



JOURNAL OF WATER PROCESS ENGINEERING

Edited by

Nicholas Hankins

Abdul Wahab Mohammad

Home (<https://www.elsevier.com/>) > Journals (<https://www.elsevier.com/catalog?producttype=jo...>)
> Journal of Water Process Engineering (<https://www.journals...>)
> Editorial Board (<https://www.journals.elsevier.com:443/journal-of-water-process-engineering/editorial-board>)

Submit Your Paper (<https://www.editorialmanager.com/JWPE/default.aspx>)

Supports Open Access (<https://www.elsevier.com/journals/journal-of-water-process-engineering/2214-7144/open-access-options>)

View Articles (<https://www.sciencedirect.com/science/journal/22147144>)

Guide for Authors

Abstracting/ Indexing (<http://www.elsevier.com/journals/journal-of-water-process-engineering/2214-7144/abstracting-indexing>)

Track Your Paper

Order Journal (<https://www.elsevier.com/journals/institutional/journal-of-water-process-engineering/2214-7144>)

Sample Issue (<https://www.sciencedirect.com/science/journal/sample//22147144>)

Journal Metrics

> CiteScore (<https://www.scopus.com/sourceid/21100324365>): **4.8** ⓘ

Impact Factor: **3.465** ⓘ

5-Year Impact Factor: **4.116** ⓘ

Source Normalized Impact per Paper (SNIP): **1.276** ⓘ

SCImago Journal Rank (SJR): **0.808** ⓘ

> View More on Journal Insights (<http://journalinsights.elsevier.com/journals/2214-7144>)



Related Links

> Author Stats (https://www.mendeley.com/stats/welcome?dgcid=journals_referral_related-links) ⓘ

> Researcher Academy (https://researcheracademy.elsevier.com)

> Author Resources (https://www.elsevier.com/authors/author-resources)

> Try out personalized alert features (https://www.sciencedirect.com/research-recommendations?

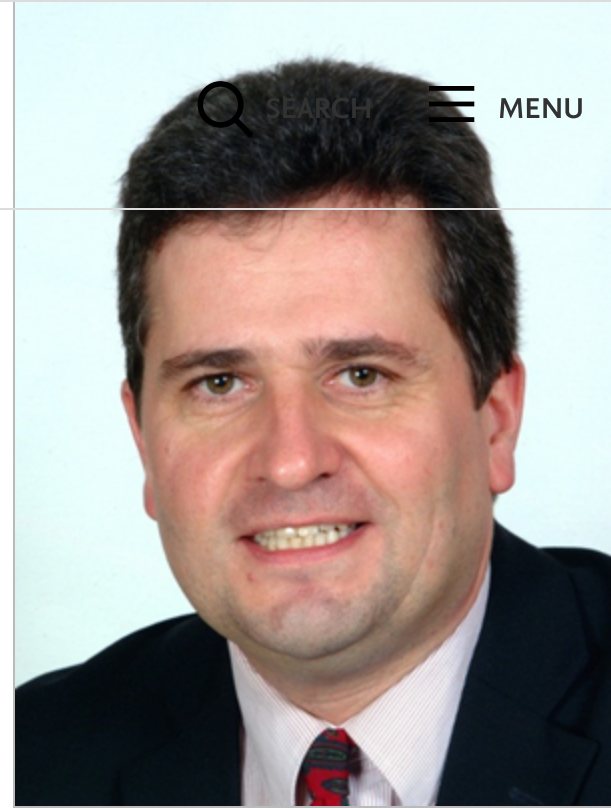
utm_campaign=STMJ_1551194499_STMJIN_OTR&utm_medium=WEB&utm_source=WEB&dgcid=STMJ_1551194499_STMJIN_OTR)

Journal of Water Process Engineering - Editorial Board

Co-Editors in Chief

Nick Hankins (https://www.journals.elsevier.com:443/journal-of-water-process-engineering/editorial-board/nick-hankins)

Department. of Engineering Science, University of Oxford, Oxford, OX1 3PJ, United Kingdom



Abdul Wahab Mohammad, PhD (<https://www.journals.elsevier.com:443/journal-of-water-process-engineering/editorial-board/abdul-wahab-mohammad-phd>)

Research Centre for Sustainable Process Technology Universiti Kebangsaan Malaysia, 43600 UKM Selangor, Malaysia

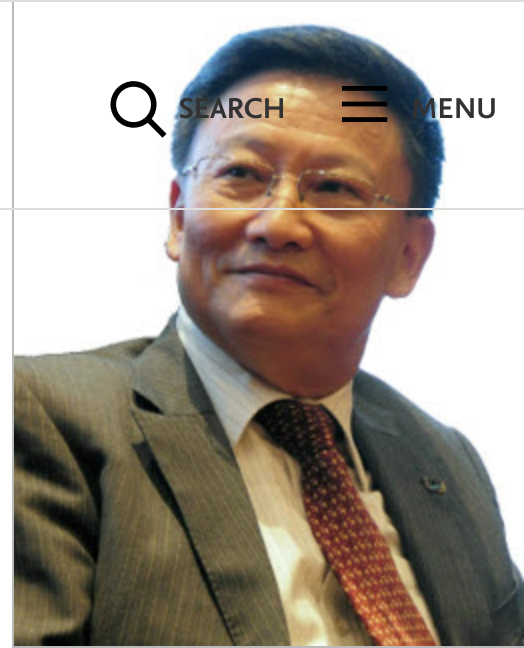
Application of membrane and separation technology in particular for water and wastewater treatment



Xiaochang C. Wang (<https://www.journals.elsevier.com:443/journal-of-water-process-engineering/editorial-board/xiaochang-c-wang>)

Xi'an University of Architecture & Technology, School of Environmental & Municipal Engineering,
No. 13, Yanta Road, 710055, Xi'an, Shaanxi, China

Water, Wastewater, Aquatic environment, Sustainability, Ecological safety



Editors

Rong Chen, PhD (<https://www.journals.elsevier.com:443/journal-of-water-process-engineering/editorial-board/rong-chen-phd>)

Xi'an University of Architecture & Technology, School of Environmental & Municipal Engineering, Xi'an, China

Biological wastewater treatment, anaerobic digestion, membrane bioreactor, Anammox



Ludovic Dumeé (<https://www.journals.elsevier.com:443/journal-of-water-process-engineering/editorial-board/ludovic-dumeé>)

Institute for Frontier Materials, Geelong, Australia

Materials engineering, Porous materials design and characterization, Membrane fabrication and operation, Heterogeneous catalysis, Water specific – microplastics, PFAS, NOM, desalination



(<https://www.elsevier.com>)

ELSEVIER
ELSEVIER

SEARCH

MENU



Wenshan Guo (<https://www.journals.elsevier.com:443/journal-of-water-process-engineering/editorial-board/wenshan-guo>)
University of Technology Sydney Faculty of Engineering and Information Technology,
Sydney, Australia



Membrane bioreactor, advanced biological treatment technologies,
micropollutants, resource and energy recovery, wastewater treatment

Chong Tzyy Haur, PhD
(<https://www.journals.elsevier.com:443/journal-of-water-process-engineering/editorial-board/chong-tzyy-haur-phd>)
Nanyang Technological University School of
Civil and Environmental Engineering,
Singapore, Singapore

(a) Advanced membrane science and
technology (b) Process intensification,
engineering for efficiency and sustainability (c)
System integration, membrane module design
and hydrodynamics (d) Process modelling and
optimization (e) Sensors for water systems (f)
Fouling and control strategies for process
units



Guangming Jiang (<https://www.journals.elsevier.com:443/journal-of-water-process-engineering/editorial-board/guangming-jiang>)
University of Wollongong, School of Civil, Mining and Environmental Engineering, Wollongong,
Australia
Environmental biotechnology; Environmental health; Sewage epidemiology; Micropollutants;
Wastewater processes



(<https://www.elsevier.com>)

ELSEVIER
ELSEVIER

SEARCH MENU



Impact factor 7.97, low cost

International Open Access Journal & ISSN Approved, Peer-reviewed, Refereed Journals

jetir Research Journal

OPEN

Journal of Water Process Engineering

35

H Index

Country [United Kingdom](#) - [SJR Ranking of United Kingdom](#)

Subject Area and Category [Biochemistry, Genetics and Molecular Biology](#)
[Biotechnology](#)

[Chemical Engineering](#)
[Process Chemistry and Technology](#)

[Engineering](#)
[Safety, Risk, Reliability and Quality](#)

[Environmental Science](#)
[Waste Management and Disposal](#)
[Water Science and Technology](#)

Publisher [Elsevier Ltd.](#)

Publication type Journals

ISSN 22147144

Coverage 2014-2020

Scope Water process engineering is interpreted by us as the understanding and application of the fundamental laws and principles of nature that allow us to transform raw or waste water sources into products that are useful to society, while operating at laboratory, pilot or full industrial scale. These products include clean water, energy and material resources. Our scope focuses on the design, operation, control, modelling, optimization and intensification of chemical, physical, and biological processes for water treatment. We emphasize the process engineering aspects of water treatment processes, for which the focus of the study is on the engineered application and practice rather than the fundamental and underlying science.

[Homepage](#)

[How to publish in this journal](#)

[Join the conversation about this journal](#)

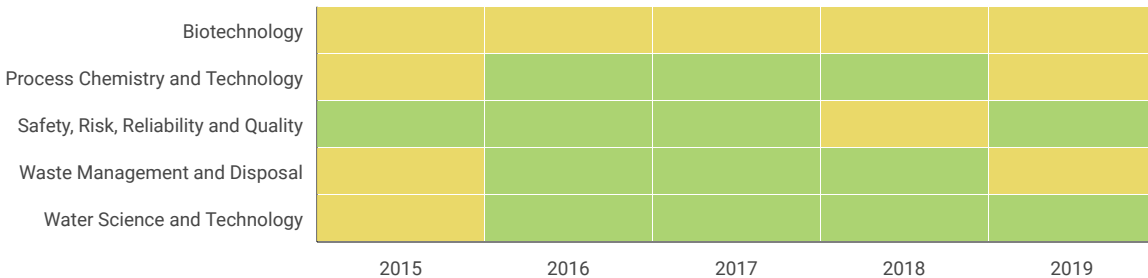
Free Grammar Checker

Eliminate grammar errors instantly and enhance your writing with Grammarly

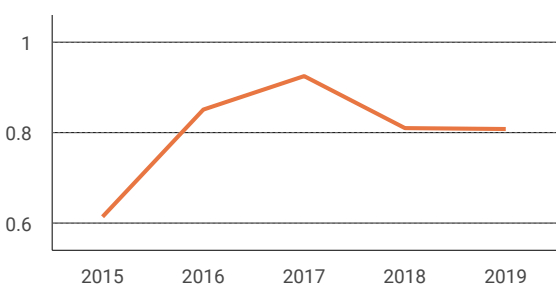
Grammarly

DOWNLOAD

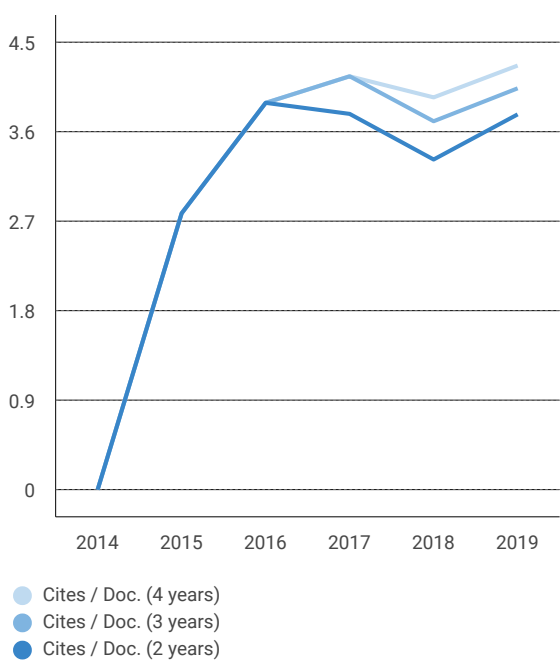
Quartiles



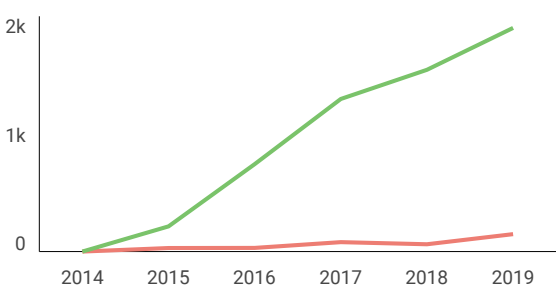
SJR



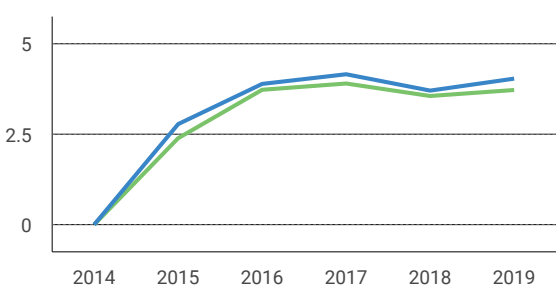
Citations per document



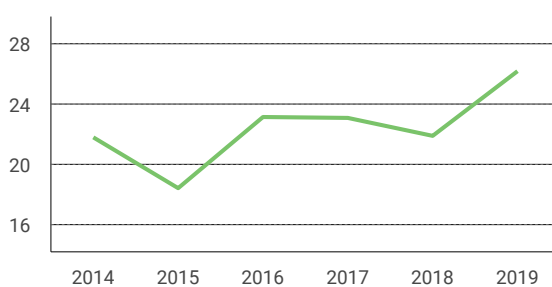
Total Cites Self-Cites



External Cites per Doc Cites per Doc



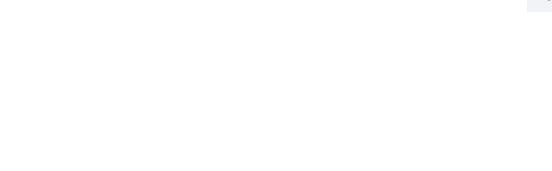
% International Collaboration



Citable documents Non-citable documents



Cited documents Uncited documents



We are sorry to tell you that SClmago Journal & Country Rank is not a journal. SJR is a portal with scientometric indicators of journals indexed in Elsevier/Scopus. Unfortunately, we cannot help you with your request, we suggest you visit the journal's homepage or contact the journal's editorial staff , so they could inform you more deeply. Best Regards, SClmago Team

F **Fernando Valenzuela** 2 years ago

Thanks Elena. Last question: the SClmago Journal Quartile Ranking is the same that the JCR Journal Quartile Rank?.

Example: if Journal of Water process Engineering is Q1 in SClmago, should be Q1 in JCR ?

Fernando
Universidad de Chile

reply

F **Fernando Valenzuela Lozano** 2 years ago

I just need to know if this journal will be included in the Journal Citation Report (JCR) during 2019, because this year is not in the list of journal. It looks like a Q1 journal, but has not a 5-years impact. Why??

Fernando

reply



Elena Corera 2 years ago

SClImago Team

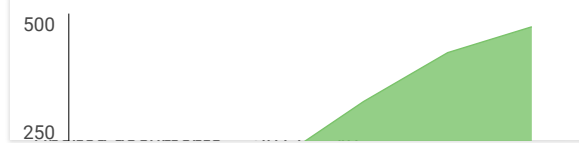
Dear Fernando, SJR uses Scopus data, our impact indicator is the SJR. Check our page to locate the journal. We suggest you consult the Journal Citation Report for other indicators with a Web of Science data source. 2019 has not yet happened, the articles of that year have not been published, let alone cited. It is impossible to know if the journal will be in a database and if the articles of that year will receive the same citation flow that they have received so far. Best Regards, SClmago Team

Leave a comment

Name

Email

(will not be published)



Journal of Water Process Engineering

Q1

Safety, Risk, Reliability and Quality
best quartile

SJR 2019

0.81

powered by scimagojr.com

← Show this widget in your own website

Just copy the code below and paste within your html code:

```
<a href="https://www.scimag
```

UGC approved Journal

research journal, Call for Paper, paper Publication, Research Paper, Review Paper

jetir.org

OPEN

S **surahman** 2 months ago

How to the publish journal?

reply



Melanie Ortiz 2 months ago

SCImago Team

Dear Surahman, thank you very much for your comment, we suggest you look for author's instructions/submission guidelines in the journal's website. Best Regards, SCImago Team

H **Heba** 2 months ago

Please, i want to ask about the time spent to know the first decision for the manuscript

Thanks

reply



Melanie Ortiz 2 months ago

SCImago Team

Dear Heba,
thank you for contacting us.

I'm not a robot
reCAPTCHA
[Privacy](#) - [Terms](#)

Submit

The users of Scimago Journal & Country Rank have the possibility to dialogue through comments linked to a specific journal. The purpose is to have a forum in which general doubts about the processes of publication in the journal, experiences and other issues derived from the publication of papers are resolved. For topics on particular articles, maintain the dialogue through the usual channels with your editor.

Developed by:



Powered by:

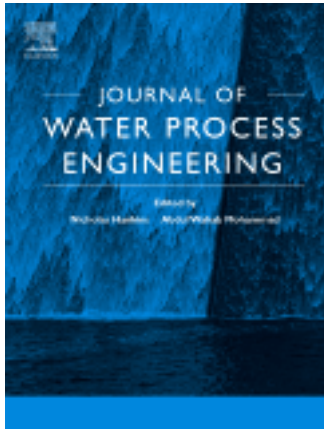


Follow us on [@ScimagoJR](#)

Scimago Lab, Copyright 2007-2020. Data Source: Scopus®

EST MODUS IN REBUS

Horatio (Satire 1,1,106)



(<https://www.sciencedirect.com/science/journal/2147144>)

[Visit journal homepage >](#)

[Submit your paper >](#)

[Open access options >](#)

[Guide for authors >](#)

[Track your paper >](#)

[Order journal >](#)

[View articles >](#)

[Free sample >](#)

[Editorial board >](#)

[Browse journals \(/c... > Journal of Water... > Abstracting and ...](#)

Abstracting and Indexing

- [Science Citation Index Expanded](#)



Solutions



Solutions

Researchers



Researchers

About Elsevier



About Elsevier

How can we help?



How can we help?



Select location/language

(https://www.elsevier.com)
(https://www.elsevier.com)
(https://www.elsevier.com)
(https://www.elsevier.com)

🌐 Global - English (/location-selector)



Copyright © 2020 Elsevier, except certain content provided by third parties

Cookies are used by this site. To decline or learn more, visit our Cookies (/legal/use-of-cookies) page.

Terms and Conditions (/legal/elsevier-website-terms-and-conditions) Privacy Policy (/legal/privacy-policy) Sitemap (/sitemap) Accessibility (/about/accessibility)



(https://www.elsevier.com)



(https://www.relx.com/)

ELSEVIER



(https://www.relx.com/)

Search in this journal

Volume 38

In progress (December 2020)

This issue is in progress but contains articles that are final and fully citable.

[Download full issue](#)

[← Previous vol/issue](#)

[Next vol/issue >](#)

Receive an update when the latest issues in this journal are published

[Sign in to set up alerts](#)

[Review article](#) [Full text access](#)

The role of wastewater treatment plants as tools for SARS-CoV-2 early detection and removal

Alain Lesimple, Saad Y. Jasim, Daniel J. Johnson, Nidal Hilal

Article 101544

[Download PDF](#) [Article preview](#) ✓

[Erratum](#) [Full text access](#)

Retraction notice to “Polyethersulfone-CaCu₃Ti₄O₁₂ hollow fiber membrane with enhanced photocatalytical activity and water permeability” [J. Water Process Eng. 33 (2020) 101072]

Tunmise Ayode Otitoju, Yang Li, Renjie Liu, Jincan Wang, ... Sanxi Li

Tuning the synthetic conditions of graphene oxide/magnetite/ hydroxyapatite/cellulose acetate nanofibrous membranes for removing Cr(VI), Se(IV) and methylene blue from aqueous solutions

Reem Al-Wafi, M.K. Ahmed, S.F. Mansour

Article 101543

[Purchase PDF](#) Article preview 

Research article Abstract only

Kinetic modelling and performance evaluation of vertical subsurface flow constructed wetlands in tropics

G.M.P.R. Weerakoon, K.B.S.N. Jinadasa, Jagath Manatunge, Buddhi Wijesiri, Ashantha Goonetilleke

Article 101539

[Purchase PDF](#) Article preview 

Research article Abstract only

Technical and economic feasibility of phosphorus recovery from wastewater in São Paulo's Metropolitan Region

Antonio Santos Sánchez

Article 101537

[Purchase PDF](#) Article preview 

Research article Abstract only

Operating parameters optimization of combined UF/NF dual-membrane process for brackish water treatment and its application performance in municipal drinking water treatment plant

Gongduan Fan, Zhongsheng Li, Zhongsen Yan, Zhongqing Wei, ... Haiqing Chang

Article 101547

[Purchase PDF](#) Article preview 

Research article Abstract only

Removal of oil contents and salinity from produced water using microemulsion

J.S.B. Souza, J.M. Ferreira Júnior, G. Simonelli, J.R. Souza, ... L.C.L. Santos

Article 101548

[Purchase PDF](#) Article preview 

[Purchase PDF](#) [Article preview](#) 

Research article Abstract only

Nattokinase production from *Bacillus subtilis* using cheese whey: Effect of nitrogen supplementation and dynamic modelling

Ansuman Sahoo, Biswanath Mahanty, Achlesh Daverey, Kasturi Dutta

Article 101533

[Purchase PDF](#) [Article preview](#) 

Research article Abstract only

Carbon templated strategies of mesoporous silica applied for water desalination: A review

Muthia Elma, Erdina L.A. Rampun, Aulia Rahma, Zaini L. Assyaifi, ... Adi Darmawan

Article 101520

[Purchase PDF](#) [Article preview](#) 

Research article Abstract only

Energy coverage of ataköy-ambarlı municipal wastewater treatment plants by salinity gradient power

Ali Zoungrana, Oruç Kaan Türk, Mehmet Çakmakci

Article 101552

[Purchase PDF](#) [Article preview](#) 

Research article Abstract only

Packing granular activated carbon into a submerged gravity-driven flat sheet membrane module for decentralized water treatment

P. Schumann, J.A. Ordóñez Andrade, M. Jekel, A.S. Ruhl

Article 101517

[Purchase PDF](#) [Article preview](#) 

Research article Abstract only

'Polycation' modified PVDF based antibacterial and antifouling membranes and 'point-of-use supports' for sustainable and effective water decontamination

Research article Abstract only

Microalgae fuel cell for wastewater treatment: Recent advances and challenges

Krishna Kumar Jaiswal, Vinod Kumar, M.S. Vlaskin, Nishesh Sharma, ... P.K. Chauhan

Article 101549

[Purchase PDF](#) Article preview

Research article Abstract only

Acetic acid and methanol recovery from dimethyl terephthalate process wastewater using pressure membrane and membrane distillation processes

Ozay Yasin, Isik Zelal, Dizge Nadir

Article 101532

[Purchase PDF](#) Article preview

[< Previous vol/issue](#)

[Next vol/issue >](#)

ISSN: 2214-7144

Copyright © 2020 Elsevier Ltd. All rights reserved



[About ScienceDirect](#)

[Remote access](#)

[Shopping cart](#)

[Advertise](#)

[Contact and support](#)

[Terms and conditions](#)

[Privacy policy](#)

 RELX™



Access through your institution



Outline Get Access Share Export

Journal of Water Process Engineering

Volume 38, December 2020, 101520

Carbon templated strategies of mesoporous silica applied for water desalination: A review

Muthia Elma ^{a, b} , Erdina L.A. Rampun ^b, Aulia Rahma ^b, Zaini L. Assyaifi ^{a, b}, Anna Sumardi ^{a, b}, Aptar E. Lestari ^{a, b}, Gesit S. Saputro ^b, Muhammad Roil Bilad ^c, Adi Darmawan ^d

Show more

<https://doi.org/10.1016/j.jwpe.2020.101520>

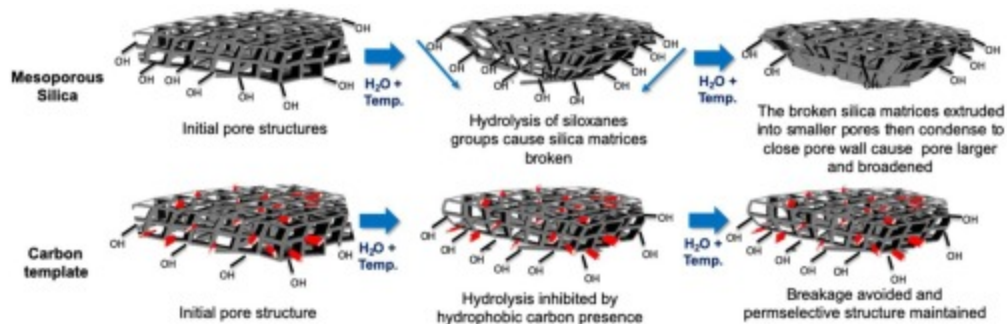
[Get rights and content](#)

Abstract

Porous materials have attracted attention in many practical fields, including for water desalination. Carbon templated is an attractive method in enhancing the properties of mesoporous silica materials used as membrane materials. This review mainly focuses on the strategies of carbon templates of mesoporous silica materials essentially applied for water desalination. Numerous strategies for carbon templated mesoporous silica are briefly discussed. In addition, most carbon-silica based membranes for desalination are detailed and their performances are discussed. Moreover, application of carbon-silica templates for wetland saline water desalination are also discussed in great detail. The comparison between carbon-silica based materials and silica-based membranes of recent techniques, fabrication, trend, application and operation condition for further improvement of membrane performance are also thoroughly reviewed.

Graphical abstract

Carbon templated presence in a mesoporous silica matrix can prevent the mobility of silica groups from hydrolytic attack and can inhibit micropore shrinkage.



[Download : Download high-res image \(251KB\)](#)

[Download : Download full-size image](#)

[Previous](#)

[Next](#)

Keywords

Carbon templated; Mesoporous silica; Carbon-silica based materials; Water and wetland saline water desalination

[Recommended articles](#)

[Citing articles \(0\)](#)

[View full text](#)

© 2020 Elsevier Ltd. All rights reserved.



[About ScienceDirect](#)

[Remote access](#)

[Shopping cart](#)

[Advertise](#)

[Contact and support](#)

[Terms and conditions](#)

[Privacy policy](#)

RELX™

We use cookies to help provide and enhance our service and tailor content and ads. By continuing you agree to the [use of cookies](#).

Copyright © 2020 Elsevier B.V. or its licensors or contributors. ScienceDirect® is a registered trademark of Elsevier B.V.

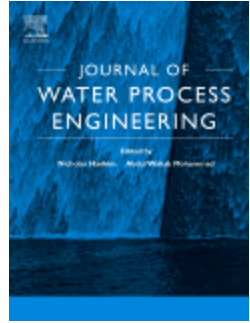
ScienceDirect® is a registered trademark of Elsevier B.V.



(https://
www.elsevier.com)

Home (https://www.elsevier.com/) > Journals (https://www.elsevier.com/catalog?producttyp...

> Journal of Water Process Engineering (https://www.journals.elsevier.com:443/journal-of-water-process-engineering)



(https://www.sciencedirect.com/science/journal/22147144)

ISSN: 2214-7144

f (jou (http
rnal- s://w
(http (http of- ww.
s://w s://t wate else
ww.f witte r- vier.
ace r.co proc com
boo m/el ess- /Pref
k.co sevi engi eren
m/El erch neer ceC
sevi eme ing/r entr
erC ng) ss) e)
hem
Eng/
)

Journal of Water Process Engineering

Co-Editors in Chief: Nick Hankins (https://www.journals.elsevier.com:443/journal-of-water-process-engineering/editorial-board/nick-hankins), Abdul Wahab Mohammad, PhD (https://www.journals.elsevier.com:443/journal-of-water-process-engineering/editorial-board/abdul-wahab-mohammad-phd), Xiaochang C. Wang (https://www.journals.elsevier.com:443/journal-of-water-process-engineering/editorial-board/xiaochang-c-wang)

> View Editorial Board (https://www.journals.elsevier.com:443/journal-of-water-process-engineering/editorial-board)

> **CiteScore:** (https://www.scopus.com/sourceid/21100324365) **4.8** i **Impact Factor:** **3.465** i

Submit Your Paper (https://www.editorialmanager.com/JWPE/default.aspx)

Supports Open Access (https://www.elsevier.com/journals/journal-of-water-process-engineering/2214-7144/open-access-options)

View Articles (https://www.sciencedirect.com/science/journal/22147144)



Abstracting/Indexing (<http://www.elsevier.com/journals/journal-of-water-process-engineering/2214-7144/abstracting-indexing>)

Track Your Paper

Order Journal (<https://www.elsevier.com/journals/institutional/journal-of-water-process-engineering/2214-7144>)

Sample Issue (<https://www.sciencedirect.com/science/journal/sample//22147144>)

Journal Metrics

► CiteScore (<https://www.scopus.com/sourceid/21100324365>): **4.8** i

Impact Factor: **3.465** i

5-Year Impact Factor: **4.116** i

Source Normalized Impact per Paper (SNIP): **1.276** i

SCImago Journal Rank (SJR): **0.808** i

► View More on Journal Insights (<http://journalinsights.elsevier.com/journals/2214-7144>)

Your Research Data

► Share your research data (<https://www.elsevier.com/authors/author-resources/research-data>)

► Data in Brief co-submission (<https://www.elsevier.com/authors/author-resources/research-data/data-articles/DIB-co-submission>)

► MethodsX co-submission (<https://www.elsevier.com/authors/author-resources/research-data/materials-and-methods/mex-co-submission>)

Related Links

► Author Stats (https://www.mendeley.com/stats/welcome?dgcid=journals_referral_related-links) i

► Researcher Academy (<https://researcheracademy.elsevier.com>)

► Author Resources (<https://www.elsevier.com/authors/author-resources>)

Aims

The Journal of Water Process Engineering aims to be the premier international forum for the publication of world leading, high impact research on the sustainable engineering of water and wastewater treatment processes.

Scope

Water process engineering is interpreted by us as the understanding and application...

Read more

Most Downloaded Recent Articles Most Cited Open Access Articles

Most Downloaded Articles



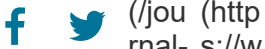
Recent Articles



Most Cited Articles



Recent Open Access Articles



(<http://www.elsevier.com/locate/journal-of-water-process-engineering>)

Announcements (<https://www.journals.elsevier.com:443/journal-of-water-process-engineering/announcements>)

In support of equality, inclusion & diversity (<https://www.journals.elsevier.com:443/journal-of-water-process-engineering/announcements/in-support-of-equality-inclusion-diversity>)

Elsevier stands against racism and discrimination and fully supports the joint commitment for action in inclusion and diversity in publishing (<https://www.rsc.org/new-perspectives/talent/joint-commitment-for-action-inclusion-and-diversity-in-publishing/>).

In partnership with the communities we serve; we redouble our deep commitment to inclusion and diversity within our editorial, author and reviewer networks.

Visibility. Trust. Choice. Only some of the benefits of publishing open access with Elsevier

(<https://www.journals.elsevier.com:443/journal-of-water-process-engineering/announcements/benefits-of-publishing-open-access-with-elsevier>)



SEARCH

MENU

Discover how our open access options can help you maximize reach and impact

Results in Engineering Partner Journal (<https://www.journals.elsevier.com:443/journal-of-water-process-engineering/announcements/results-in-engineering-partner-journal>)

This journal has partnered with *Results in Engineering* (<http://www.journals.elsevier.com/results-in-engineering>), an open access journal from Elsevier publishing peer reviewed research across all engineering disciplines. *Results in Engineering's* team of experts provide editorial excellence, fast publication, and high visibility for your paper. Authors can quickly and easily transfer their research from a Partner Journal to *Results in Engineering* without the need to edit, reformat or resubmit.

> Learn more at Results in Engineering (<https://www.journals.elsevier.com/development-engineering/announcements/results-in-engineering-partner-journal>)

> View All (<https://www.journals.elsevier.com:443/journal-of-water-process-engineering/announcements>)

Latest Mendeley Data Datasets (<https://www.journals.elsevier.com:443/journal-of-water-process-engineering/mendeley-data>)

Mendeley Data Repository is free-to-use and open access. It enables you to deposit any research data (including raw and processed data, video, code, software, algorithms, protocols, and methods) associated with your research manuscript. Your datasets will also be searchable on Mendeley Data Search, which includes nearly 11 million indexed datasets. For more information, visit Mendeley Data (<https://data.mendeley.com/datasets>).

Data for: Micellar enhanced ultrafiltration (MEUF) of mercury-contaminated wastewater: Experimental and artificial neural network modeling (<https://data.mendeley.com/datasets/92ncbyx5h9>)

Seung Hwan Lee | Muhammad Yaqub

1 file (2019)

Data for: Field performance of two on-site wastewater treatment systems using reactive media layers for nutrient and pathogen removal (<https://data.mendeley.com/datasets/gn2zp9wtwh>)

Alexandra Suhogusoff | David Blowes | ...

2 files (2019)

Data for: Field performance of two on-site wastewater treatment systems using reactive media layers for nutrient and pathogen removal (<https://data.mendeley.com/datasets/pvmcht7kbp>)

Alexandra Suhogusoff | David Blowes | ...

2 files (2019)

> View All (<https://www.journals.elsevier.com:443/journal-of-water-process-engineering/mendeley-data>)



Special issues published in Journal of Water Process Engineering.

Sustainable Water Processing (<https://www.sciencedirect.com/science/journal/22147144/vsi/108T4KHFHQD>)

Nicolas Hankins | Sher Jamal Khan

SI: Sust Water Processing (<http://www.sciencedirect.com/science/journal/22147144/30>)

Sustainable Water Engineering (<http://www.sciencedirect.com/science/journal/22147144/15>)

Ooi Boon Seng

➤ View All (<https://www.journals.elsevier.com:443/journal-of-water-process-engineering/special-issues>)

PlumX Metrics (<https://www.journals.elsevier.com:443/journal-of-water-process-engineering/top-articles>)

Below is a recent list of 2019—2020 articles that have had the most social media attention. The Plum Print next to each article shows the relative activity in each of these categories of metrics: Captures, Mentions, Social Media and Citations. Go here (<http://plumanalytics.com/learn/about-metrics/>) to learn more about PlumX Metrics.

Removal of dye from polluted water using novel nano manganese oxide-based materials (<https://plu.mx/a?doi=10.1016/j.jwpe.2019.100911>)

Removal of dye from polluted water using novel nano manganese oxide-based materials (<https://dx.doi.org/10.1016/j.jwpe.2019.100911>)

Macroscopic and modeling evidence for nickel(II) adsorption onto selected manganese oxides and boehmite (<https://plu.mx/a?doi=10.1016/j.jwpe.2019.100964>)

Macroscopic and modeling evidence for nickel(II) adsorption onto selected manganese oxides and boehmite (<https://dx.doi.org/10.1016/j.jwpe.2019.100964>)

Microalgae fuel cell for wastewater treatment: Recent advances and challenges (<https://plu.mx/a?doi=10.1016/j.jwpe.2020.101549>)

Microalgae fuel cell for wastewater treatment: Recent advances and challenges (<https://dx.doi.org/10.1016/j.jwpe.2020.101549>)

➤ View All (<https://www.journals.elsevier.com:443/journal-of-water-process-engineering/top-articles>)

Call for Papers (<https://www.journals.elsevier.com:443/journal-of-water-process-engineering/call-for-papers>)

Special Issue on Novel materials for water and wastewater treatment

(<https://www.journals.elsevier.com:443/journal-of-water-process-engineering/call-for-papers/special-issue-on-novel-materials-for-water-and-wastewater>)

Special Issue on Novel bioprocesses and technologies for enhanced recovery of value-added products from wastewater (<https://www.journals.elsevier.com:443/journal-of-water-process-engineering/call-for-papers/novel-bioprocesses-and-technologies>)



ELSEVIER evier.co

Special Issue on Anaerobic process for simultaneous wastewater treatment and biogas production in agro industries in ASEAN (<https://www.journals.elsevier.com:443/journal-of-water-process-engineering/call-for-papers/special-issue-on-anaerobic-process-for-simultaneous-wastewat>)

> [View All \(https://www.journals.elsevier.com:443/journal-of-water-process-engineering/call-for-papers\)](https://www.journals.elsevier.com:443/journal-of-water-process-engineering/call-for-papers)

News (<https://www.journals.elsevier.com:443/journal-of-water-process-engineering/news>)

News

Partnership With Case Studies in Chemical and Environmental Engineering (<https://www.journals.elsevier.com:443/journal-of-water-process-engineering/news/partnership-with-case-studies-jwpe>)

First issue now published (<https://www.journals.elsevier.com:443/journal-of-water-process-engineering/news/first-issue-now-published>)

> [View All \(https://www.journals.elsevier.com:443/journal-of-water-process-engineering/news\)](https://www.journals.elsevier.com:443/journal-of-water-process-engineering/news)

Journal of Water Process Engineering

Readers

[View Articles \(https://www.sciencedirect.com/science/journal/22147144\)](https://www.sciencedirect.com/science/journal/22147144)

[Sample Issue \(https://www.sciencedirect.com/science/journal/sample//22147144\)](https://www.sciencedirect.com/science/journal/sample//22147144)

[Volume/ Issue Alert \(https://www.sciencedirect.com/user/alerts\)](https://www.sciencedirect.com/user/alerts)

[Personalized Recommendations \(https://www.sciencedirect.com/user/register?](https://www.sciencedirect.com/user/register?utm_campaign=sd_recommender_ELSJLS&utm_channel=elseco&dgcid=sd_recommender_ELSJLS)

[utm_campaign=sd_recommender_ELSJLS&utm_channel=elseco&dgcid=sd_recommender_ELSJLS\)](https://www.sciencedirect.com/user/register?utm_campaign=sd_recommender_ELSJLS&utm_channel=elseco&dgcid=sd_recommender_ELSJLS)

[Authors \(http://www.elsevier.com/authors/home\)](http://www.elsevier.com/authors/home)

[Author Information Pack \(https://www.elsevier.com/journals/journal-of-water-process-engineering/2214-7144?generatepdf=true\)](https://www.elsevier.com/journals/journal-of-water-process-engineering/2214-7144?generatepdf=true)

[Submit Your Paper \(https://www.editorialmanager.com/JWPE/default.aspx\)](https://www.editorialmanager.com/JWPE/default.aspx)

[Track Your Paper \(http://help.elsevier.com/app/answers/detail/a_id/89/p/8045/\)](http://help.elsevier.com/app/answers/detail/a_id/89/p/8045/)

[Early Career Resources \(http://www.elsevier.com/early-career-researchers/training-and-workshops\)](http://www.elsevier.com/early-career-researchers/training-and-workshops)

[Rights and Permissions \(https://www.elsevier.com/about/policies/copyright/permissions\)](https://www.elsevier.com/about/policies/copyright/permissions)

[Support Center \(https://service.elsevier.com/app/home/supporthub/publishing/#authors\)](https://service.elsevier.com/app/home/supporthub/publishing/#authors)

[Librarians \(https://www.elsevier.com/librarians\)](https://www.elsevier.com/librarians)

[Ordering Information and Dispatch Dates \(http://www.elsevier.com/journals/journal-of-water-process-engineering/2214-7144/order-journal\)](http://www.elsevier.com/journals/journal-of-water-process-engineering/2214-7144/order-journal)

Abstracting/ Indexing (<http://www.elsevier.com/journals/journal-of-water-process-engineering/2214-7144/abstracting-indexing>)
Editors (<https://www.elsevier.com/editors/home>)
Publishing Ethics Resource Kit (<http://www.elsevier.com/editors/perk>)
Support Center (<https://service.elsevier.com/app/home/supporthub/publishing/#editors>)

Reviewers (<http://www.elsevier.com/reviewers/home>)
Log in as Reviewer (<https://www.editorialmanager.com/JWPE/default.aspx>)
Reviewer Recognition (<https://www.elsevier.com/reviewers/becoming-a-reviewer-how-and-why#recognizing>)
Support Center (<https://service.elsevier.com/app/home/supporthub/publishing/#reviewers>)
Societies (<http://www.elsevier.com/societies/home>)

 (<https://www.elsevier.com>)

ELSEVIER




Copyright © 2020 Elsevier B.V.

Careers (<https://www.elsevier.com/careers/careers-with-us>) - Terms and Conditions
(<https://www.elsevier.com/legal/elsevier-website-terms-and-conditions>) - Privacy Policy
(<https://www.elsevier.com/legal/privacy-policy>)

Cookies are used by this site. To decline or learn more, visit our Cookies (/Cookies) page.

 (<https://www.elsevier.com>)  RELX Group™ (<http://www.reedelsevier.com/>)

ELSEVIER

   (<https://www.linkedin.com/company/elsevier>)  RELX Group™ (<http://www.reedelsevier.com/>)

10.1016_j.jwpe.2020.101520.pdf

by

Submission date: 04-Aug-2020 10:50AM (UTC+0700)

Submission ID: 1365732133

File name: 10.1016_j.jwpe.2020.101520.pdf (4.48M)

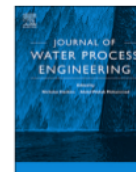
Word count: 16995

Character count: 93671



Contents lists available at ScienceDirect

Journal of Water Process Engineering

journal homepage: www.elsevier.com/locate/jwpe

Carbon templated strategies of mesoporous silica applied for water desalination: A review



Muthia Elma^{a,b,*}, Erdina L.A. Rampun^b, Aulia Rahma^b, Zaini L. Assyaifi^{a,b}, Anna Sumardi^{a,b}, Aptar E. Lestari^{a,b}, Gesit S. Saputro^b, Muhammad Roil Bilad^c, Adi Darmawan^d

^a Chemical Engineering Department, Lambung Mangkurat University, Jl. A. Yani KM 36, Banjarbaru, South Kalimantan 70714, Indonesia

^b Materials and Membranes Research Group (M²ReG), Lambung Mangkurat University, Jl. A. Yani KM 36, Banjarbaru, South Kalimantan 70714, Indonesia

^c Department of Chemical Engineering, Universiti Teknologi Petronas, Seri Iskandar, Perak 32610, Malaysia

^d Department of Chemistry, Diponegoro University, Semarang 50275, Indonesia

ARTICLE INFO

Keywords:

Carbon templated

Mesoporous silica

Carbon-silica based materials

Water and wetland saline water desalination

ABSTRACT

Porous materials have attracted attention in many practical fields, including for water desalination. Carbon templated is an attractive method in enhancing the properties of mesoporous silica materials used as membrane materials. This review mainly focuses on the strategies of carbon templates of mesoporous silica materials essentially applied for water desalination. Numerous strategies for carbon templated mesoporous silica are briefly discussed. In addition, most carbon-silica based membranes for desalination are detailed and their performances are discussed. Moreover, application of carbon-silica templates for wetland saline water desalination are also discussed in great detail. The comparison between carbon-silica based materials and silica-based membranes of recent techniques, fabrication, trend, application and operation condition for further improvement of membrane performance are also thoroughly reviewed.

1. Introduction

Porous materials have attracted attention in many practical fields, such as chemical, medical, optic, electronic, biotechnological, environmental and/or energy applications. Porous materials pose regular pore structures and high surface area useful for materials adsorption, storage [1,2]. According to the IUPAC definition, porous materials are classified into three categories depending on their pore sizes: microporous < 2 nm, mesoporous 2–50 nm, and macroporous > 50 nm [3]. Since the first mesoporous material of MCM-41 was introduced in 1990s, the developments of other mesoporous materials have been extensive [4].

Basic preparation of mesoporous materials are done using template synthesis self-assembled micelles structure from cost-effective silica and carbon sources [1]. It is done by employing organic template molecules under various processes or by employing textural templates where the inorganic precursor condenses [4]. Extensive reports are available on custom developments of novel mesoporous materials for catalyst, sorption, sensing, optics, drug delivery or separation. Mesoporous materials are also attractive for wrapping siRNA to enhance the therapeutic effect on cancer for medical treatment [5,6]. They have been explored to encapsulate fragrances for controlled release and storage of

the odorants [7]. Mesoporous materials such as zeolite and silica are also highly attractive as support for catalyst [8,9] thanks to their inherent selectivity and high surface area [10].

Membranes processes have long been established with widespread applications. They are mostly used to produce potable water from saline water, to treat industrial wastewater effluents and to recover valuable resources from wastewater (via concentration and purification) and to fractionate macromolecular mixtures in the food and drug industries. They have also been established for separation of gases, energy conversion systems artificial organs and drug delivery. The membrane materials employed in those diverse applications differ widely in their structure and function.

Diverse membrane base processes have recently been emerging molecular separations, fractionations, concentrations, purifications, clarifications, emulsifications, crystallization, etc. It is mainly because of the inherent characteristic of high efficiency; operational simplicity, stability and flexibility; high selectivity and permeability in separation applications; low energy requirements; environment compatibility, easy to control and scale-up. Apart for being applied as standalone unit, membrane processes are also very common in hybrid system involving process intensification. They include but not limited to membrane reactors, membrane bioreactors, membrane contactors.

* Corresponding author at: Chemical Engineering Department, Lambung Mangkurat University, Jl. A. Yani KM 36, Banjarbaru, South Kalimantan 70714, Indonesia.

E-mail address: melma@ulm.ac.id (M. Elma).

<https://doi.org/10.1016/j.jwpe.2020.101520>

Received 4 April 2020; Received in revised form 2 July 2020; Accepted 8 July 2020

2214-7144/© 2020 Elsevier Ltd. All rights reserved.

However, all membranes have several features in common that make them particularly attractive for the separation. The separation is performed by physical means (mostly) at ambient temperature without chemically altering the feed mixture. This is mandatory for applications in artificial organs and in many drug delivery systems as well as in the food and drug industry or in downstream processing of bioproducts where temperature-sensitive substances are handled. The membrane materials used in those applications differ widely in their structure, function and the way they operate. Membrane properties can thus be tailored and adjusted to specific applications.

The versatility of membrane structures and functions makes a precise and complete definition of a membrane rather difficult. A membrane is a barrier that separates and/or contacts two different phases and controls the exchange of matter and energy between the phases. The membrane can be a selective or simply acts as a contacting barrier. In the first case, it controls the exchange between the two phases adjacent to it in a very specific manner; in the second case, it functions as contactor of the two phases in which the transport occurs.

Ones can distinguish between biological membranes, which are part of the living organism, and synthetic membranes that are man-made. The structure and function of synthetic membranes are much simpler than the biological membranes. They only facilitate passive transport and are less selective. However, they are chemically and mechanically more stable especially at high temperature. The selectivity of synthetic membranes is dictated by sieving property of the pore or the solute solubility and diffusivity within the membrane matrix. The permeability of the membrane for different components, however, is only one parameter determining the flux through the membrane.

Membrane based processes are also driven by different forces, such as concentration different, pressure different, or temperature gradients, or an electrical potential for the charged components. The use of different driving forces results in a number of processes such as reverse osmosis, micro-, ultra- and nanofiltration, dialysis, electro-dialysis, pervaporation, gas separation, membrane contactors, membrane distillation, membrane-based solvent extraction, membrane reactors, etc. [11].

Mesoporous silica materials are frequently applied for membrane fabrication in the gas and the water separation and thus worthy of detailed overview. The interaction between the permeating molecule and the membrane material often dictate the separation process. Gas steams or water vapor are abundant with water molecules that easily reacts with the hydrophilic sites in the silica thin films created chemical and microstructural instability. For instance, Giessler, Diniz da Costa [12] reported that sol-gel derived films produced the silanols from hydrolysis and condensation reactions. The presence of silanol bonds collapses of the film structure that lowers the pore volume. Silanol groups form weakly branched fractal systems and has hydrophilic properties. They easily react with water altering the matrix of silica-derived materials. These include organic covalent templates such as methyl groups and noncovalently bonded organic templates such as C6 and C16 surfactants and alkyltriethoxysilanes [12].

To overcome the detrimental interaction of water with the silica material, various templating methods have been developed. It is generally divided into 3 steps: 1) preparation, 2) method selection (i.e., hydrothermal, precipitation, and sol-gel), and 3) templating (dissolution, sintering, etc.). Regular template is sorted into two categories of materials that is naturally and synthesis. One strategy to obtain a good hydro stability of silica is by embedding carbon molecules into the silica matrix. Various materials have been used earlier as carbon sources such as P123 [13], F127 [14], and F108 [15], or citric acid [16]. Recently, more sustainable and low-cost carbon sources have also been explored, such as pectin (from apple peel) [17], banana peel [18]), and also glucose [19]. The Si-O-C bond can be formed after adding carbon materials into the silica matrix. The presence of carbon prevents silica pore from collapsing especially when the material is applied for water desalination. Carbon material also reported has strong covalent bonding

[20] which enhances the mechanical strength.

In this review, we overview of the progress of the advantageous strategies of carbon templates of mesoporous silica materials essentially applied for water desalination. Numerous strategies for carbon templated mesoporous silica were discussed. Finally, applications of carbon templated mesoporous silica materials in water desalination are also discussed.

2. Advanced carbon templated strategies

Materials with nanopore structure allow interaction at atomic, ionic and molecular level since they have large surface area and limited spatial space [21,22]. Nanopores can be classified into macro-porous (> 50 nm), Mesoporous (2 nm – 50 nm) and microporous (< 2 nm). Materials with nanopore has been used in adsorption [23], separation [24,25], catalysts [26,27], and electronics [28,29]. Among many application of nanopores, nanopore carbons (NPCs) have regular inter-penetrations which leads to desirable chemical and physical properties, namely high specific surface, uniform pore structure, good heat resistance and chemical stability, low density and many others [28]. NPCs have been then implemented in hydrogen storage [30], adsorption [31,32], energy storage [33,34] and electronic devices [35].

The most commonly used carbon templating methods include physical (destruction, adhesion and spray) and chemical methods (precipitation, sol-gel, hydrothermal and template) [36,37]. Template synthesis is a method that has been developed since the 1990-an and still widely applied currently. The method is also very easy to do and provide ample flexibility in controlling the structure, morphology and particle size of the resulting materials [38].

Morphology is an important parameter to determine the character of the particle size and pore structure [39,40]. The template method changes the morphology of the product by controlling the nucleation and growth of crystals during the nano-material preparations. It generally consists of 3 steps: 1) template preparation, 2) methods selection (hydrothermal, precipitation, and sol-gel), and 3) templated (dissolution, sintering, etc.). Regular template can be classified into materials that is naturally and synthetic. Also, it is based on the difference between the structure of the template. The templating method is divided into hard templates and soft templates [41,42].

One strategy to obtain a good hydro stability of silica matrix is by embedding carbon molecules into the silica. Various materials have been used earlier as carbon sources such as P123 [13], F127 [14], and F108 [15], or citric acid addition [16]. Recently, more sustainable and low-cost carbon sources have also been explored: pectin (from apple peel) [17], banana peel [18]), and also glucose [19]. The Si-O-C bond can be formed after adding carbon materials into the matrix. The presence of carbon prevents silica pore from collapsing especially when applied for water desalination. Carbon material also has strong covalent bonding [20] which enhances the mechanical strength of the resulting matrix.

2.1. Soft and hard templating methods

The soft templating uses a nano-structure formed through inter-molecular interactions as a template [43]. They do not have permanent rigid structures. During the synthesis of nanoparticles, certain structural aggregates are formed through molecular or intra-molecular (hydrogen bonds, chemical bonds, and static electricity) interactions [38]. The soft template materials are typically organic surfactants and/or copolymer blocks that can interact with metal ions and merge into a liquid crystal phase through the sol-gel process. Pores are obtained after the removal of soft templates via calcination. The soft templating method allows easy control of the structure and pore size relative to the hard template method [43]. The crucial step in the soft templating is the transition of sol-gel precursors in the form of a surfactant/copolymer block [44–46].

The hard templating method is known as nano-casting, mostly

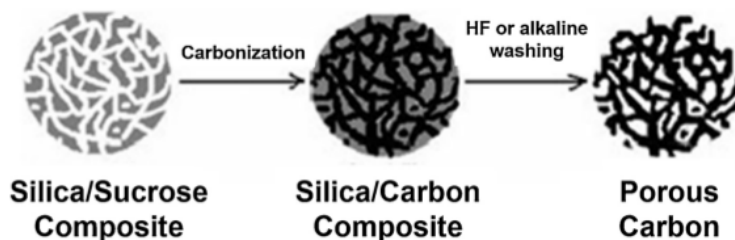


Fig. 1. Principles of porous carbon making [48].

attractive for synthesis of mesoporous materials. Nano-casting uses a solid mould as the template to which a material or precursor is filled. Later, after the formation of the porous material the main mould is removed [43]. For nano-casting of M-TMO, it consists of 3 steps: synthesis of mesoporous replica (eg: silica, carbon, alumina); a metal interphyracy of precursors and decomposition to form materials into crystals; and lastly, removal of the mould to obtain pores.

2.2. Synthesis of carbon templating

The porous carbon synthesis using a particular template necessitate the feasibility to remove the template without damaging the resulting structure [47]. For example, in a method illustrate in Fig. 1, silica and carbon sources are firstly mixed, then the mixture is heated to form solid composites. In the final phase, silica is removed by using the alkaline solvent (Fig. 1) [48].

Synthesis of porous carbon is also applicable to biomass-based carbon by applying a specific template into a carbohydrate-containing biomass [49]. Pang, Li [48] synthesized porous carbon form sucrose with the template of tetra ethyl ortho (TEOS) to form porous carbon (Fig. 2). It was done by applying hydrofluoric acid to leach the silica after carbonization step. The product was a carbon sheet that has pore diameter of 2 nm (Fig. 2). Porous carbon nanoparticles can also be made poly methyl meta acrylates (PMMA) by using silica as the pore-former [49]. The resulting nanoparticles have pore size of 300 nm (Fig. 3).

Liu, Gan [51] synthesized porous carbon from liquid paraffin by using silica as the regulator of carbon porcelain and surfactants to disperse paraffin in water. The synthesis process consisted of two main steps: formation of carbon/silica composite using paraffin carbonization method, followed by elimination of carbon silica by using hydrofluoric acid (HF) or potassium hydroxide (KOH). The illustration of the sythesis process and morphology of the resulting porous carbon are shown in Fig. 4.

Brun, Sakaushi [53] prepared porous carbon from monosaccharides (xylose and glucose) using hydrothermal methods backed by carbonization and silica derived from the synthesis of the Stober method using TEOS as a template. After the composite of carbon and silica was formed, the silica was removed using the ammonium hydrogen di-fluoride. The morphologies of the obtained porous carbon are shown in Fig. 5, which have pore size of 100 nm and 5–8 nm.

Liu, Yao [54] prepared microporous carbon particles from poly (furfuryl alcohol) through carbonization. In this sythesis method, furfuryl polymerization of alcohol was limited from stem-shaped by adding silica or slowed by using surfactants. The detail of preparation steps and the morphology of the resulting microporous carbon with pores of 260–320 nm are shown in Fig. 6.

Porous carbon synthesis can also be done through the hydrothermal method [54]. In this method, the common carbon sources used are hydrolysed hemicellulose, corn cob, and glucose and the template for pore formation is silica nanoparticles. The morphology of the resulting porous carbon can be seen in Fig. 7.

2.3. Mesoporous carbon through mesoporous silica templated

2.3.1. Carbon (C)

Synthesis of porous carbonaceous materials using silica template had been started since 1980s. The porous membranes were developed from a phenol-hexamine mixture as the carbon precursor and silica gel as the template. The carbon can easily be filled thanks to the spacious structure of silica gel [56]. Another templates, such as MgO, have been introduced [57–59]. MgO can be removed by using light acid, but the homogeneity of the resulting mesoporous is lower than the ones with the silica template. Silica template is highly recommended for synthesis of very organized mesoporous architecture coupled with an acid treatment for the template removal [60]. However, the procedure for the template can cause serious environmental problems from the use of the harmful etchants [61].

Template method is superior to control MCs pore structure. MCs with controlled pore structures can be formed by templating mesoporous silica such as Mobil Crystalline Material-48 (MCM-48). Typically, the synthesize of MCs steps involves infiltration of inorganic templates using carbon precursors, followed by template removal [62]. Although this method results in asymmetric membrane, it yields an ordered mesoporous carbon (OMC) [60], like the one obtained using MCM-48 as the hard template. OMC has symmetrical structure and narrow pore-size distribution. Common silica templates for mesoporous carbon fabrication are MCM, Santa Barbara Amorphous (SBA), Fudan University (FDU), MSU-H, and Hexagonal mesoporous silica (HMS) [60]. The pores size of mesoporous silica materials has been listed in Table 1.

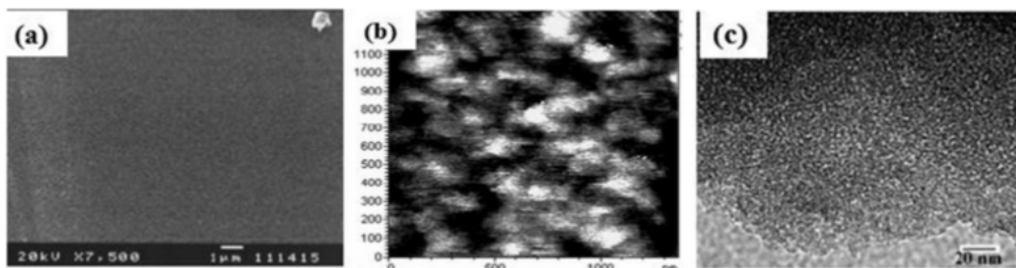


Fig. 2. Morphology of Film Carbon characterization results: (a) SEM appears above, (b) AFM, and (c) TEM [48].

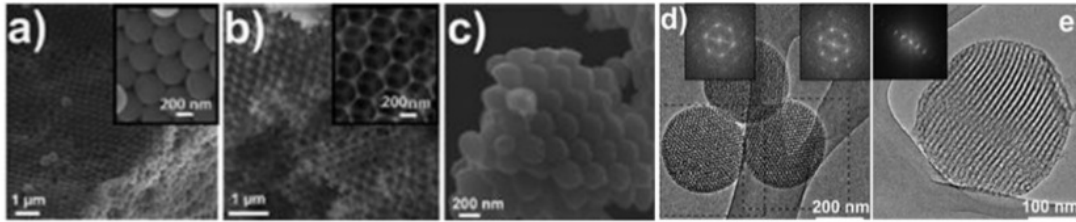


Fig. 3. Morphology of the materials during formation of porous carbon from PMMA as the carbon sources: (a) PMMA, (b) silica, (c) porous carbon products, (d, E) TEM of porous carbon products [50].

Carbon membranes have gained huge interests for desalination [68] and gas separation [69]. MCs based membrane has high pore volume and surface area, high resistance in rigorous circumstances, and is easy to regenerate. The pore size of a MC-based membrane is affected by the carbon precursors and the treatment method [62]. Carbon precursors such as thermosetting phenol resin (TPR), mesophase pitch (MP), and polyacrylonitrile (PAN) have been introduced for fabrication of MCs. MP is attractive to fabricate the porous material with excellent performances due to good graphitizability, high carbonization, and low organic content [62]. TPR offers higher surface area and pore volume of than MP and PAN. However, MP seems more stable during heat treatment [62]. The pores of MCs are formed by letting the small molecules of carbon precursors leach out during carbonization and by removal of the nanosized particles. The resulting pore properties are also affected by dispersion of the nanosized silica and the thermal stabilities.

2.3.2. Mobil crystalline material

Some researchers studied mesoporous silica structure as a template using MCM-48 [70], MCM-41 [71,72], MCM-50. The MCM-48 is very attractive as template for production of MCs because the precursor can form periodic pores arrangement with three-dimensional system. Homogeneous pores are contained in the MCM-48 molecular sieves [73]. MCM-41 is naturally hexagonal mesoporous silica with high surface, pore volume with the pores sizes ranging from 20 to 100 Å [74,75]. MCM-50 has pillared layer or lamellar pores. Among all, MCM-41 has gained the most interest because of its simple structure as shown in Fig. 8. In particular, the porous silica was created using sodium silicate or TEOS as the silicon source, and alkyl ammonium salts as the structure directing agent [74].

2.3.3. Santa Barbara Amorphous (SBA)

SBA-15 as a mesoporous material that has two-dimensional (2-D) hexagonal $p6mm$ symmetry and a channel-type or 3-D mesopore structure. It contains the micropores inside the pore walls [77]. The pore wall structure of SBA-15 is thicker than the MCM-41 [78,79]. SBA-15 can be prepared from TEOS or sodium silicate [80,81] or sodium silicate derived from oil palm ash [82]. It has controllable pore sizes of 5–30 nm range [77,78] with good thermal and hydrothermal stability due to thick pore walls (2–6 nm). SBA-15 may show variety of morphologies such as rods, fibres, spheres, gyroids, doughnut-like and discoid-like shape depending on fabricate conditions [77,83,84].

Various methods of SBA-15 fabrication have been reported, to name a few: grafting and impregnation, direct synthesis, sol-gel and immobilization. Synthetic grafting and impregnation are used to produce covalent attachment of functional groups between organo-silane with silanol groups on surface material [85]. Direct synthesis is a method where the metal source is added directly to the synthesis gel. This method results in SBA-15 of high specific area and pore volumes, but owing to low pH, it requires a high amount of the extra aluminium network [86]. Pore structure, size and shape of SBA-15 can be properly arranged when employing sol-gel synthesis method that works under modest temperature and results in high purity [87].

2.3.4. Fudan University (FDU)

The 3D pore structures of FDU-12 s are face-centred cubic structure with close packing of spherical cages, each is connected to 12 nearest neighboring cages [88]. It can be fabricated from non-ionic triblock copolymer F127 as a template, TEOS as silica precursor with 1,3,5-trimethylbenzene (TMB) and potassium chloride (KCl) as additives.

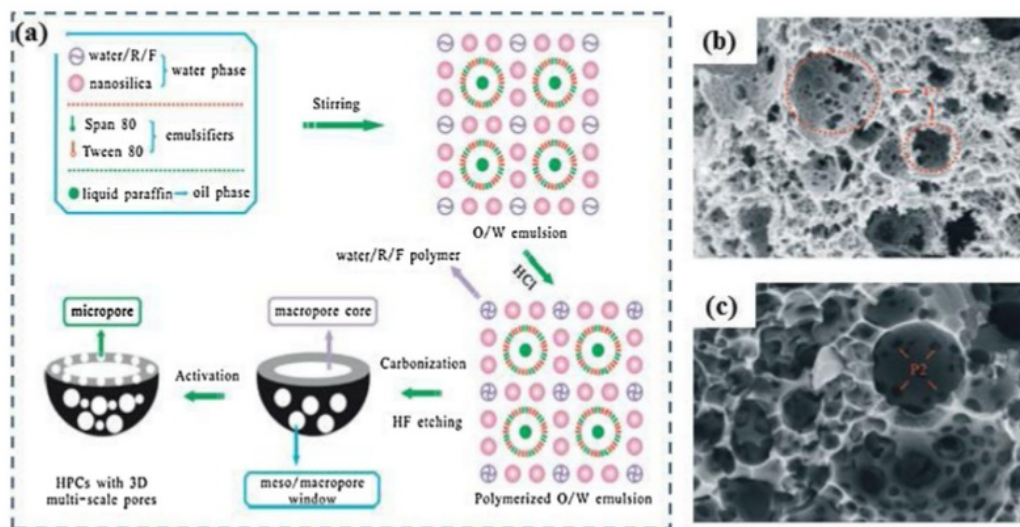


Fig. 4. (a) illustration of the porous carbon synthesis process, visualizing SEM from porous carbon with magnification: (b) Low and (c) high [52].

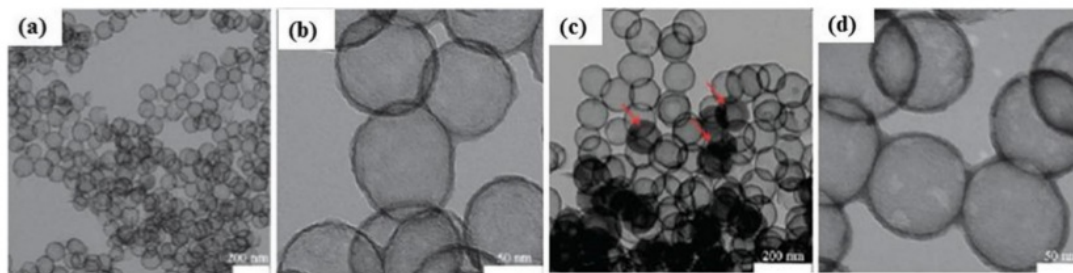


Fig. 5. TEM of carbon-based products: (A, B) Xylose and (c, D) glucose [52].

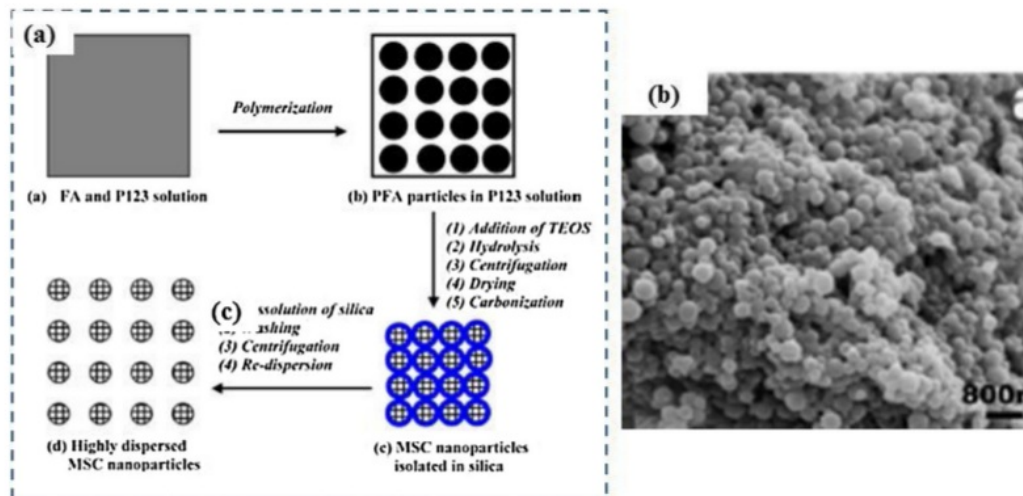


Fig. 6. (a) Illustration of porous carbon synthesis and (b) TEM of carbon [54].

TMB is used to enhance the volumetric ratio of the hydrophobic core and to turn it hydrophilic, which leads the structure changes from a body-centred cubic to a face-centred cubic [89]. Fabrication at low temperature (15 °C) results in highly ordered cubic of FDU-12 silica with pore diameters of 22–27 nm [89].

2.3.5. Mesoporous MSU-H

The porous framework of MSU-H is similar to that of SBA-15 that consists of ordered large pores connected by micropores [90]. These large two-dimensional pore channels allow easy penetration of carbon with better pore sizes adjustment compared to the SBA-15 or the MCM-

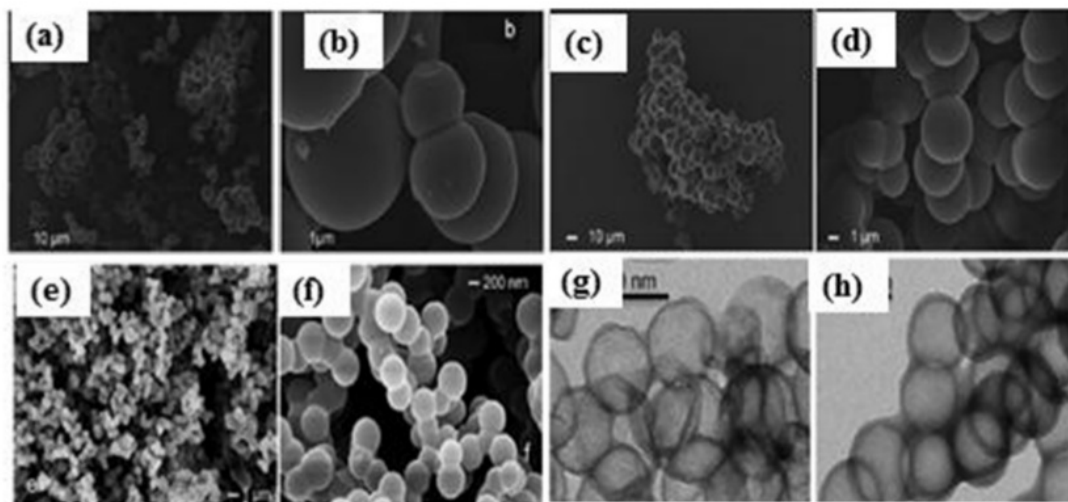


Fig. 7. Morphologies of porous carbon prepared from hydrothermal method: (A, b) hemicellulose hydrolysis, (c, D) Corn Cob, (e, F) glucose, and (g, h) TEM of carbon nanoparticle Products [55].

Table 1
List of pore size of mesoporous silica used as template for porous carbon membrane synthesis.

Material type	Pore size (nm)	References
MCM-48	2–5	[63,64]
MCM-41	1.5–8	[63,64]
MCM-50	2–5	[65]
SBA-15	6	[63]
FDU-12	5–36	[66]
MSU-H	3–10	[64]
HMS	2.9–4.1	[67]

41 [91]. MSU-H silica can be obtained from sodium silicate under neutral pH in the presence of triblock copolymer [92]. OMC membrane using sucrose as precursor and MSU-H as hard template was successfully fabricated Zeng, Zhao [91]. The resulting OMC has a large surface area of $1019 \text{ m}^2 \text{ g}^{-1}$, large volume ($1.46 \text{ cm}^3 \text{ g}^{-1}$) and uniform mesoporous structure (with pore size distribution with modus at 4.2 nm).

2.3.6. Hexagonal mesoporous silica

HMS is a mesoporous silica template with high surface area [93], prepared via soft templating from neutral long chain of *n*-dodecyl amine [94,95]. The long range hexagonal structure can be formed from a long chain template. There are few advantages of using HMS over MCM-48, namely inexpensive structure-directing agent (primary alkyl amines), high silica recovery yield (> 95 %, higher than the MCM-48 of ~ 50 %), fast synthesis (18 h for HMS and 4 days for MCM-48), does not involve hydrothermal reaction [96], thicker walls than SBA-15 [79], and the template is easy to remove. HMS has also been considered as a potential template for drug carriers thanks to its volume for drug molecule loadings [97].

2.4. Mesoporous silica through mesoporous carbon templated

Owing to excellent chemical, mechanical, thermal and molecular sieving properties [98–100], the mesoporous silica membranes have been favorably applied for gas and water desalination processes. The fabrications of such membranes involve several types of silica precursors such as TEOS as the most popular [101], tetramethoxysilane (TMOS), methyltrimethoxysilane (MTMS), and methyltriethoxysilane (MTES) [102].

In recent studies, ethyl orthosilicate-40 (ES-40) [103,104] was employed to fabricate this membrane. ES-40 contains about 40 wt% SiO_2 and an average of five Si atoms per molecule. It is produced by reacting ethanol, water and silicon tetrachloride or through partial hydrolysis and condensation processes of TEOS. However, unlike TEOS, ES40 has lower hydrolysis rate but higher condensation rate [105]. The produced silica is stable for up to 250 h of long term performance test [106]. However, the silica pores collapse easily because the hydrophilic silanol group (Si–OH) is reactive with water [107,108]. The hydro-stability can be enhanced by templating the carbon source into the

silica resulting in improved properties of high mechanical strength, good electrochemical performance, and good thermal and adsorption properties [109] [110].

2.4.1. Pluronic surfactant

Pluronic has been used as a template during formation of CPM to create ordered porous structure. The pluronic concentration and the initial temperature are important aspects of forming a micelle. After the micelle formation in acid solution, poly(ethylene oxide) (PEO) blocks in micelle can interact with the framework precursor (TEOS or TMOS) [111]. Because of the high acidity of the solution, the framework condenses and forms a silica network around the micelle as shown in Fig. 9. During the synthesis of mesoporous organo-silica (PMO), PMO is formed when nonionic surfactant consisting of PEO is added. It results in formation of Si-C bonds through condensation of templated carbon surfactant, such as $(\text{RO})_3\text{-Si-R}^*\text{-Si}(\text{OR})_3$. Then, hydrolysis and cross-link occur between the terminal groups of the bridged bis(trialoxysilyl) organo-silanes [112,113].

SBA-16 can be prepared by employing Pluronic F127 to form high quality mesostructured [114]. Some studies report smaller pore sizes of SBA-16 from copolymer blends of P123 and F127 [115] or nonionic oligomeric surfactants [116]. F127 has critical micelle temperature of 31°C at 0.1 % w/v. At higher concentration of 0.25 % w/v, the CMT is diminished at the 28°C [111].

When Pluronic-123 (P123) as a carbon source is incorporated into silica structures, it produces more robust structures demonstrated by high performance of membrane filtration when using the silica-P123 than the pure-silica [103]. It was also found that at low P123 concentrations, the carbonized templates uniformly attached onto the silica matrix forming more microporous network. Higher concentrations of P123 lead to higher hydro-stability.

2.4.2. Natural carbon sources material

To address the challenge of providing renewable resources at low cost, it is very important to utilize non-food related materials as the carbon sources. Several studies report the use of pectin extracted from apple [118] and banana peel [119] as the carbon sources to fabricate carbon templated silica. The pectin in the silica matrix prevents the silica networks from collapsing toward water. The polysaccharides from pectin allow formation mesoporous structure. Sucrose has also been used as the carbon precursor through hard-template method for formation of MCM [120]. Sucrose is environmentally benign material that contains multiple adjacent hydroxyl groups that form hydrogen bonding with silica oligomers. However, there are only a few reports of sucrose incorporated into silica via the soft template.

3. Mesoporous silica materials

3.1. Recent techniques, fabrication and application

3.1.1. In-situ synthesis

In the modified in-situ synthesis, cetyltrimethylammonium (CTAB)

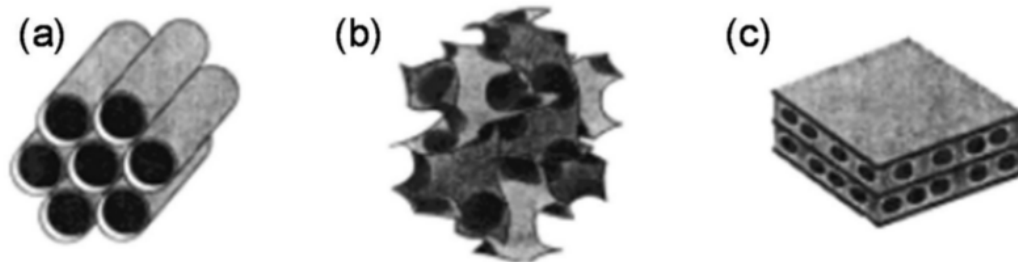


Fig. 8. Visualization of pore structures in MCM-41, MCM-48 and MCM-50 [76].

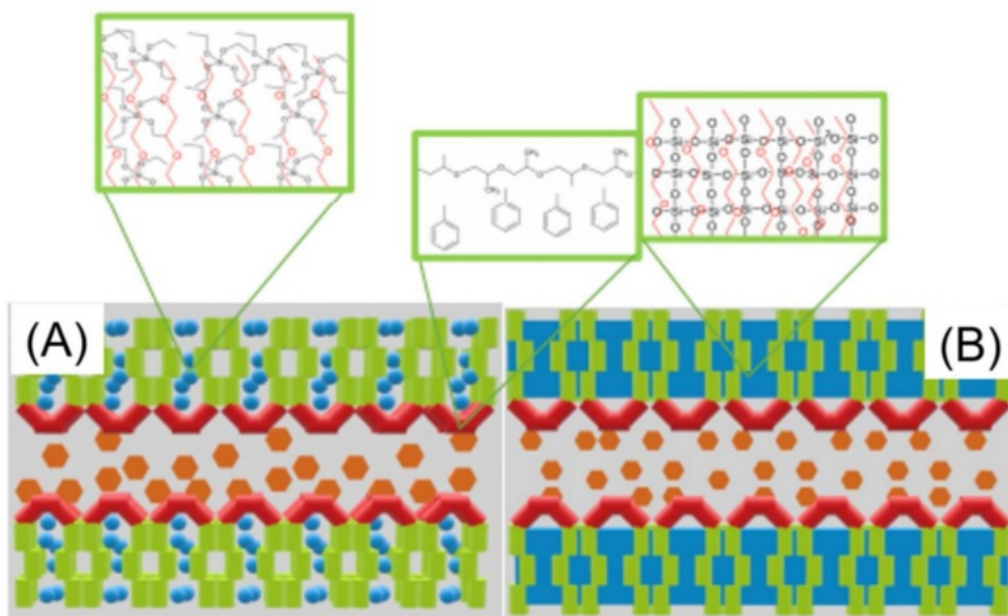


Fig. 9. Illustration of micelles formation with Pluronic-silica precursor and swelling agent before (A) after condensation (B) [117].

and urea were firstly dissolved in water. Next, cyclohexane, MI IPA, TEOS of 2.5 mL 3% mol (2-cyanoethyl)triethoxysilane (CETEOS) were added drop-wise [121]. After stirring for 30 min at room temperature, it was heated to 70 °C and was allowed to react for 16 h. The results obtained were silica fibrous particles or SiO₂-CN₃. By adopting the same method and by employing pure TEOS, it resulted in formation of Fi-SiO₂ [122].

Although in-situ synthesis produces mesoporous sizes of 10–20 nm on Fi-SiO₂, SiO₂-CN₃ or SiO₂-CN400, addition of N₂ during the N₂ adsorption-desorption analysis increases the absorption and hysteresis H₃ at P/P* > 0.95. It suggests that there are a number of macropore gaps related to the SiO₂ microspheres fibrous morphology [123,124], higher than the F-SiO₂ (of 55 nm). Both 1-SiO₂-CN₃ and F-SiO₂ microspheres have relatively high specific surface area and total pore volume of microspheres [125,126]. The specific surface area (m² g⁻¹) sizes of 399.2 for F-SiO₂, 252 for SiO₂-CN₃ and 298 for SiO₂-CN400 and the total pore volumes (cm³ g⁻¹) for F-SiO₂, SiO₂-CN₃, SiO₂-CN400 are 1.14, 0.99 and 0.89, respectively. Based on available data it shows that the in-situ method may produce mesoporous silica.

3.1.2. The spinning coating

Thin film synthesis using the spinning coating process has also been reported [127]. The fabrication starts from a mixture of NaOH, cetyltrimethylammonium chloride, CTAC, water and methanol mixture, tetramethylorth-silicate, mixture of MOS and aminopropyltrimethoxysilane and APT-MS to form a sol. The formed sol is stirred for 12 h at room temperature and is let idle for 8 h. To prepare a thin film via the spinning coating processes, a template of mesopore-free silica particles is dispersed in ethanol by ultrasonication at 2.5–10 % w/w. The dispersion is then coated on a substrate and spun at 500–2000 rpm for 40 s as detailed elsewhere [128].

The BET characterization shows that the resulting particles have diameter of 2.6 nm and surface area 499–942 m² g⁻¹, suggesting that they are mesoporous in structure. SEM images reveals that there are still some structural defects with variation in the thicknesses due to the presence of agglomerates either in the original dispersion or formed during spinning. In order to study the generality of the used spinning coating process, corresponding films were also prepared using amino-

functionalized mesoporous silica nanoparticles under otherwise identical conditions. The surface chemical properties of the nanoparticles are found to be important affecting the interactions of the nanoparticles and the biological environment [129].

3.1.3. The electrospinning coating

Mesoporous silica can also be prepared through the electrospinning coating process as reported elsewhere [130]. The base materials are TEOS mixture with H₃PO₄ that drop-wise added during stirring/mixing. Then a 10 % PVA solution is added into the silica sol as additive to ease the spinning. Next, an alumina sol with a molar composition of Al(NO₃)₃·9H₂O:AlCl₃·6H₂O:Al(O-i-Pr)₃:Al:H₂O of 1:1:2:4:178 is prepared through hydrolysis and condensation reactions under constant stirring at 80 °C. An appropriate amount of HNO₃ is then added to the mixture to adjust the reaction rate and control the pH of the final sol from 3.24 to 4.23. Then, 0.1 g of PEO and 6.0 g of P123 are added into 40 mL of as-prepared alumina to improve the spinnability of the sol and to direct the pore structure formation, respectively. The mixture is then stirred for 12 h to form a spinnable sol. To fabricate SiO₂/Al₂O₃ core-shell fibrous membrane, the sol silica and sol alumina are put into A separated syringes. The one for sol silica is connected to a core needle (d = 0.4 mm), while the one for alumina sol is connected to a shell needle with an inner diameter of 1 mm. The flows in the needle are set alike at 2 mL/h. The distance between the spinneret and the aluminium collector is 17 cm and the voltage of 18 kV. The spinning is conducted under ambient condition. The electrospun xerogel core-shell fibrous membranes are collected on the aluminium foil and are further dried at 90 °C for 12 h, and then are calcined at 700, 800 or 900 °C for 2 h at a heating rate of 10 °C min⁻¹ [131].

The BET analysis reveals that higher calcination temperature leads to lower specific surface areas [132], with the values of 134, 104 and 79 m²/g at 700, 800 and 900 °C, respectively. The pH of the precursor also affects the pore volumes in which the pHs of 3.24, 3.53 and 4.23 correspond to the pore volumes are 0.387, 0.589 and 0.655 cm³ g⁻¹, respectively. Considering that the high surface area corresponds to a large adsorption capacity, the reports [133] select the precursor pH of 4.23 as the most promising condition to fabricate the shell in the coaxial electrospinning process.

3.1.4. Extraction from pumice stone

Mesoporous silica can be fabricated from pumice via extraction. The resulting mesoporous silica has a high purity and shows the presence of siloxane and silanol groups. However, the extraction process takes so many steps and over a very long period. The fabrication process starts with dissolving a pumice in 3 M NaOH solutions in a three necks flask equipped with a condenser for 24 h at 100 °C and a stirring speed of 300 rpm to produce sodium silica. The obtained sodium silica is then washed and heated with distilled water. Silica settles at pH below 10, which is required to form silica gel under acidic condition. Furthermore, the solution is titrated with H₂SO₄ (5 M) until reaching pH 7, then is let idle for 24 h to allow formation of a white precipitate. The precipitate is then filtered, and the solid residue is dried at 80 °C for 24 h. The residue is then refluxed with 1 M HCl at 110 °C for 3 h to purify silica from other soluble minerals (Al, Ca, Fe and Mg). The refluxed solution is then filtered and dried at 110 °C. The last step is calcination at 800 °C to produce a white silica powder [134].

The resulting pumice powder composes of mostly silica (confirmed from FTIR and chemical analysis) main minerals content of clinopyroxene (diopside, augite or basanite types), forsterite and other (apatite and haematite) in minor quantities [135–138]. The pure silica structure is amorphous as demonstrated by strong peak at 2θ of 15–30°. FTIR peaks analysis show the narrow band centred at wavelength 1039 cm⁻¹ may be attributed to the presence of silica with the highest percentage [139], as also confirmed by chemical analysis. The predominant bands at wavelength 1101 cm⁻¹ and the shoulder at 1193 cm⁻¹ are associated with asymmetric stretching-vibrations of siloxane (Si-O-Si). The presence of bands at 470 cm⁻¹ and 810 cm⁻¹ is from symmetric siloxane groups (Si-O-Si). The existence of a band at 950 cm⁻¹ is associated with Si-OH groups from silanol groups with smaller particle sizes [140]. The shoulder appeared at 3750 cm⁻¹ indicates the presence of hydrogen bonds from interaction between the silanol groups (Si-OH) located at the surface of the nanosilica material [141]. BET results show that the pore size of the silica is in range of 2–6 nm indicating of the mesoporous structure, with a pore volume of 0.645 that exceeds the size of the nanoparticles of 0.195 cm³ g⁻¹ with the surface area of 422 m² g⁻¹.

3.2. Recent trends on the ordered and the disordered mesoporous silica materials

Summary of structure and pore size distribution of silica-carbon base materials is presented in Table 2. It summarizes the main properties of recently developed ordered and disordered mesoporous silica materials discussed in this sub-section.

3.2.1. TEOS : EtOH : C₆H₁₂O₆ : H₂O

Ordered mesoporous silica materials is a promising material in the field of technology membrane filtration. Synthesis of order mesoporous silica have recently been developed by directly assembly of organic or carbon template [149]. Elma et al. reported development of direct acid catalyst for preparation of mesoporous carbon template silica membranes with ordered structure on porous a α-alumina support. The

ordered mesoporous silica membranes made from organocatalytic posed relatively high surface area and pore volume of 354 m² g⁻¹ and 0.215 cm³ g⁻¹, respectively. The citric acid catalyst acts as a carbon source in the silica matrix and increases the hydro-stability of silica networks. Absorption of the N₂ curve shows xerogels refluxed at 0 and 50 °C are included in type IV H4 [142]. While Elma et al. work found surface area and pore size of 475 m² g⁻¹ and 1.94 cm³ g⁻¹ [143].

3.2.2. TEOS : EtOH : HNO₃ : H₂O : NH₃

Modified the sol-gel process is needed to reduce the amount of silanol group. Reflux temperature can be adjusted to get optimum condition for ordered mesoporous silica. The ordered mesoporous silica materials were also preserved during reflux temperature on sol-gel process. The sol-gel was refluxed at 0 and 50 °C to achieve the lowest and the highest silanol concentrations with calcined xerogel at a pH of 6 or 9. Xerogel at pH 6 and 9 shows a tendency to form micro and mesoporous materials as adsorption saturation is achieved above 0.65 P/P⁰ with capillary condensation leads to hysteresis near 0.5 P/P⁰. The average pore diameter each was measured around 2.6–2.7 nm and showed type IV isotherm curves with hysteresis loops indicating the mesopore structures. In other hand, silica-based materials of pH 7 and 8 had type I isotherms curves without hysteresis indicating of microporous material. The BET surface area (~ 420 m² g⁻¹) and total pore volume (~ 0.18 cm³ g⁻¹) were proportional to the pore size of about 1.8 nm. Therefore, micro-porosity was correlated well with high concentrations of silanol groups [143]. While silica sol mixed with various variations of cobalt oxide (5 %–35 % w/v) obtained at pH 6 and produced mesoporous membrane. The BET results show that the isotherms of the two samples were type IV, ascribing the characteristics of the mesoporous material. The greater addition of Si-Co concentration, the larger was the surface area, volume and pore size. This was because the cobalt oxide in xerogel increased the silanol and siloxane groups to enlarge the pores [150].

3.2.3. TEOS : TEVS : EtOH : HNO₃ : H₂O : NH₃ : P123

Triethoxyvinylsilane (TEVS) is frequently used to produce microporous silica membranes on interlayer porous substrates [146]. It contains vinyl groups as silica ligand pendants. The silica methyl ligand pendant group is known to produce high-quality microporous silica membranes. In order to form mesoporous structures, TEVS and other silica precursors are combined using TEOS with the addition of P123 non-ligand triblock copolymer as a template. Then the sol-gel synthesis is carried out with a base catalyst which allows its deposition directly to the porous substrate without using interlayers. The non-ligand surfactant is embedded into the silica matrix followed by carbonization. High-quality carbon can be prepared using ligand and non-ligand templates together with the co-polymerization reaction of two different silica precursors where TEOS does not have a template while TEVS has a ligand template based on the vinyl group. Then the xerogel and silica membrane are calcined under vacuum or N₂ atmosphere. Carbon silica hybrid membranes are represented as CS-N₂ (calcined under N₂) and CS-Vc (calcined under vacuum air) calcined at 450 °C. The isotherms of the order P123 template TEOS-TEVS is type IV of the mesoporous

Table 2
Summary of silica-carbon base material structure and pore size distribution.

Material type	Calcine technique/ temp. (°C)	BET surface area (m ² g ⁻¹)	Pore volume cm ³ g ⁻¹	Pore size (nm)	Ref
Organosilica	RTP (inert atm)/200	315	0.16	2.5	[142]
Pure silica	CTP (vacuum)/600	420	0.18	1.8	[143]
Silica P123	RTP (inert atm)/350	572	0.31	2.2	[144]
Silica P123	CTP (vacuum).450	965	0.50	2.3	[145]
TEVS	CTP (vacuum)/350	761	0.55	< 2	[146]
CTAB	CTP/550	925.1	0.20	3.1	[147]
Ni-Si	CTP	450	-	2.5	[148]

material. The interlayer-free carbon-silica hybrid membranes were successfully prepared by adding template of pluronic triblock copolymer (P123) and vinyl pendant ligands in TEVS in synthesis sol-gel also contain TEOS as the second silica precursor. Both the vacuum calcined and the N_2 samples exhibit mesoporous properties with high pore volume, but the calcined vacuum samples (CS-Vc) produces more carbon structure in the silica matrix resulting in better desalination performance. Surface area and pore volume of CS- N_2 membrane are $754 \text{ m}^2 \text{ g}^{-1}$ and $0.546 \text{ cm}^3 \text{ g}^{-1}$ while CS-Vc membrane are $761 \text{ m}^2 \text{ g}^{-1}$ and $0.615 \text{ cm}^3 \text{ g}^{-1}$. The CS-Vc membrane produces water flux much higher than previously reported for processing saltwater. The combine method of organo-silica hybrid with polymer template and vacuum calcination produces mesoporous silica membrane carbonization very well for the separation of water from hydrated salt ions, and exhibits high water flux especially for processing brine salt solutions [148].

3.2.4. TEOS : TEVS : EtOH : HNO_3 : H_2O : NH_3 : $K_2S_2O_8$

Hybrid silica membranes can be prepared by mixing TEOS and TEVS using $K_2S_2O_8$ (KPS) as an initiator Elma, Wang [146]. The KPS provides radical polymerization to create C–C bonds as a secondary network and then to produce more space in the silica network. The radical polymerization formed by KPS affects the growth of oriented particles. In order to avoid decomposition of C–C groups in the silica matrices, the calcination process is held up to 350°C . Densification is then formed when the ratio of TEVS is greater than TEOS composition. The TEVS: TEOS molar ratio is 10:90 and produces micro-porosity. Pure TEVS is not suitable to produce amorphous silica material, because the functional groups formed were found blocked inside the pores. As such, the xerogel hybrids containing TEVS become microporous. The isotherms found the saturation process at very low relative pressures ($p/p^* < 0.05$). It is due to the mixing between TEVS and TEOS is greatly reduced and this trend continues as a function of TEVS [146].

3.2.5. TEOS : EtOH : NH_3 : H_2O : CTAB (cetyltrimethylammonium bromide)

Mesoporous silica carbon template materials have been explored and developed very fast to competes in desalination application. Carbon template is one of effective strategy to stabilized the silanol group of silica membrane. Recently, Ashrafi-Shahria, Ravaria [147] used CTAB surfactants as template to embedded into silica. Silica precursors were synthesized at 550°C to remove cationic templates from CTAB required to form the mesoporous structures. Order mesoporous silica (MS) nanoparticles were synthesized and then functioned by Eriochrome Black T (ECBT) as a corrosion inhibitor. Composite coating systems (a combination between Ti-Zr conversion layers and organic/inorganic hybrid sol-gel) were applied instead of simple sol-gel films to provide better corrosion protection and adhesive strength. Nitrogen adsorption-desorption isotherms were plotted with BJH plots from MS nanoparticles before and after loading of the inhibitors. The N_2 physisorption data showed that the surface area and pore volume of MS were $925.1 \text{ m}^2 \text{ g}^{-1}$ and $0.2025 \text{ cm}^3 \text{ g}^{-1}$, while the surface area and pore volume of MS-ECBT were $103.1 \text{ m}^2 \text{ g}^{-1}$ and $0.0561 \text{ cm}^3 \text{ g}^{-1}$. It is clear that the specific surface area of MS nanoparticles is greatly decreased by the final functionalization process due to the addition of ECBT molecules in the mesoporous space. In addition, the pore volume of MS nanoparticles is greatly decreased by loading of inhibitors. However, the pore diameter of MS nanoparticles did not change significantly after the loading inhibitor because the structure of nanoparticles could not be affected by the functionalization process [147]. This is also similar to that study explained by Vazquez, Gonzalez [151], in which surfactants play an important effect in changing the morphology of particles, but it cannot change pore size and pore diameter.

3.2.6. TEOS : EtOH : $Ni(NO_3)_2 \cdot 6H_2O$: H_2O_2 : H_2O

The ordered of nickel oxide sol are synthesized by hydrolysis and condensation of TEOS in ethanol with and without 30 % H_2O_2 water

and nickel nitrate hexahydrate ($Ni(NO_3)_2 \cdot 6H_2O$). The tendency of the silanol/siloxane ratio clearly showed that the role of H_2O_2 was favoured by the formation of silanol groups and slightly inhibited the condensation reaction. The presence of H_2O_2 acidified the the sol-gel process by the presence of nitric acid which promoted the formation of silanol groups and microporous materials.

Nitrogen adsorption isotherm of ordered xerogel doped with nickel by addition of H_2O_2 produced a type I isotherm curves ascribed by very strong initial adsorption at very low partial pressures ($P/P^* < 0.2$) followed by saturation ascribing the characteristic of type I micropores. Whereas nickel doped xerogels without H_2O_2 formed mesopores with higher adsorption saturation capacities above $0.4 P/P^*$ and hysteresis with subtle inflection indicating the type IV isotherms. Surface area for ordered mesoporous nickel oxide with 10 % H_2O_2 was affected by the Ni/Si molar ratio. The average pore diameter with H_2O_2 remained constant at $2.1 \pm 0.05 \text{ nm}$. Addition of nickel oxide to silica gel matrix with H_2O_2 could maintain the micro-porosity of amorphous silica xerogel. Whereas samples without H_2O_2 produced meso-porosity that increased significantly as a function of Ni content as the average pore size increased while the BET surface area decreased for a Ni/Si ratio of 25–50%. This effect had also been observed for cobalt silica oxide, and increased meso-porosity is associated with cobalt oxide agglomeration. Perhaps, the same effect also occurs on increasing the shaft as a function of the Ni/Si molar ratio in this work [52].

4. The application of carbon templated mesoporous silica materials

Carbon templated mesoporous silica membranes are excellent material for pervaporation, a process to separate liquid mixtures by vaporization and selective permeation and through a membrane [152]. It uses molecular sieve type of membranes that permits only passage to water molecules under driving force of a water vapor pressure difference [10]. Highly permeable and selective membranes can be prepared via sol-gel method that offers great advantages in the control of pore sizes [10,143,152,153]. Recent advances in the preparation of carbon template mesoporous silica membranes have opened avenue to substantially improve pervaporation performance with respect to flux, selectivity and stability. Conscientious adjusting of carbon-silica template mesoporous structures makes it possible to design membranes as coveted of respective separation applications.

Carbon template silica membranes have also widely been applied for gas separation, particularly the ones with microporous structures [154–157]. Microporous molecular sieve carbon-silica base membranes can also offer the considerable advantages in comparison to the zeolite, the polymeric or the carbon-based membranes [157]. Whereas, membrane materials with mesoporous structure are more appropriate for water desalination [143,158,159]. The carbon templated molecular sieve mesoporous silica materials are gaining popularity for desalination, which is detailed in the following section.

4.1. Hydro-stability of silica-carbon templated and current strategies for water desalination

Desalination via pervaporation is promising to produce fresh water from non-potable saline sources. It offers advantages of a high salt rejection and the capability of treating a high salinity solution. Novel mesoporous silica base membranes for desalination have recently been developed. Because of the affinity of amorphous silica for water adsorption, pure silica-derived membranes suffer from structural degradation when in contact with water, leading to a loss of selectivity. Hydro-stability is therefore a severe problem which prompts the recent studies on altering the surface properties of the silica to lessen the interaction of water molecules with the membrane structure.

One strategy to address hydro-stability problems is by introducing a non-covalently bonded organic templates into the pure silica matrix

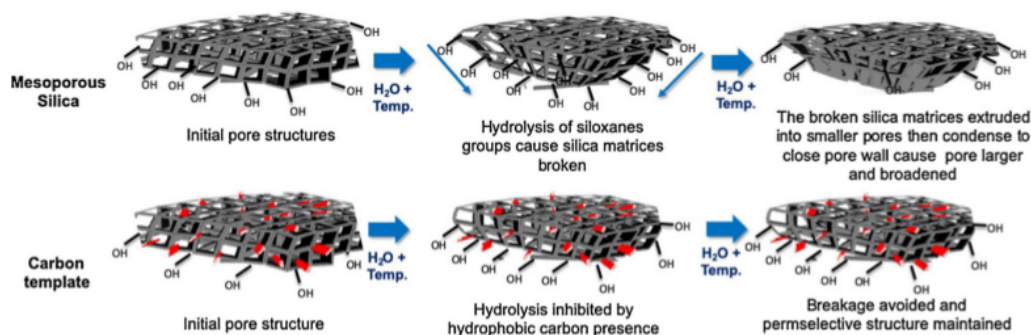


Fig. 10. Schematic of mechanism for stabilization of the carbon template silica pore structure.

[12,157,160]. The existence of carbon moieties embedded into the silica framework can inhibit the mobility of soluble silica groups under hydrolytic attack and consequently hinders micropore from collapsing [10,154]. The carbon templates and silanol groups (Si-OHs) interact weakly via the electrostatic interaction to form a peculiar structure derived from a hydrophobic core and hydrophilic exterior properties [161]. The carbon templates obstruct the micropore spaces to forbid the mobility and degradation of the silanol groups.

For the first time, Raman and Brinker [160] demonstrated a breakthrough organic templating approach to fabricate the molecular sieving organo-silica membranes. It results in high flux and selectivity membrane for gas separation. The hydrophobic carbon template improves the hydrothermal stability of the silica membranes. In similar research done by Duke, da Costa [154] report carbonized template molecular sieve silica (CTMSS) as new material for wet gas separation. The C6 surfactant hexyl trimethyl ammonium bromide is embedded into CTMSS as carbon template to achieve a great hydro-stability via hydrophobic surface functionalization. The mechanism of carbon templates in imposing hydro-stabilization toward exposure to water is illustrated in Fig. 10.

Both mesoporous silica and template carbon materials alter the surface chemistry to limit water in breaking the siloxane groups (hydrolysis) and allowing for dissociative chemisorption, as detailed elsewhere [162]. Normally, the rehydration on the silica surface is done by a physisorption of water to form a hydroxyl group, followed by a chemisorption with the nearby siloxane groups. As more silanol groups are formed, more sites become available for H₂O sorption and a chain reaction of siloxane breakage occurs across the surface. The mobility of silica groups then becomes localized in the higher-attraction-energy regions in the smaller pores, where thermal condition above 180 °C causes a subsequent cross-pore condensation leading to their closure.

Fig. 10 demonstrates how the carbon moieties templated into silica matrices prevent the mobility of silica groups under hydrolytic attack and inhibits micropore cave in. The entrapment of carbon moieties in the carbon template silica matrix is facilitated by carbonization of the templates under vacuum or an inert atmosphere, leading to a hybrid silica/carbon membrane. Carbon template membranes thus offers a great potential for achieving hydro-stability without compromising the selectivity [162]. The carbon-silica template membranes have also been tested for desalination of saline water (NaCl 3.5 wt%), demonstrating high salt rejection [163].

Carbon templated mesoporous silica materials have a pore size of 0.3–10 nm and thus are very suitable for desalination applications [145,158,163–165]. Wijaya, Duke [166] reported the investigation of carbon chain length of ionic surfactants effect toward CTMSS membranes for desalination by preparing sol-gels with C6, C12 and C16. The CTMSS membrane fabricated with the longest carbon chain C16 surfactant delivered the highest salt rejection, whilst also given the largest pore volume and surface area. Interestingly, the average pore sizes of

the membranes were identical for the three surfactants used.

Ladewig, Tan [165] investigated the potential of a polyethylene glycol-polypropylene glycol-polyethylene glycol (PEG-PPG-PEG) as the template non-ionic surfactant. The enhanced carbon content up to 10% increased the pore volume and the specific surface area. Consequently, the membrane demonstrated a slightly higher flux of $3.7 \text{ kg}\cdot\text{m}^{-2}\cdot\text{h}^{-1}$ and 985% of salt rejection at room temperature compared to the surfactant template membranes mentioned above, that is 2.2 and 3 $\text{kg}\cdot\text{m}^{-2}\cdot\text{h}^{-1}$, respectively. The embedded carbon has a beneficial role in silica matrices and the amount embedded has a direct impact to performance of the carbon-silica template.

4.1.1. Effect of operation condition on performance of carbon template silica membranes

Table 3 summarizes the reports on carbon template silica performance in terms of water flux and salt rejection. Performance of membrane in pervaporation is affected by the testing conditions such as feed temperature, feed salt concentration and permeate vapor pressure. To achieve optimum performance, it is necessary to study the effect of testing parameters on water flux and salt rejection. A change of feed concentration directly affects sorption at the liquid/membrane interface [161]. Since diffusion in the membrane is concentration dependent, the water flux generally decreases with increasing salt concentration in the feed [10,145]. Mass transfer in the liquid feed side may be limited by the extent of concentration polarization. In general, when the feed flow rate increases, water flux also increases due to a reduction of transport resistance in the liquid boundary layer and reduction of the concentration polarization.

The feed temperature exponentially increases the water flux. It is because when feed temperature increases, the vapor pressure on the feed side increases exponentially, while the vapor pressure on the permeate side remains constant. The raising of vapor pressure leads to an increase in the driving force of the water vapor transport, thus improving the water flux. The diffusion coefficient of water vapor increases by four times as the feed temperature is raised from 20 to 65 °C [153]. Moreover, high temperature increases the frequency and amplitude of thermal motions of the polymer chains, which can bring about the free channels of polymer promoting the water vapor transport. The carbon templated silica membranes have been widely reported and developed for water desalination application [17,19,99,109,144–146,159,163,164,166–170].

Pervaporation using inorganic membranes based on mesoporous silica offers high salt rejection, but rather low in water fluxes especially for saline solution (NaCl 3.5 wt%). These low performances diminish the chance of the pervaporation using inorganic membranes to compete against the reverse osmosis (RO) processes. It is, however, worth noting that the results are dependent upon many parameters related to testing condition, including the feed concentration, the feed temperature, the permeate vapor pressure and the fouling/scaling tendencies. In

Table 3
The summary of carbon template silica performance in terms of water flux and salt rejection in pervaporation for desalination.

Membrane types	Condition testing (calcination technique/ ΔP)	NaCl conc. (wt.%)	Water Flux ($\text{kg} \cdot \text{m}^{-2} \cdot \text{h}^{-1}$)	Salt Rejection (%)	Ref.
Silica-pectin	RTP inert atmosphere/1 atm/25 °C	3.5	0.22–5.7	> 99	[107]
	CTP vacuum/7 bar/25 °C	0.3	3.2	86	[163]
CTMSS C6	CTP vacuum/7 bar/25 °C	3.5	1.4	92	[163]
		0.3	2.8	86	
		3.5	1.6	94	
CTMSS C12	CTP vacuum/7 bar/25 °C	0.3	2.8	86	[163]
		3.5	1.6	94	
CTMSS C16	CTP vacuum/7 bar/25 °C	0.3	2.1	> 98	[163]
		3.5	1.9	> 98	
P123 Carbonized template silica	CTP vacuum/1 atm/22–60 °C	0.3	6–8.4	> 98	[145]
		3.5	2.4–7.8	> 98	
		7.5	1.8–6.6	> 98	
CTMSS C6	CTP vacuum/1 atm/22 °C	0.3	3.2	92	[166]
		3.5	2.2	97	
Glucose carbonized template silica	RTP inert atmosphere/1 atm/25–60 °C	7.5	0.4–2.3	> 92	[19]
	P123/TEVS/TEOS	CTP vacuum/1 atm/25–60 °C	0.3	10–27	> 98
Interlayer-free silica-pectin	RTP inert atmosphere/1 atm/25–60 °C	3.5	9–17	> 98	[17]
		7.5	8–16	> 98	
		3.5	5.9–8.9	> 99	

addition, the listed membranes on Table 3 may have different geometries (flat, hollow fibre or tubular and sizes) and architecture (thickness of top layer, number interlayers or top layer, porosity and substrate) as such, all these factors play a role in the final performances.

Duke, O'Brien-Abraham [171] reported that a MTES membrane with pore diameter of 0.5 nm exhibits a higher water flux than carbonized template molecular sieve silica (CTMSS) membrane with pore diameters of 0.3 nm but with lower salt rejection. The comparison of three kinds of inorganic membranes: alumina, MTES and CTMSS for desalination by pervaporation have also been reported. Among them, CTMSS displayed the best performance with a flux of $2.2 \text{ kg} \cdot \text{m}^{-2} \cdot \text{h}^{-1}$, a rejection > 99.9 % and long-term testing at 25 °C was stable for 5 h. The findings suggest that the incorporation of carbon in a silica matrix plays a role in increasing salt rejection as well as matrix stabilization.

Wijaya, Duke [166] reported a CTS membrane derived from long carbon chain surfactant (C16) showed high salt rejection of up to 97 % with a flux of $3 \text{ kg} \cdot \text{m}^{-2} \cdot \text{h}^{-1}$. Carbon chain length of surfactants templates is a crucial factor that give direct impact in terms of desalination performance. The amount of embedded carbon has a beneficial role in silica matrices and is directly related to the number of residual carbons after the carbonization. However, if the surfactants concentration is too high, it forms micelles which block the possibility of using the sol-gel to coat the substrates.

Ladewig, Tan [165] to use the tri-block copolymer (polyethylene glycol)-(polypropylene glycol)-(polyethylene glycol) (PEG-PPG-PEG) as the template. The surfactant templates tend to form micelles at high concentrations and precipitate if in excess of 3 wt.% in the silica sol-gel. When the carbon content increased to 10 %, there was a rise in porosity despite still remained microporous. Consequently, the membrane demonstrated a slightly higher flux of $3.7 \text{ kg} \cdot \text{m}^{-2} \cdot \text{h}^{-1}$ and 985% of salt rejection for system operating at room temperature. Further increases of the tri-block copolymer to 20 wt.% altered the structure becomes mesopores. The performance is slightly higher than the surfactant template membranes (2.2 and $3 \text{ kg} \cdot \text{m}^{-2} \cdot \text{h}^{-1}$) mentioned earlier.

Mesopore CTAB silica membranes exhibited an excellent salt rejection > 99 % and water flux $2.6 \text{ kg} \cdot \text{m}^{-2} \cdot \text{h}^{-1}$ in seawater desalination at 25 °C. However, when it is exposed to high feed temperature (> 40 °C), the barrier layer of the mesostructured formed by a weak electrostatic interaction between CTAB and silica may suffer a disturbance, leading to a release of NaCl molecules to the permeate side and thus drastically decreases the salt rejection. This effect of temperature was reversible. The rejection came back to normal when reversed to lower feed temperature [172].

Recently, P123 carbon template silica prepared by the CTP technique by Elma, Wang [13] were successfully fabricated using the dual catalyst sol-gel method. Embedded P123 loading from 0–50 wt.% into

silica sol exhibited salt rejection of 99 %. The water fluxes varied depending on the loading of P123 in the silica sol, the feed temperature and the salt concentration in the feed. The water flux of the Silica-P123 membranes varied between 0.5 – $4.5 \text{ kg} \cdot \text{m}^{-2} \cdot \text{h}^{-1}$ (P123 5 wt. %), 0.9 – $5.5 \text{ kg} \cdot \text{m}^{-2} \cdot \text{h}^{-1}$ (P123 20 wt. %), 1.4 – $6.3 \text{ kg} \cdot \text{m}^{-2} \cdot \text{h}^{-1}$ (P123 35 wt. %), and 1.5 – $8.5 \text{ kg} \cdot \text{m}^{-2} \cdot \text{h}^{-1}$ (P123 50 wt.%). The major finding here was that the effect of salt concentration polarization was greatly reduced as the concentration of P123 in the silica matrix increased from 5 to 50 wt.%. Hence, high carbon content conferred salt concentration anti-polarization to the membrane surface as compared to the high silica content.

Glucose template silica membranes were investigated by Mujiyanti, Elma [19] for brine water desalination. The C-H stretching vibration showed from FTIR results indicating carbon from glucose successfully induced into the silica matrices. Silica-glucose membrane showed good performance with salt rejection of 93 %, but rather low water flux of 0.22 – $2.28 \text{ kg} \cdot \text{m}^{-2} \cdot \text{h}^{-1}$ under feed temperatures of 25, 40 and 60 °C). This work concluded that the addition of glucose as carbon template agents strengthen the silica network becomes stronger even though the water fluxes remains a bit lower.

Elma, Pratiwi [17] produced potable water from NaCl 3.5 wt.% solution. They found that the pectin template silica membranes gave similar water fluxes of 5.9 – $8.66 \text{ kg} \cdot \text{m}^{-2} \cdot \text{h}^{-1}$ (25–60 °C) with salt rejections of > 99.3 %, depending on the testing conditions and amount of pectin loading (2.5 wt.%, calcined at 300 °C). The membranes work well thanks to the presence of carbon chains from the pectin apple which strengthened silica membrane pore structure.

Syauqiyah, Elma [109] reported silica-P123 membrane for seawater desalination prepared under different calcined technique of (RTP). The RTP technique offered faster fabrication time with competitive performance against the CTP technique. This work reported comparing performance of silica-pectin and silica-P123 membranes by measuring water flux and salt rejection. Silica-pectin membrane displayed prominent water flux of 3 folds higher than the silica-P123. It is suggested that the number of carbon chains of P123 joined to silica matrices densified the membranes film.

Liang, Zhan [173] prepared GO (graphene oxide) films coated on polyacrylonitrile (PAN) by vacuum filtration method. As the new intriguing material, GO has ultra-thin two-dimensional structure with abundant functional groups such as epoxide, carbonyl on the surface. The resulting membrane displayed outstanding water permeability (of up to $65 \text{ kg} \cdot \text{m}^{-2} \cdot \text{h}^{-1}$) and salt rejection of > 99.8 % for desalination NaCl 3.5 wt.% via pervaporation at 90 °C. GO-based membranes have the potentials to become the preferred candidates to next-generation high performing membranes. However, fabrication method of GO membranes is rather complex, and the GO membranes tend to quickly

Table 4
Summary of carbon template based membranes for wetland saline water desalination.

Membrane	Feed temperature (°C)	NaCl conc. (wt%)	Water Flux (kg.m ⁻² .h ⁻¹)	Salt Rejection (%)	Ref
Silica-P123	25	3.2	1.3–1.7	66–96	[169]
Silica-pectin	25	3.4	4.48	> 99	[174]
Pure silica	25–60	3.2	0.8–1.2	70–85	[168]
Organosilica	25	3	1.2	> 99	[99]

swell when immersed in water on a large scale. Recent results show that pervaporation using inorganic membranes have undergone major improvement as water fluxes are now reaching values as high as 65 kg.m⁻².h⁻¹ (for feed of NaCl 3.5 wt.%). These results clearly show that pervaporation using inorganic membranes has closed the performance gap with the pervaporation using organic/polymer-based membrane, with performances now in the same range as commercial RO membranes.

4.1.2. Desalination of wetland saline water by carbon template silica membranes

Desalination of wetland saline water is an interesting application for pervaporation by carbon template silica membranes. Reports on desalination of wetland saline water by pervaporation using carbon-silica template membrane are listed on Table 4. Wetland saline water is abundant in Indonesia, especially in South Kalimantan. Generally, wetland saline water has unique characteristics such as low pH, brownish colour and consists of high natural organic matter (NOM) [99], that typically increases membrane vulnerability from fouling. Even more, sea water infiltrates into wetland aquifers during the rainy season and increase the salinity of the wetland water. In many wetland areas, wetland water is often seen as the only water resource, but its utilization is highly limited by the salt concentration and NOM contents.

Elma, Fitriani [169] reported the application of mesopore carbonized template silica membrane by employing P123 triblock copolymers calcinated at different temperatures (350–600 °C) for desalination of wetland saline water. The silica-P123 membranes showed good water flux and salt rejection. The water flux of silica-P123 increased from 1.3 to 1.7 kg.m⁻².h⁻¹ by raising the calcination temperatures from 300 to 600 °C. In the contrary, the salt rejection decreased sharply from 96 % to 66 %. Such behaviours are attributed to the carbon moieties tight at low temperature in arranging the silica pore structure leading to the reduction of water fluxes. Therefore, silica-P123 membranes calcined at high temperature having loose indeed the membrane structure become unstable and force the selectivity decreases.

In another study Elma, Hairullah [168], pure silica membrane was proved effective to reduce the salt concentration of wetland saline water feed via pervaporation process. The highest water flux obtained at feed temperature of 60 °C was 1.2 kg.m⁻².h⁻¹. Unfortunately, the salt rejection was still poor, only 69 % at the highest feed temperature. A phenomena equivocal with the one discussed earlier. Interestingly, another study Lestari, Elma [99] also reported organosilica membrane with similar water flux of 1.2 kg.m⁻².h⁻¹ at lower feed temperature (25 °C) coupled with high salt rejection over 99 % (Fig. 11). The organosilica membranes was prepared by employing citric acid with dual roles as the carbon sources and catalyst. Such membrane poses advantages such as inexpensive, easy to fabricate and fast in production. The pure mesoporous silica has slightly lower performance than other carbon mesopore template silica membranes. Overall it can be deduced that carbon template effective and yet affordable material for preparation of silica-based membranes for wetland saline water desalination.

Silica-pectin membrane showed excellent water fluxes of 2–3 folds higher than various silica-based membranes applied for wetland saline

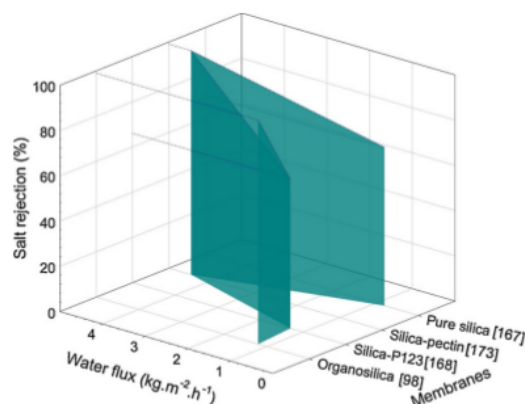


Fig. 11. Pervaporation performance at room temperature (25 °C) for desalination of wetland saline water.

water desalination (Fig. 11). Rahma, Elma [174] investigated pectin templated silica membrane and claimed that it achieved almost complete salt rejection of > 99 %. The NOM content was effectively reduced by incorporating a coagulation process as the pre-treatment. The highest NOM (UV₂₅₄) rejection was over 90 % [174]. Mechanism of pervaporation process for wetland saline water using carbon-silica template membrane is shown in Fig. 12.

Selectively of pure silica membranes are greatly reduced as the mobility of the silica enlarge the pore in the silica film facilitating salt diffusion. Water molecules react with the hydrophilic silanol groups because the silica matrix becomes mobile. The carbon template provides a barrier in the silica matrix that blocks the mobility of silica (Fig. 12). In this application, carbon can be attributed as a strong agent that switches the weakly silanol groups to avoid shrinkage of the silica matrices. At higher temperature, carbon-silica template materials are needed.

4.1.3. Long term stability of carbon template silica membranes

The stability of pervaporation process is judged by the ability to maintain the performance over time. Flux decline can happen due to hydration of the ions in solution and on the pore mouths which blocks the entry of water molecules. Therefore, during long-time testing the membrane fouling becomes critical due to the tendency of salt deposition that block the membrane pores. Deposition of salt shrinks the pore structure that block the transport of water which lowers the flux [143,153]. Fig. 13 summarizes the stability performance of various membranes types for desalination application.

Regarding the long-term testing of pure silica membrane (inorganic based material), an excellent result was reported by Elma, Yacou [143] for desalination of feed solution of 3.5 wt.% of NaCl. It was observed that pure silica membranes have stable long-term performances for 250 h at feed temperature of 22 °C. The first part of the operation of 150 h showed water fluxes ~8.5 kg.m⁻².h⁻¹, and the 250 h test yielded the water fluxes of 6.7 kg.m⁻².h⁻¹. The salt rejections were maintained high (of > 98 %). However, Elma, Yacou [143] also reported that water flux slightly reduced attributed to micropore blocking by hydrated salt ions due to the pure silica matrices cave during the submergence in water.

Despite the importance of performance stability, only a few reports are available (Table 5). In the longest performance evaluation reported so far, Lin, Ding [175] demonstrated cobalt oxide silica membranes (CoOxSi) est with multiples salt solutions i.e. 1 % (288 h), 3.5 wt.% (144 h), 7.5 wt.% (72 h) and 15 wt.% (72 h), totalling of 570 h. Water flux of the CoOxSi membrane tended to stabilize after 5 days ascribed to initial structural changes in the CoOxSi matrices. The long-term testing successfully demonstrated the improved hydro-stability of CoOxSi

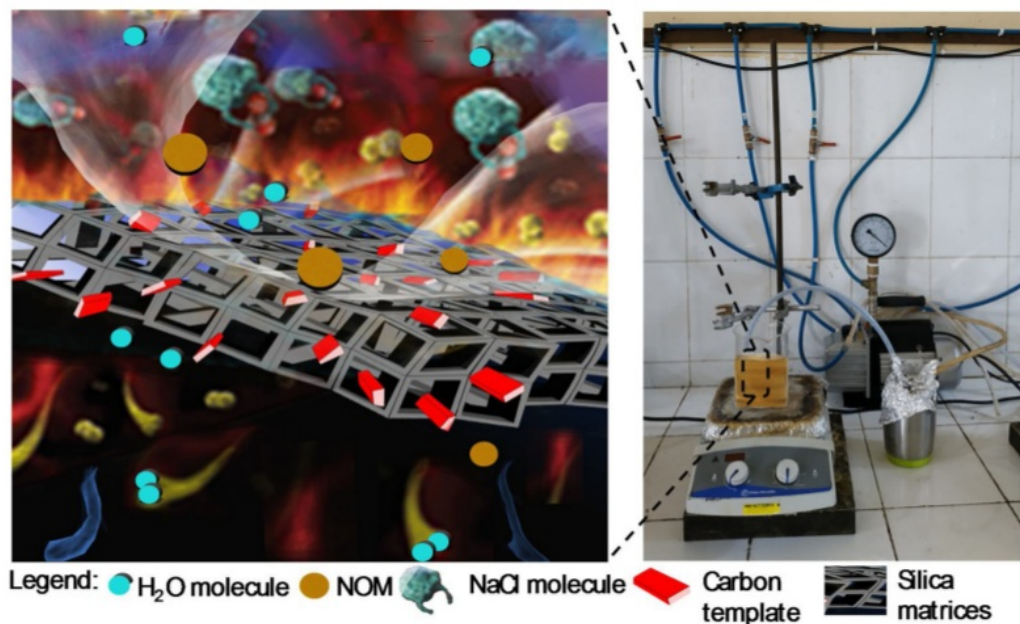


Fig. 12. Illustration of pervaporation mechanism of wetland saline water desalination via carbon template silica matrices.

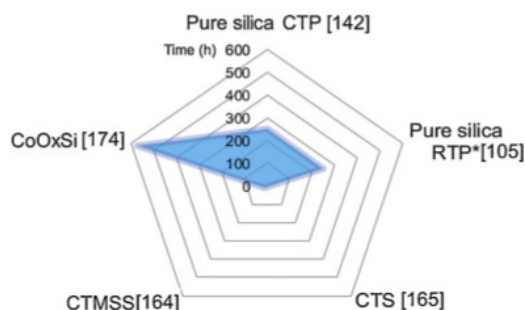


Fig. 13. Stability of various membranes type toward operation time (hour) for desalination of seawater and *wetland saline water.

membranes at various feed concentrations. In the several other studies, CTMSS (C6) membranes showed stable performance over 5 h, Wijaya, Duke [166] and over 12 h [165] due to the benefit of the carbonized templating method to improve the hydro-stability of the silica membranes. The report of long term stability study of carbon templated mesoporous silica membranes is still limited.

Zwijenberg, Koops [176] demonstrated the longest stability performance of non-porous polyether amide membranes using solar driven pervaporation. The test was carried out using three different feed: de-oiled formation water, untreated seawater and artificial seawater (3.5 wt.% NaCl). The water flux remained stable over 250 day. In the

beginning of the experiment, a slightly lower flux was observed due to the hold-up volume on the permeate side of the system. However, water flux reached a steady state after 10 days tests. The occurrence of membrane fouling was not obvious over the experiment duration. The decrease in water flux due to fouling also reduced the heat loss via evaporation. This automatically resulted in an increase in the feed temperature. Consequently, the increased feed temperature enhanced the evaporation rate to about the same level that occurred as that without fouling.

4.2. Future challenges

Carbon template silica-based membranes for desalination application are still at the premature stages of research and development. Therefore, this type of material requires significant enhancements to be able to compete against both established membranes and/or established technologies. Indeed, the RO process using polymeric based membranes is now the golden standard as a result of major research, development, and deployment in the last 30 years.

Silica based membranes have shown potential in providing excellent molecular sieving properties for gas separation applications, but less so in water desalination. It is primarily due to the shortage of hydro-stability of silica structures when contact with water. The final challenge for the membrane researchers is to establish the carbon materials which are favourable, most technically and economically viable applied for water desalination using silica-based membranes. GO and polyetherimide materials have been reported to be effective carbon

Table 5

The stability performance of silica based membranes for water desalination.

Membrane type	Testing condition (Pressure, Temp.)	Feed salt conc. (wt%) Lower/Higher	Water Flux (Kg. m ⁻² . h ⁻¹)	Salt Rejection (%)	Long Term Stability test	Ref
Pure silica CTP	ΔP < 1 bar, 22 °C	3.5	8.5–6.89	> 98	250 h	[143]
Pure silica RTP	ΔP < 1 bar, 25 °C	3.2 (wetland saline water)	1.7–1.25	98–92	250 h	[106]
CTS	P = 7 bar, 20 °C	0.3/3.5	2.1/1.9	99.9/98	5 h	[166]
CTMSS	ΔP < 1 bar, 20 °C	0.3/3.5	6.3/4.9	87/97	12 h	[165]
CoOxSi	ΔP < 1 bar, 20 °C	0.3/15	0.4/0.3	99.7/99.9	570 h	[175]

template into silica matrices. In wetland saline water desalination, improvement is required to have membrane material that can handle the presence of NOM in the feed.

Application of mesoporous carbon template silica membranes by pervaporation is also restricted by the high energy input in comparison to the RO. Analysis of the thermodynamics also indicates that parity will never be reached when utilizing primary energy sources. However, if the pervaporation process is successfully integrated with solar heat sources, waste heat or other sustainable energy source then the technology may be attractive for niche applications such as brine processing or salt recovery.

Currently, there is limited study on membrane fouling for the silica-carbon based membranes mainly due to the immature stages of the testing. Most studies still utilize laboratory scale using artificial salt-water as the feed. Similarly, for fouling study of wetland saline water desalination. Given the scale of the problem for RO membranes, this is a problem that will require substantial research in the future to ensure that mesoporous carbon template silica membranes can be deployed in an industrial context.

5. Conclusions

Many approaches have been developed to prepare carbon templated mesoporous silica. Hard templating methods have often been applied, in which the incorporated carbon sources are deposited through mesoporous silica. However, this method is costly, involves toxic substances and complicated, which limit its application. Soft templating is favourable strategies to tailor well defined mesoporous structure. Sustainable carbon sources material as templating agents are very attractive technically and economically. Sucrose has been explored as carbon templates because it is an environmentally friendly product and contains multiple adjacent hydroxyl groups which will make the formation of hydrogen bonding with silica oligomers possible. In addition, GO and polyetherimide material can also be considered as effective carbon templating into silica matrices due to their excellent properties. Application of carbon templated mesoporous silica membranes is promising for water desalination. Future challenges for desalination of wetland saline water are on improve membrane performances (high flux and salt rejection), as well as handle NOM content. To tackle the energy input issue, application of mesoporous carbon template silica membranes by pervaporation systems can be coupled with renewable energy such as solar heat sources, waste heat or others as such it can be competitive against RO for niche applications such as brine processing or salt recovery.

Declaration of Competing Interest

The authors report no declarations of interest.

Acknowledgements

Muthia thanks to Applied Research Universities Grant 2019-2020, Thesis Magister Grant 2019-2020, World Class Research Grant 2020-2022 Deputy of Research and Development National Research and Innovation Agency, The Ministry of Research and Technology Republic of Indonesia and Lambung Mangkurat University Research Grant 2020.

References

- [1] K. Ariga, et al., Nanoarchitectonics for mesoporous materials, *Bull. Chem. Soc. Jpn.* 85 (1) (2012) 1–32, <https://doi.org/10.1246/bcsj.20110162>.
- [2] X. Zhu, et al., Facile surface modification of mesoporous silica with heterocyclic silanes for efficiently removing arsenic, *Chinese Chem. Lett.* 30 (6) (2019) 1133–1136, <https://doi.org/10.1016/j.ccl.2019.02.022>.
- [3] U. Ciesla, F. Schüth, Ordered mesoporous materials, *Microporous Mesoporous Mater.* 27 (2) (1999) 131–149, [https://doi.org/10.1016/S1387-1811\(98\)00249-2](https://doi.org/10.1016/S1387-1811(98)00249-2).
- [4] V. Meynen, P. Cool, E.F. Vansant, Verified syntheses of mesoporous materials, *Microporous Mesoporous Mater.* 125 (3) (2009) 170–223, <https://doi.org/10.1016/j.micromeso.2009.03.046>.
- [5] W. Cheng, et al., A multifunctional nanoplatform against multidrug resistant Cancer: merging the best of targeted Chemo/Gene/Photothermal therapy, *Adv. Funct. Mater.* 27 (45) (2017) 1704135, <https://doi.org/10.1002/adfm.201704135>.
- [6] W. Zeng, et al., Dual-response oxygen-generating MnO₂ nanoparticles with poly-dopamine modification for combined photothermal-photodynamic therapy, *Chem. Eng. J.* 389 (2020) 124494, <https://doi.org/10.1016/j.cej.2020.124494>.
- [7] W. Ji, et al., Mesoporous silica nanospheres with the ability of photo-driven releasing sandela 803 for the application to wallpaper, *Chinese Chem. Lett.* 30 (03, 2019-03-22) (2019) 747–749, <https://doi.org/10.1016/j.ccl.2018.09.015>.
- [8] F. Schüth, W. Schmidt, Microporous and mesoporous materials, *Adv. Eng. Mater.* 4 (5) (2002) 269–279, [https://doi.org/10.1002/1527-2648\(20020503\)4:5<269::Aid-adem269>3.0.Co;2-7](https://doi.org/10.1002/1527-2648(20020503)4:5<269::Aid-adem269>3.0.Co;2-7).
- [9] A. Taguchi, F. Schüth, Ordered mesoporous materials in catalysis, *Microporous Mesoporous Mater.* 77 (1) (2005) 1–45, <https://doi.org/10.1016/j.micromeso.2004.06.030>.
- [10] M. Elma, et al., Microporous silica based membranes for desalination, *Water.* 4 (2012) 629–649, <https://doi.org/10.3390/w4030629>.
- [11] Heiner Strathmann, Enrico Drioli L.G, An Introduction to Membrane Science and Technology, Consiglio Nazionale Delle Ricerche, Italy, 2006.
- [12] S.J.C. Giessler, Dinizda Costa, G. Lu, Hydrophobicity of templated silica xerogels for molecular sieving applications, *J. Nanosci. Nanotechnol.* 1 (3) (2001) 331–336.
- [13] M. Elma, et al., Interlayer-free P123 carbonised template silica membranes for desalination with reduced salt concentration polarisation, *J. Memb. Sci.* 475 (2015) 376–383, <https://doi.org/10.1016/j.memsci.2014.10.026>.
- [14] C. Liang, S. Dai, Synthesis of mesoporous carbon materials via enhanced hydrogen-bonding interaction, *J. Am. Chem. Soc.* 128 (16) (2006) 5316–5317, <https://doi.org/10.1021/ja060242k>.
- [15] S. Tanaka, N. Nishiyama, Morphology control of ordered mesoporous carbon using organic-templating approach, *Progress in Molecular and Environmental Bioengineering-From Analysis and Modeling to Technology Applications*, IntechOpen, 2011.
- [16] R. Ayu Lestari, et al., Functionalization of Si-C Using TEOS (Tetra Ethyl Ortho Silica) As Precursor and Organic Catalyst, 148, (2020) 07008.
- [17] M. Elma, et al., The performance of membranes interlayer-free silica-pectin templated for seawater desalination via pervaporation operated at high temperature of feed solution, *Mater. Sci. Forum* 981 (2020) 349–355.
- [18] M. Elma, et al., Effect of banana pectin concentration on silica membran performance for brackish water, *Jurnal Teknik Lingkungan* 5 (2) (2019) 60–66, <https://doi.org/10.20527/jukung.v5i2.7318>.
- [19] D.R. Mujiyanti, M. Elma, M. Amalia, Interlayer-free glucose carbonised template silica membranes for brine water desalination, *MATEC Web Conf.* 280 (2019) 03010.
- [20] R. Babicheva, et al., New carbon membrane for water desalination via reverse osmosis, *IOP Conference Series: Materials Science and Engineering*, IOP Publishing, 2018.
- [21] V. Malgras, et al., Templated synthesis for nanoarchitected porous materials, *Bull. Chem. Soc. Jpn.* 88 (9) (2015) 1171–1200.
- [22] V. Malgras, et al., Nanoarchitectures for mesoporous metals, *Adv. Mater.* 28 (6) (2016) 993–1010.
- [23] N.L. Rosi, et al., Hydrogen storage in microporous metal-organic frameworks, *Science.* 300 (5622) (2003) 1127–1129.
- [24] Y.S. Bae, R.Q. Snurr, Development and evaluation of porous materials for carbon dioxide separation and capture, *Angew. Chemie Int. Ed.* 50 (49) (2011) 11586–11596.
- [25] Y.H. Deng, et al., A drying-free, water-based process for fabricating mixed-matrix membranes with outstanding pervaporation performance, *Angew. Chemie Int. Ed.* 55 (41) (2016) 12793–12796.
- [26] H.-L. Jiang, et al., Synergistic catalysis of Au@Ag core-shell nanoparticles stabilized on metal-organic framework, *J. Am. Chem. Soc.* 133 (5) (2011) 1304–1306.
- [27] Y.D. Chiang, et al., Functionalized Fe₃O₄@silica core-shell nanoparticles as microalgae harvester and catalyst for biodiesel production, *ChemSusChem.* 8 (5) (2015) 789–794.
- [28] Y.-H. Yang, et al., Hollow mesoporous hydroxyapatite nanoparticles (hmHANPs) with enhanced drug loading and pH-responsive release properties for intracellular drug delivery, *J. Mater. Chem. B* 1 (19) (2013) 2447–2450.
- [29] N.L. Torad, et al., MOF-derived nanoporous carbon as intracellular drug delivery carriers, *Chem. Lett.* 43 (5) (2014) 717–719.
- [30] R.E. Morris, P.S. Wheatley, Gas storage in nanoporous materials, *Angew. Chemie Int. Ed.* 47 (27) (2008) 4966–4981.
- [31] J. Ruparella, et al., Potential of carbon nanomaterials for removal of heavy metals from water, *Desalination* 232 (1-3) (2008) 145–156.
- [32] F.-K. Shieh, et al., Size-adjustable annular ring-functionalized mesoporous silica as effective and selective adsorbents for heavy metal ions, *RSC Adv.* 3 (48) (2013) 25686–25689.
- [33] S. Dutta, A. Bhaumik, K.C.-W. Wu, Hierarchically porous carbon derived from polymers and biomass: effect of interconnected pores on energy applications, *Energy Environ. Sci.* 7 (11) (2014) 3574–3592.
- [34] C. Van Nguyen, et al., A metal-free, high nitrogen-doped nanoporous graphitic carbon catalyst for an effective aerobic HMF-to-FDCA conversion, *Green Chem.* 18 (22) (2016) 5957–5961.
- [35] N.-L. Liu, et al., ZIF-8 derived, nitrogen-doped porous electrodes of carbon

- polyhedron particles for high-performance electrosorption of salt ions, *Sci. Rep.* 6 (1) (2016) 1–7.
- [36] Y. Gao, et al., Preparation of polyaniline nanotubes via “thin glass tubes template” approach and its gas response, *Macromol. Rapid Commun.* 28 (3) (2007) 286–291.
- [37] Y. Xie, et al., The effect of novel synthetic methods and parameters control on morphology of nano-alumina particles, *Nanoscale Res. Lett.* 11 (1) (2016) 1–11.
- [38] Y. Xie, et al., Review of research on template methods in preparation of nanomaterials, 2016 (2016).
- [39] M. Zhou, Z. Wei, H. Qiao, et al., Particle size and pore structure characterization of silver nanoparticles prepared by confined arc plasma, *Contributions to Atmospheric Physics* 2009 (8) (2009) 219–229.
- [40] E.M. Johansson, J.M. C’ordoba, M. Od’en, Effect of heptane addition on pore size and particle morphology of mesoporous silica SBA-15, *Microporous Mesoporous Mater.* 133 (1–3) (2010) 66–74.
- [41] H. Tamon, et al., Preparation of mesoporous carbon by freeze drying, *Carbon* 37 (12) (1999) 2049–2055.
- [42] K. Nielsch, et al., Self-ordering regimes of porous alumina: the 10 porosity rule, *Nano Lett.* 2 (7) (2002) 677–680.
- [43] L. Zhang, et al., Templated growth of crystalline mesoporous materials: from Soft/Hard templates to colloidal templates, *Front. Chem.* 7 (2019) 22.
- [44] Y. Meng, et al., Ordered mesoporous polymers and homologous carbon frameworks: amphiphilic surfactant templating and direct transformation, *Angew. Chemie Int. Ed.* 44 (43) (2005) 7053–7059.
- [45] W. Li, et al., A perspective on mesoporous TiO₂ materials, *Chem. Mater.* 26 (1) (2014) 287–298.
- [46] H.N. Lokupitiya, et al., Ordered mesoporous to macroporous oxides with tunable isomorphic architectures: solution criteria for persistent micelle templates, *Chem. Mater.* 28 (6) (2016) 1653–1667.
- [47] M.D. Goodman, et al., Enabling new classes of templated materials through mesoporous carbon colloidal crystals, *Adv. Opt. Mater.* 1 (4) (2013) 300–304.
- [48] J. Pang, et al., Silica-templated continuous mesoporous carbon films by a spin-coating technique, *Adv. Mater.* 16 (11) (2004) 884–886.
- [49] B. Hu, et al., Functional carbonaceous materials from hydrothermal carbonization of biomass: an effective chemical process, *J. Chem. Soc. Dalton Trans.* (40) (2008) 5414–5423.
- [50] J. Schuster, et al., Spherical ordered mesoporous carbon nanoparticles with high porosity for lithium–sulfur batteries, *Angew. Chemie Int. Ed.* 51 (15) (2012) 3591–3595.
- [51] M.-X. Liu, et al., Synthesis and electrochemical performance of hierarchical porous carbons with 3D open-cell structure based on nanosilica-embedded emulsion-templated polymerization, *Chinese Chem. Lett.* 25 (6) (2014) 897–901.
- [52] A. Darmawan, et al., Structural evolution of nickel oxide silica sol-gel for the preparation of interlayer-free membranes, *J. Non. Solids* 447 (2016) 9–15.
- [53] N. Brun, et al., Hydrothermal carbon-based nanostructured hollow spheres as electrode materials for high-power lithium–sulfur batteries, *J. Chem. Soc. Faraday Trans.* 15 (16) (2013) 6080–6087.
- [54] J. Liu, et al., Highly dispersible microporous carbon particles from furfuryl alcohol, *NSTI Nanotech.* (2005).
- [55] C. Falco, et al., Hydrothermal carbons from hemicellulose-derived aqueous hydrolysis products as electrode materials for supercapacitors, *ChemSusChem* 6 (2) (2013) 374–382.
- [56] J.H. Knox, K.K. Unger, H. Mueller, Prospects for carbon as packing material in high-performance liquid chromatography, *J. Liq. Chromatogr.* 6 (sup001) (1983) 1–36, <https://doi.org/10.1080/01483918308067647>.
- [57] T. Morishita, et al., A review of the control of pore structure in MgO-templated nanoporous carbons, *Carbon* 48 (10) (2010) 2690–2707, <https://doi.org/10.1016/j.carbon.2010.03.064>.
- [58] Y. Yan, et al., Controlled synthesis of mesoporous carbon nanosheets and their enhanced supercapacitive performance, *J. Solid State Electrochem.* 17 (6) (2013) 1677–1684, <https://doi.org/10.1007/s10008-013-2025-3>.
- [59] X. He, et al., Synthesis of mesoporous carbons for supercapacitors from coal tar pitch by coupling microwave-assisted KOH activation with a MgO template, *Carbon* 50 (13) (2012) 4911–4921, <https://doi.org/10.1016/j.carbon.2012.06.020>.
- [60] A. Eftekhari, Z. Fan, Ordered mesoporous carbon and its applications for electrochemical energy storage and conversion, *Mater. Chem. Front.* 1 (6) (2017) 1001–1027, <https://doi.org/10.1039/C6QM00298F>.
- [61] S.B. Yoon, et al., New mesoporous silica/carbon composites by in situ transformation of silica template in carbon/silica nanocomposite, *J. Exp. Nanosci.* 9 (3) (2014) 221–229, <https://doi.org/10.1080/17458080.2011.654275>.
- [62] Z.-h. Tang, et al., Properties of mesoporous carbons prepared from different carbon precursors using nanosize silica as a template, *New Carbon Mater.* 25 (6) (2010) 465–469, [https://doi.org/10.1016/S1872-5805\(09\)60045-7](https://doi.org/10.1016/S1872-5805(09)60045-7).
- [63] S.J.M. Wang, Ordered mesoporous materials for drug delivery, *Microporous Mesoporous Mater.* 117 (1–2) (2009) 1–9.
- [64] H.I. Lee, et al., Rational synthesis pathway for ordered mesoporous carbon with controllable 30- to 100-Angstrom pores, *Adv. Mater.* 20 (4) (2008) 757–762, <https://doi.org/10.1002/adma.200702209>.
- [65] S. Wang, H.J.M. Li, Structure directed reversible adsorption of organic dye on mesoporous silica in aqueous solution, *Microporous Mesoporous Mater.* 97 (1–3) (2006) 21–26.
- [66] L. Huang, M. Kruk, Synthesis of ultra-large-pore FDU-12 silica using ethylbenzene as micelle expander, *J. Colloid Interface Sci.* 365 (1) (2012) 137–142, <https://doi.org/10.1016/j.jcis.2011.09.044>.
- [67] T.R. Pauly, T.J. Pinnavaia, Pore size modification of mesoporous HMS molecular sieve silicas with wormhole framework structures, *Chem. Mater.* 13 (3) (2001) 987–993, <https://doi.org/10.1021/cm000762t>.
- [68] R.I. Babicheva, et al., New carbon membrane for water desalination via reverse osmosis, *IOP Conference Series: Materials Science and Engineering* 447 (2018) 012053, <https://doi.org/10.1088/1757-899x/447/1/012053>.
- [69] B. Zhang, et al., Towards the preparation of ordered mesoporous Carbon/Carbon composite membranes for gas separation, *Sep. Sci. Technol.* 49 (2014), <https://doi.org/10.1080/01496395.2013.838684>.
- [70] R. Ryoo, S.H. Joo, S. Jun, Synthesis of highly ordered carbon molecular sieves via template-mediated structural transformation, *J. Phys. Chem. B* 103 (37) (1999) 7743–7746, <https://doi.org/10.1021/jp991673a>.
- [71] C. Lin, et al., Synthesis of ordered mesoporous carbon using MCM-41 mesoporous silica as template, *Adv. Mat. Res.* 11–12 (2006) 543–546, <https://doi.org/10.4028/www.scientific.net/AMR.11-12.543>.
- [72] M. Brankovic, et al., Mesoporous silica (MCM-41): Synthesis/modification, characterization and removal of selected organic micro-pollutants from water, *Adv. Technol.* 6 (2017) 50–57, <https://doi.org/10.5937/savtehl701050B>.
- [73] K. Erdmann, et al., Al-MCM-48 As a Template for Synthesis of Porous Carbons – Adsorption Study, (2005).
- [74] C. Kresge, et al., Ordered mesoporous molecular sieves synthesized by a liquid-crystal template mechanism, *nature* 359 (6397) (1992) 710–712.
- [75] J.S. Beck, et al., A new family of mesoporous molecular sieves prepared with liquid crystal templates, *J. Am. Chem. Soc.* 114 (27) (1992) 10834–10843.
- [76] J.C. Vartuli, et al., Chapter 1 - designed synthesis of mesoporous molecular sieve systems using surfactant-directing agents, in: W.R. Moser (Ed.), *Advanced Catalysts and Nanostructured Materials*, Academic Press, San Diego, 1996, pp. 1–19.
- [77] A. Sayari, B.-H. Han, Y. Yang, Simple synthesis route to monodispersed SBA-15 silica rods, *J. Am. Chem. Soc.* 126 (44) (2004) 14348–14349, <https://doi.org/10.1021/ja0478734>.
- [78] D. Zhao, et al., Triblock copolymer syntheses of mesoporous silica with periodic 50 to 300 angstrom pores, *Science* 279 (5350) (1998) 548–552, <https://doi.org/10.1126/science.279.5350.548>.
- [79] D. Zhao, et al., Nonionic triblock and star diblock copolymer and oligomeric surfactant syntheses of highly ordered, hydrothermally stable, mesoporous silica structures, *J. Am. Chem. Soc.* 120 (24) (1998) 6024–6036, <https://doi.org/10.1021/ja974025i>.
- [80] P. Fulvio, S. Pikus, M. Jaroniec, Short-time synthesis of SBA-15 using various silica sources, *J. Colloid Interface Sci.* 287 (2005) 717–720, <https://doi.org/10.1016/j.jcis.2005.02.045>.
- [81] J. Wang, et al., Hydrothermal synthesis of SBA-15 using sodium silicate derived from coal gangue, *J. Nanomaterials* 2013 (2013), <https://doi.org/10.1155/2013/352157> Article 6.
- [82] H. Razak, et al., Refluxed synthesis of SBA-15 using sodium silicate extracted from Oil Palm Ash for dry reforming of methane, *Mater. Today Proc.* 19 (2019) 1363–1372, <https://doi.org/10.1016/j.matpr.2019.11.150>.
- [83] A. Sayari, Y. Yang, SBA-15 templated mesoporous carbon: new insights into the SBA-15 pore structure, *Chem. Mater.* 17 (24) (2005) 6108–6113, <https://doi.org/10.1021/cm050960q>.
- [84] M. Koh, et al., Surface morphology and physicochemical properties of ordered mesoporous silica SBA-15 synthesized at low temperature, *IOP Conference Series: Materials Science and Engineering* 206 (2017) 012056, <https://doi.org/10.1088/1757-899X/206/1/012056>.
- [85] N. Rahmat, A.Z. Abdullah, A. Mohamed, A review: mesoporous silica SBA-15, types, synthesis and its applications towards biorefinery production, *Am. J. Appl. Sci.* 7 (2010), <https://doi.org/10.3844/ajassp.2010.1579.1586>.
- [86] M.S.Md. Oliveira, et al., Incorporating aluminum into the structure of SBA-15 by adjusting the pH and adding NaF, *Mater. Res.* 22 (2019).
- [87] E. Rivera-Muñoz, R. Huirache-Acuña, Sol gel-derived SBA-16 mesoporous material, *Int. J. Mol. Sci.* 11 (2010) 3069–3086, <https://doi.org/10.3390/ijms11093069>.
- [88] T. Yu, et al., Pore structures of ordered large cage-type mesoporous silica FDU-12s, *J. Phys. Chem. B* 110 (43) (2006) 21467–21472, <https://doi.org/10.1021/jp064534j>.
- [89] J. Fan, et al., Cubic mesoporous silica with large controllable entrance sizes and advanced adsorption properties, *Angew. Chem. Int. Ed. Engl.* 42 (27) (2003) 3146–3150, <https://doi.org/10.1002/anie.200351027>.
- [90] S.S. Kim, et al., Synthesis and characterization of ordered, very large pore MSU-H silicas assembled from water-soluble silicates, *J. Phys. Chem. B* 105 (32) (2001) 7663–7670, <https://doi.org/10.1021/jp010773p>.
- [91] J. Zeng, et al., Ordered mesoporous carbon/Nafion as a versatile and selective solid-phase microextraction coating, *J. Chromatogr. A* 1365 (2014) 29–34, <https://doi.org/10.1016/j.chroma.2014.08.094>.
- [92] S.-S. Kim, T.J. Pinnavaia, A low cost route to hexagonal mesostructured carbon molecular sieves, *Chem. Commun.* 23 (2001) 2418–2419, <https://doi.org/10.1039/B107896H>.
- [93] Á.A. Beltrán-Osuna, J.E. Perilla, Colloidal and spherical mesoporous silica particles: synthesis and new technologies for delivery applications, *J. Solgel Sci. Technol.* 77 (2) (2016) 480–496.
- [94] D. Macquarrie, et al., Organomodified hexagonal mesoporous silicates, *New J. Chem.* 23 (5) (1999) 539–544.
- [95] F. Farjadian, et al., Phosphinite-functionalized silica and hexagonal mesoporous silica containing palladium nanoparticles in Heck coupling reaction: synthesis, characterization, and catalytic activity, *RSC Adv.* 5 (97) (2015) 79976–79987.
- [96] P.T. Tanev, T.J. Pinnavaia, A neutral templating route to mesoporous molecular sieves, *Science* 267 (5199) (1995) 865–867, <https://doi.org/10.1126/science.267.5199.865>.

- [97] M.A. Al Roaya, F. Manteghi, M. Haghverdi, Synthesis and characterization of hollow mesoporous silica spheres and studying the load and release of dexamethasone, *Silicon* 11 (3) (2019) 1401–1411, <https://doi.org/10.1007/s12633-018-9943-8>.
- [98] M. Elma, et al., Microporous silica based membranes for desalination, *Water* 4 (3) (2012) 629, <https://doi.org/10.3390/w4030629>.
- [99] R.A. Lestari, et al., Organo silica membranes for wetland saline water desalination: effect of membranes calcination temperatures, *E3S Web Conf.* 148 (2020) 07006.
- [100] S. Benfer, et al., Development and characterization of ceramic nanofiltration membranes, *Sep. Purif. Technol.* 22–23 (2001) 231–237, [https://doi.org/10.1016/S1383-5866\(00\)00133-7](https://doi.org/10.1016/S1383-5866(00)00133-7).
- [101] R. Ayu Lestari, et al., Functionalization of Si-C using TEOS (Tetra ethyl ortho silica) as precursor and organic catalyst, *E3S Web Conf.* 148 (2020) 07008.
- [102] D. Nadargi, A. Rao, Methyltriethoxysilane: New precursor for synthesizing silica aerogels, *Journal of Alloys and Compounds - J ALLOYS COMPOUNDS* 467 (2009) 397–404, <https://doi.org/10.1016/j.jallcom.2007.12.019>.
- [103] Maimunawaro, et al., Deconvolution of carbon silica templated thin film using ES40 and P123 via rapid thermal processing method, *Mater. Today Proc.* (2020), <https://doi.org/10.1016/j.matpr.2020.01.195>.
- [104] S.K. Rahmalan, et al., Functionalization of hybrid organosilica based membranes for water desalination – preparation using Ethyl Silicate 40 and P123, *Mater. Today Proc.* (2020), <https://doi.org/10.1016/j.matpr.2020.01.187>.
- [105] J. Ghláf, Hydrolysis and polycondensation of ethyl silicates. 2. Hydrolysis and polycondensation of ETS40 (ethyl silicate 40), *Colloids Surf. A Physicochem. Eng. Asp.* 70 (3) (1993) 253–268, [https://doi.org/10.1016/0927-7757\(93\)80299-T](https://doi.org/10.1016/0927-7757(93)80299-T).
- [106] M. Elma, N. Riskawati, Marhamah, Silica membranes for wetland saline water desalination: performance and long term stability, *IOP Conference Series: Earth and Environmental Science* 175 (1) (2018) 012006, <https://doi.org/10.1088/1755-1315/175/1/012006>.
- [107] E.L.A. Rampun, et al., Interlayer-free silica-pectin membrane for sea-water desalination, *Membr. Technol.* 2019 (12) (2019) 5–9, [https://doi.org/10.1016/S0958-2118\(19\)30222-8](https://doi.org/10.1016/S0958-2118(19)30222-8).
- [108] E.L.A. Rampun, et al., Interlayer-free Silica Pectin Membrane for Wetland Saline Water via Pervaporation, *J. Kim. Sains Dan Apl.* 22 (3) (2019) 6 10.14710/jksa.22.3.99-104.
- [109] I. Syaunyah, et al., Interlayer-free silica-carbon template membranes from pectin and P123 for water desalination, *MATEC Web Conf.* 280 (2019) 03017.
- [110] A. Lamy-Mendes, R.F. Silva, L. Durães, Advances in carbon nanostructure-silica aerogel composites: a review, *J. Mater. Chem. A* 6 (4) (2018) 1340–1369, <https://doi.org/10.1039/C7TA08959G>.
- [111] P. Alexandridis, J.F. Holzwarth, T.A. Hatton, Micellization of poly(ethylene oxide)-Poly(propylene oxide)-Poly(ethylene oxide) triblock copolymers in aqueous solutions: thermodynamics of copolymer association, *Macromolecules* 27 (9) (1994) 2414–2425, <https://doi.org/10.1021/ma00087a009>.
- [112] B. Hatton, et al., Past, present, and future of periodic mesoporous organosilicas-the PMOs, *Acc. Chem. Res.* 38 (4) (2005) 305–312, <https://doi.org/10.1021/ar040164a>.
- [113] F. Hoffmann, et al., Periodic mesoporous organosilicas (PMOs): past, present, and future, *J. Nanosci. Nanotechnol.* 6 (2) (2006) 265–288, <https://doi.org/10.1166/jnn.2006.902>.
- [114] D. Zhao, et al., Triblock copolymer syntheses of mesoporous silica with periodic 50 to 300 angstrom pores, *Science* 279 (5350) (1998) 548–552.
- [115] T.-W. Kim, et al., Tailoring the pore structure of SBA-16 silica molecular sieve through the use of copolymer blends and control of synthesis temperature and time, *J. Phys. Chem. B* 108 (31) (2004) 11480–11489.
- [116] L. Wang, et al., Synthesis and characterization of small pore thick-walled SBA-16 templated by oligomeric surfactant with ultra-long hydrophilic chains, *Microporous Mesoporous Mater.* 67 (2–3) (2004) 135–141.
- [117] G. Farid, Flexible and Versatile Soft Templates for Mesoporous Silicas and Organosilicas Based on Pluronic Block Copolymer Surfactants and Their Mixtures, (2018).
- [118] A.E. Pratiwi, et al., Innovation of carbon from pectin templated in fabrication of interlayer-free silica-pectin membrane, *J. Kim. Sains Dan Apl.* 22 (3) (2019) 6, <https://doi.org/10.14710/jksa.22.3.93-98>.
- [119] M. Elma, et al., The effect of banana pectin concentration on silica membrane performance for brackish water, *Jukung Jumal Teknik Lingkungan* 5 (2) (2019) 45–51.
- [120] R. Zhong, et al., An eco-friendly Soft template synthesis of mesostructured silica-carbon nanocomposites for acid catalysis, *ChemCatChem* 7 (2015), <https://doi.org/10.1002/cctc.201500728> n/a-n/a.
- [121] C.M. Yang, B. Zibrowius, F. Schuth, Formation of cyanide-functionalized SBA-15 and its transformation to carboxylate-functionalized SBA-15, *Chemistry* (2004) 2461–2467.
- [122] Yunyun Xie, Mozhen Wang J.W, Xuewu Ge, Fabrication of fibrous amidoxime-functionalized mesoporous silicamicrosphere and its selectively adsorption property for Pb²⁺ in aqueous solution, *J. Hazard. Mater.* 297 (2015) 66–73.
- [123] S. Brunauer, W.E. Deming, E. Teller, On a theory of the van der Waals adsorption of gases, *J. Am. Chem. Soc.* 62 (1940) 1723–1732.
- [124] K.S.W. Sing, R.A.W. Haul, I. Moscou, R.A. Pierotti, J. Rouquerol, T. Siemieniowska, Reporting physisorption data for gas/solid systems with special reference to the determination of surface area and porosity (recommendations 1984), *Pure Appl. Chem.* 57 (1985) 603–619.
- [125] D.S. Moon, J.K. Lee, Tunable synthesis of hierarchical mesoporous silicananoparticles with radial wrinkle structure, *Langmuir* 28 (2012) 12341–12347.
- [126] F. Juillerat, P.B., H. Hofmann, 22 (2006) 5287–5291.
- [127] J.M. Rosenholm, E. Peuhu, R. Niemi, J.E. Eriksson, C. Sahlgren, *MI INDEN, ACS Nano* 3 (2009) 197–268.
- [128] Oliver Wiltshchka, D. Böcking, Larissa Miller, Rolf E. Brenner, Cecilia Sahlgren, Mika Lindén, Preparation, characterization, and preliminary biocompatibility evaluation of particulate spin-coated mesoporous silica films, *Microporous Mesoporous Mater.* 188 (2013) 203–209.
- [129] J.H. Prosser, S.Lee T.B, A.J. Nolte, D. Lee, *Nano Lett.* 11 (1999) 2132–2140.
- [130] X. Mao, Y. Chen, L. Yang, F. Zhao, B. Ding, J. Yu, *RSC Adv.* (2012) 12216–12223.
- [131] Yang Wang, Xiuling Jiao W.D, Dairong Chen, Electrospun flexible self-standing silica/mesoporous alumina core-shell fibrous membranes as adsorbents toward Congo red, *RSC Adv.* 30790 (2014).
- [132] S. Zhan, X. Jiao, C. Tao, *J. Phys. Chem. B* 110 (11199-11204) (2006).
- [133] J.H. Yu, S.V. Fridrikh, G.C. Rutledge, *Adv Mater* 16 (1562-1566) (2004).
- [134] Asmaa Mourhly, Adnane E. Hamidi, Mohammed Kacimi, Mohammed Halim, Said Arsalane, The synthesis and characterization of low-cost mesoporous silica SiO₂ from local pumice rock, *Nanomater. Nanotechnol.* (2015).
- [135] S. Nasser, M. Heidari, Evaluation and comparison of aluminum coated-pumice and zeolite in arsenic removal from water resources, *Iranian J. Environ. Health Sci. Eng.* 9 (2012) 256–268.
- [136] A.H. Mahvi, A. Mesdaghinia, A.R. Yari, Fluoride adsorption by pumice from aqueous solutions, *E-journal Chem.* 9 (2012) 1843–1853.
- [137] M. Tapan, Use of pumice and scoria aggregates, *Problems of Minerals Processing* 50 (2014) 467–475.
- [138] B. Cekova, B. Pavlovski, D. Spasev, A. Reka, Structural examinations of natural raw materials pumice and tephel from republic of Macedonia, *Balkan Mineral Processing Congress, Bulgaria*, 2013, pp. 73–75.
- [139] M.N. Sepehr, Kazemian Z.M, H. Amrane, A. Yaghmaian, K. Ghaffar, Removal of hardness agents, calcium and magnesium, by natural and alkaline modified pumice stones in single and binary systems, *Appl. Surf. Sci.* 274 (2013) 295–305.
- [140] I.A. Rahman, P. Vejayakumaran, C.S. Sipaut, J. Ismail, C.K. Chee, Size-dependent physicochemical and optical properties of silica nanoparticles, *Mater. Chem. Phys.* 114 (2009) 328–332.
- [141] J. Yang, E. Wang, Reaction of water on silica surfaces, *Curr. Opin. Solid State Mater. Sci.* 10 (2006) 33–39.
- [142] M. Elma, et al., Fabrication of interlayer-free silica-based membranes – effect of low calcination temperature using an organo-catalyst, *Membr. Technol.* 2019 (2) (2019) 6–10, [https://doi.org/10.1016/S0958-2118\(19\)30037-0](https://doi.org/10.1016/S0958-2118(19)30037-0).
- [143] M. Elma, et al., Performance and Long Term Stability of Mesoporous Silica Membranes for Desalination, *Membranes* 3 (2013) 136–150, <https://doi.org/10.3390/membranes3030136>.
- [144] M. Elma, et al., Fabrication of interlayer-free P123 carbonised template silica membranes for Water desalination: conventional versus Rapid thermal processing (CTP vs RTP) techniques, *IOP Conference Series: Materials Science and Engineering*, IOP Publishing, 2019.
- [145] M. Elma, et al., Interlayer-free P123 carbonised template silica membranes for desalination with reduced salt concentration polarisation, *J. Memb. Sci.* 475 (2015) 376–383, <https://doi.org/10.1016/j.memsci.2014.10.026>.
- [146] M. Elma, et al., Interlayer-Free hybrid organo-silica membranes based teos and tevs for Water desalination, *International Conference on Oleo and Petrochemical Engineering* (2015) 49–57 https://www.researchgate.net/publication/294715939_INTERLAYER-FREE_HYBRID_ORGANO-SILICA_MEMBRANES_BASED_TEOS_AND_TEVS_FOR_WATER_DESALINATION.
- [147] S.M. Ashrafi-Shahria, F. Ravaria, D. Seifzadeh, Smart Organic/Inorganic sol-gel nanocomposite containing functionalized mesoporous silica for corrosion protection, *Progress in Organic Coatings* 133 (2019) 44–54.
- [148] H. Yang, et al., Interlayer-free hybrid carbon-silica membranes for processing brackish to brine salt solutions by pervaporation, *J. Memb. Sci.* (2017).
- [149] S. Tanaka, et al., Preparation of ordered mesoporous carbon membranes by a soft-templating method, *Carbon* 49 (10) (2011) 3184–3189, <https://doi.org/10.1016/j.carbon.2011.03.042>.
- [150] M. Elma, G.S. Saputro, Performance of cobalt-silica membranes through pervaporation process with different feed solution concentrations, *Mater. Sci. Forum* 981 (2020) 342–348.
- [151] N.I. Vazquez, et al., Synthesis of mesoporous silica nanoparticles by sol-Gel as nanocontainer for future drug delivery applications, *Boletín De La Sociedad Espanola De Ceramica y Vidrio* 56 (2017) 139–145.
- [152] H. Nagasawa, T. Tsuru, Chapter 9 - silica membrane application for pervaporation process, in: A. Basile, K. Ghasemzadeh (Eds.), *Current Trends and Future Developments on (Bio-) Membranes*, Elsevier, 2017, pp. 217–241.
- [153] Q. Wang, et al., Desalination by pervaporation: a review, *Desalination* 387 (2016) 46–60, <https://doi.org/10.1016/j.desal.2016.02.036>.
- [154] M.C. Duke, et al., Hydrothermally robust molecular sieve silica for wet gas separation, *Adv. Funct. Mater.* 16 (9) (2006) 1215–1220, <https://doi.org/10.1002/adfm.200500456>.
- [155] P.-S. Lee, et al., Carbon molecular sieve membranes on porous composite tubular supports for high performance gas separations, *Microporous Mesoporous Mater.* 224 (2016) 332–338, <https://doi.org/10.1016/j.micromeso.2015.12.054>.
- [156] S.M. Saufi, A.F. Ismail, Fabrication of carbon membranes for gas separation—a review, *Carbon* 42 (2) (2004) 241–259, <https://doi.org/10.1016/j.carbon.2003.10.022>.
- [157] G. Komeritakis, et al., Organic-templated silica membranes: I. Gas and vapor transport properties, *J. Memb. Sci.* 215 (1) (2003) 225–233, [https://doi.org/10.1016/S0376-7388\(02\)00616-6](https://doi.org/10.1016/S0376-7388(02)00616-6).
- [158] M. Elma, et al., High performance interlayer-free mesoporous cobalt oxide silica membranes for desalination applications, *Desalination* 365 (2015) 308–315, <https://doi.org/10.1016/j.desal.2015.02.034>.
- [159] Y. Chua, et al., Mesoporous organosilica membranes: effects of pore geometry and

- calcination conditions on the membrane distillation performance for desalination, *Desalination*. 370 (2015) 53–62, <https://doi.org/10.1016/j.desal.2015.05.015>.
- [160] N.K. Raman, C.J. Brinker, Organic "template" approach to molecular sieving silica membranes, *J. Memb. Sci.* 105 (3) (1995) 273–279, [https://doi.org/10.1016/0376-7388\(95\)00067-M](https://doi.org/10.1016/0376-7388(95)00067-M).
- [161] Z. Xie, et al., 6 - desalination by pervaporation, in: V.G. Gude (Ed.), *Emerging Technologies for Sustainable Desalination Handbook*, Butterworth-Heinemann, 2018, pp. 205–226.
- [162] M.C. Duke, et al., Hydrothermally robust molecular sieve silica for wet gas separation, *Adv. Funct. Mater.* 16 (9) (2006) 1215–1220, <https://doi.org/10.1002/adfm.200500456>.
- [163] M.C. Duke, S. Mee, J.C.D. da Costa, Performance of porous inorganic membranes in non-osmotic desalination, *Water Res.* 41 (17) (2007) 3998–4004, <https://doi.org/10.1016/j.watres.2007.05.028>.
- [164] H. Yang, et al., Hybrid vinyl silane and P123 template sol–gel derived carbon silica membrane for desalination, *J. Solgel Sci. Technol.* (2017), <https://doi.org/10.1007/s10971-017-4562-1>.
- [165] B.P. Ladewig, et al., Preparation, characterization and performance of templated silica membranes in non-osmotic desalination, *Materials*. 4 (5) (2011) 845.
- [166] S. Wijaya, M.C. Duke, J.C. Diniz da Costa, Carbonised template silica membranes for desalination, *Desalination*. 236 (1) (2009) 291–298, <https://doi.org/10.1016/j.desal.2007.10.079>.
- [167] E.L.A. Rampun, et al., Interlayer-free silica pectin membrane for wetland saline water via pervaporation, *J. Kim. Sains Dan Apl.* 22 (3) (2019) 99–104.
- [168] M. Elma, Hairullah, Z.L. Assyaifi, Desalination process via pervaporation of wetland saline Water, *IOP Conference Series: Earth and Environmental Science*, IOP Publishing, 2018.
- [169] M. Elma, et al., Silica P123 membranes for desalination of wetland saline Water in South Kalimantan, *IOP Conference Series: Earth and Environmental Science*, IOP Publishing, 2018.
- [170] Y.T. Chua, et al., Nanoporous organosilica membrane for water desalination: theoretical study on the water transport, *J. Memb. Sci.* 482 (2015) 56–66, <https://doi.org/10.1016/j.memsci.2015.01.060>.
- [171] M.C. Duke, et al., Seawater desalination performance of MFI type membranes made by secondary growth, *Sep. Purif. Technol.* 68 (3) (2009) 343–350, <https://doi.org/10.1016/j.seppur.2009.06.003>.
- [172] P.S. Singh, et al., Cetyltrimethylammonium bromide–silica membrane for seawater desalination through pervaporation, *Bull. Mater. Sci.* 38 (2) (2015) 565–572.
- [173] B. Liang, et al., High performance graphene oxide/polyacrylonitrile composite pervaporation membranes for desalination applications, *J. Mater. Chem. A* 3 (9) (2015) 5140–5147, <https://doi.org/10.1039/C4TA06573E>.
- [174] A. Rahma, et al., Removal of natural organic matter for wetland saline water desalination by coagulation-pervaporation, *J. Kim. Sains Dan Apl.* 22 (3) (2019) 85–92, <https://doi.org/10.14710/jksa.22.3.85-92>.
- [175] C.X.C. Lin, et al., Cobalt oxide silica membranes for desalination, *J. Colloid Interface Sci.* 368 (1) (2012) 70–76.
- [176] H.J. Zwijnenberg, G.H. Koops, M. Wessling, Solar driven membrane pervaporation for desalination processes, *J. Memb. Sci.* 250 (1) (2005) 235–246, <https://doi.org/10.1016/j.memsci.2004.10.029>.

ORIGINALITY REPORT

16%

SIMILARITY INDEX

7%

INTERNET SOURCES

13%

PUBLICATIONS

5%

STUDENT PAPERS

MATCH ALL SOURCES (ONLY SELECTED SOURCE PRINTED)

2%

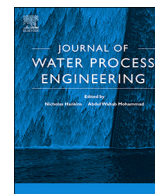
★ Elma, Muthia, Christelle Yacou, João Costa, and David Wang. "Performance and Long Term Stability of Mesoporous Silica Membranes for Desalination", Membranes, 2013.

Publication

Exclude quotes On

Exclude matches Off

Exclude bibliography On



Carbon templated strategies of mesoporous silica applied for water desalination: A review



Muthia Elma^{a,b,*}, Erdina L.A. Rampun^b, Aulia Rahma^b, Zaini L. Assyaifi^{a,b}, Anna Sumardi^{a,b}, Aptar E. Lestari^{a,b}, Gesit S. Saputro^b, Muhammad Roil Bilad^c, Adi Darmawan^d

^a Chemical Engineering Department, Lambung Mangkurat University, Jl. A. Yani KM 36, Banjarbaru, South Kalimantan 70714, Indonesia

^b Materials and Membranes Research Group (M²ReG), Lambung Mangkurat University, Jl. A. Yani KM 36, Banjarbaru, South Kalimantan 70714, Indonesia

^c Department of Chemical Engineering, Universiti Teknologi Petronas, Seri Iskandar, Perak 32610, Malaysia

^d Department of Chemistry, Diponegoro University, Semarang 50275, Indonesia

ARTICLE INFO

Keywords:

Carbon templated
Mesoporous silica
Carbon-silica based materials
Water and wetland saline water desalination

ABSTRACT

Porous materials have attracted attention in many practical fields, including for water desalination. Carbon templated is an attractive method in enhancing the properties of mesoporous silica materials used as membrane materials. This review mainly focuses on the strategies of carbon templates of mesoporous silica materials essentially applied for water desalination. Numerous strategies for carbon templated mesoporous silica are briefly discussed. In addition, most carbon-silica based membranes for desalination are detailed and their performances are discussed. Moreover, application of carbon-silica templates for wetland saline water desalination are also discussed in great detail. The comparison between carbon-silica based materials and silica-based membranes of recent techniques, fabrication, trend, application and operation condition for further improvement of membrane performance are also thoroughly reviewed.

1. Introduction

Porous materials have attracted attention in many practical fields, such as chemical, medical, optic, electronic, biotechnological, environmental and/or energy applications. Porous materials pose regular pore structures and high surface area useful for materials adsorption, storage [1,2]. According to the IUPAC definition, porous materials are classified into three categories depending on their pore sizes: microporous < 2 nm, mesoporous 2–50 nm, and macroporous > 50 nm [3]. Since the first mesoporous material of MCM-41 was introduced in 1990s, the developments of other mesoporous materials have been extensive [4].

Basic preparation of mesoporous materials are done using template synthesis self-assembled micelles structure from cost-effective silica and carbon sources [1]. It is done by employing organic template molecules under various processes or by employing textural templates where the inorganic precursor condenses [4]. Extensive reports are available on custom developments of novel mesoporous materials for catalyst, sorption, sensing, optics, drug delivery or separation. Mesoporous materials are also attractive for wrapping siRNA to enhance the therapeutic effect on cancer for medical treatment [5,6]. They have been explored to encapsulate fragrances for controlled release and storage of

the odorants [7]. Mesoporous materials such as zeolite and silica are also highly attractive as support for catalyst [8,9] thanks to their inherent selectivity and high surface area [10].

Membranes processes have long been established with widespread applications. They are mostly used to produce potable water from saline water, to treat industrial wastewater effluents and to recover valuable resources from wastewater (via concentration and purification) and to fractionate macromolecular mixtures in the food and drug industries. They have also been established for separation of gases, energy conversion systems artificial organs and drug delivery. The membrane materials employed in those diverse applications differ widely in their structure and function.

Diverse membrane base processes have recently been emerging molecular separations, fractionations, concentrations, purifications, clarifications, emulsifications, crystallization, etc. It is mainly because of the inherent characteristic of high efficiency; operational simplicity, stability and flexibility; high selectivity and permeability in separation applications; low energy requirements; environment compatibility, easy to control and scale-up. Apart for being applied as standalone unit, membrane processes are also very common in hybrid system involving process intensification. They include but not limited to membrane reactors, membrane bioreactors, membrane contactors.

* Corresponding author at: Chemical Engineering Department, Lambung Mangkurat University, Jl. A. Yani KM 36, Banjarbaru, South Kalimantan 70714, Indonesia.
E-mail address: melma@ulm.ac.id (M. Elma).

However, all membranes have several features in common that make them particularly attractive for the separation. The separation is performed by physical means (mostly) at ambient temperature without chemically altering the feed mixture. This is mandatory for applications in artificial organs and in many drug delivery systems as well as in the food and drug industry or in downstream processing of bioproducts where temperature-sensitive substances are handled. The membrane materials used in those applications differ widely in their structure, function and the way they operate. Membrane properties can thus be tailored and adjusted to specific applications.

The versatility of membrane structures and functions makes a precise and complete definition of a membrane rather difficult. A membrane is a barrier that separates and/or contacts two different phases and controls the exchange of matter and energy between the phases. The membrane can be a selective or simply acts as a contacting barrier. In the first case, it controls the exchange between the two phases adjacent to it in a very specific manner; in the second case, it functions as contactor of the two phases in which the transport occurs.

One can distinguish between biological membranes, which are part of the living organism, and synthetic membranes that are man-made. The structure and function of synthetic membranes are much simpler than the biological membranes. They only facilitate passive transport and are less selective. However, they are chemically and mechanically more stable especially at high temperature. The selectivity of synthetic membranes is dictated by sieving property of the pore or the solute solubility and diffusivity within the membrane matrix. The permeability of the membrane for different components, however, is only one parameter determining the flux through the membrane.

Membrane based processes are also driven by different forces, such as concentration different, pressure different, or temperature gradients, or an electrical potential for the charged components. The use of different driving forces results in a number of processes such as reverse osmosis, micro-, ultra- and nanofiltration, dialysis, electrodialysis, pervaporation, gas separation, membrane contactors, membrane distillation, membrane-based solvent extraction, membrane reactors, etc. [11].

Mesoporous silica materials are frequently applied for membrane fabrication in the gas and the water separation and thus worthy of detailed overview. The interaction between the permeating molecule and the membrane material often dictate the separation process. Gas steams or water vapor are abundant with water molecules that easily reacts with the hydrophilic sites in the silica thin films created chemical and microstructural instability. For instance, Giessler, Diniz da Costa [12] reported that sol-gel derived films produced the silanols from hydrolysis and condensation reactions. The presence of silanol bonds collapses of the film structure that lowers the pore volume. Silanol groups form weakly branched fractal systems and has hydrophilic properties. They easily react with water altering the matrix of silica-derived materials. These include organic covalent templates such as methyl groups and noncovalently bonded organic templates such as C6 and C16 surfactants and alkyltriethoxysilanes [12].

To overcome the detrimental interaction of water with the silica material, various templating methods have been developed. It is generally divided into 3 steps: 1) preparation, 2) method selection (i.e., hydrothermal, precipitation, and sol-gel), and 3) templating (dissolution, sintering, etc.). Regular template is sorted into two categories of materials that is naturally and synthesis. One strategy to obtain a good hydro stability of silica is by embedding carbon molecules into the silica matrix. Various materials have been used earlier as carbon sources such as P123 [13], F127 [14], and F108 [15], or citric acid [16]. Recently, more sustainable and low-cost carbon sources have also been explored, such as pectin (from apple peel) [17], banana peel [18]), and also glucose [19]. The Si-O-C bond can be formed after adding carbon materials into the silica matrix. The presence of carbon prevents silica pore from collapsing especially when the material is applied for water desalination. Carbon material also reported has strong covalent bonding

[20] which enhances the mechanical strength.

In this review, we overview of the progress of the advantageous strategies of carbon templates of mesoporous silica materials essentially applied for water desalination. Numerous strategies for carbon templated mesoporous silica were discussed. Finally, applications of carbon templated mesoporous silica materials in water desalination are also discussed.

2. Advanced carbon templated strategies

Materials with nanopore structure allow interaction at atomic, ionic and molecular level since they have large surface area and limited spatial space [21,22]. Nanopores can be classified into macro-porous (> 50 nm), Mesoporous (2 nm – 50 nm) and microporous (< 2 nm). Materials with nanopore has been used in adsorption [23], separation [24,25], catalysts [26,27], and electronics [28,29]. Among many application of nanopores, nanopore carbons (NPCs) have regular inter-penetrations which leads to desirable chemical and physical properties, namely high specific surface, uniform pore structure, good heat resistance and chemical stability, low density and many others [28]. NPCs have been then implemented in hydrogen storage [30], adsorption [31,32], energy storage [33,34] and electronic devices [35].

The most commonly used carbon templating methods include physical (destruction, adhesion and spray) and chemical methods (precipitation, sol-gel, hydrothermal and template) [36,37]. Template synthesis is a method that has been developed since the 1990-an and still widely applied currently. The method is also very easy to do and provide ample flexibility in controlling the structure, morphology and particle size of the resulting materials [38].

Morphology is an important parameter to determine the character of the particle size and pore structure [39,40]. The template method changes the morphology of the product by controlling the nucleation and growth of crystals during the nano-material preparations. It generally consists of 3 steps: 1) template preparation, 2) methods selection (hydrothermal, precipitation, and sol-gel), and 3) templated (dissolution, sintering, etc.). Regular template can be classified into materials that is naturally and synthetic. Also, it is based on the difference between the structure of the template. The templating method is divided into hard templates and soft templates [41,42].

One strategy to obtain a good hydro stability of silica matrix is by embedding carbon molecules into the silica. Various materials have been used earlier as carbon sources such as P123 [13], F127 [14], and F108 [15], or citric acid addition [16]. Recently, more sustainable and low-cost carbon sources have also been explored: pectin (from apple peel) [17], banana peel [18]), and also glucose [19]. The Si-O-C bond can be formed after adding carbon materials into the matrix. The presence of carbon prevents silica pore from collapsing especially when applied for water desalination. Carbon material also has strong covalent bonding [20] which enhances the mechanical strength of the resulting matrix.

2.1. Soft and hard templating methods

The soft templating uses a nano-structure formed through inter-molecular interactions as a template [43]. They do not have permanent rigid structures. During the synthesis of nanoparticles, certain structural aggregates are formed through molecular or intra-molecular (hydrogen bonds, chemical bonds, and static electricity) interactions [38]. The soft template materials are typically organic surfactants and/or copolymer blocks that can interact with metal ions and merge into a liquid crystal phase through the sol-gel process. Pores are obtained after the removal of soft templates via calcination. The soft templating method allows easy control of the structure and pore size relative to the hard template method [43]. The crucial step in the soft templating is the transition of sol-gel precursors in the form of a surfactant/copolymer block [44–46].

The hard templating method is known as nano-casting, mostly

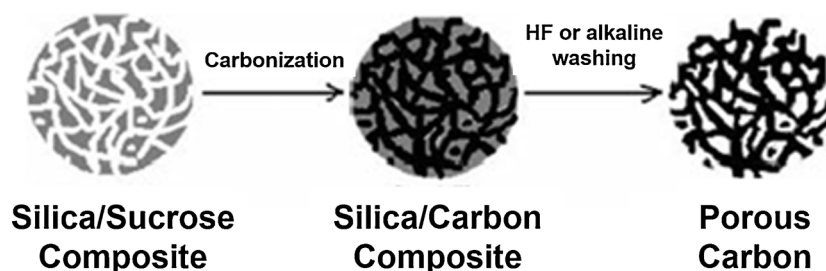


Fig. 1. Principles of porous carbon making [48].

attractive for synthesis of mesoporous materials. Nano-casting uses a solid mould as the template to which a material or precursor is filled. Later, after the formation of the porous material the main mould is removed [43]. For nano-casting of M-TMO, it consists of 3 steps: synthesis of mesoporous replica (eg: silica, carbon, alumina); a metal interphyracy of precursors and decomposition to form materials into crystals; and lastly, removal of the mould to obtain pores.

2.2. Synthesis of carbon templating

The porous carbon synthesis using a particular template necessitate the feasibility to remove the template without damaging the resulting structure [47]. For example, in a method illustrate in Fig. 1, silica and carbon sources are firstly mixed, then the mixture is heated to form solid composites. In the final phase, silica is removed by using the alkaline solvent (Fig. 1) [48].

Synthesis of porous carbon is also applicable to biomass-based carbon by applying a specific template into a carbohydrate-containing biomass [49]. Pang, Li [48] synthesised porous carbon form sucrose with the template of tetra ethyl ortho (TEOS) to form porous carbon (Fig. 2). It was done by applying hydrofluoric acid to leach the silica after carbonization step. The product was a carbon sheet that has pore diameter of 2 nm (Fig. 2). Porous carbon nanoparticles can also be made poly methyl meta acrylates (PMMA) by using silica as the pore-former [49]. The resulting nanoparticles have pore size of 300 nm (Fig. 3).

Liu, Gan [51] synthesized porous carbon from liquid paraffin by using silica as the regulator of carbon porcelain and surfactants to disperse paraffin in water. The synthesis process consisted of two main steps: formation of carbon/silica composite using paraffin carbonization method, followed by elimination of carbon silica by using hydrofluoric acid (HF) or potassium hydroxide (KOH). The illustration of the sythesis process and morphology of the resulting porous carbon are shown in Fig. 4.

Brun, Sakaushi [53] prepared porous carbon from monosaccharides (xylose and glucose) using hydrothermal methods backed by carbonization and silica derived from the synthesis of the Stober method using TEOS as a template. After the composite of carbon and silica was formed, the silica was removed using the ammonium hydrogen di-fluoride. The morphologies of the obtained porous carbon are shown in Fig. 5, which have pore size of 100 nm and 5–8 nm.

Liu, Yao [54] prepared microporous carbon particles from poly (furfuryl alcohol) through carbonization. In this sythesis method, furfuryl polymerization of alcohol was limited from stem-shaped by adding silica or slowed by using surfactants. The detail of preparation steps and the morphology of the resulting microporous carbon with pores of 260–320 nm are shown in Fig. 6.

Porous carbon synthesis can also be done through the hydrothermal method [54]. In this method, the common carbon sources used are hydrolysed hemicellulose, corn cob, and glucose and the template for pore formation is silica nanoparticles. The morphology of the resulting porous carbon can be seen in Fig. 7.

2.3. Mesoporous carbon through mesoporous silica templated

2.3.1. Carbon (C)

Synthesis of porous carbonaceous materials using silica template had been started since 1980s. The porous membranes were developed from a phenol-hexamine mixture as the carbon precursor and silica gel as the template. The carbon can easily be filled thanks to the spacious structure of silica gel [56]. Another templates, such as MgO, have been introduced [57–59]. MgO can be removed by using light acid, but the homogeneity of the resulting mesoporous is lower than the ones with the silica template. Silica template is highly recommended for synthesis of very organized mesoporous architecture coupled with an acid treatment for the template removal [60]. However, the procedure for the template can cause serious environmental problems from the use of the harmful etchants [61].

Template method is superior to control MCs pore structure. MCs with controlled pore structures can be formed by templating mesoporous silica such as Mobil Crystalline Material-48 (MCM-48). Typically, the synthesise of MCs steps involves infiltration of inorganic templates using carbon precursors, followed by template removal [62]. Although this method results in asymmetric membrane, it yields an ordered mesoporous carbon (OMC) [60], like the one obtained using MCM-48 as the hard template. OMC has symmetrical structure and narrow pore-size distribution. Common silica templates for mesoporous carbon fabrication are MCM, Santa Barbara Amorphous (SBA), Fudan University (FDU), MSU-H, and Hexagonal mesoporous silica (HMS) [60]. The pores size of mesoporous silica materials has been listed in Table 1.

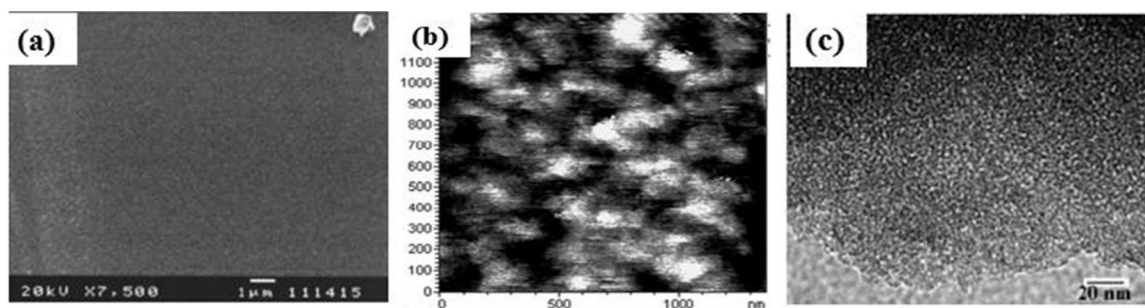


Fig. 2. Morphology of Film Carbon characterization results: (a) SEM appears above, (b) AFM, and (c) TEM [48].

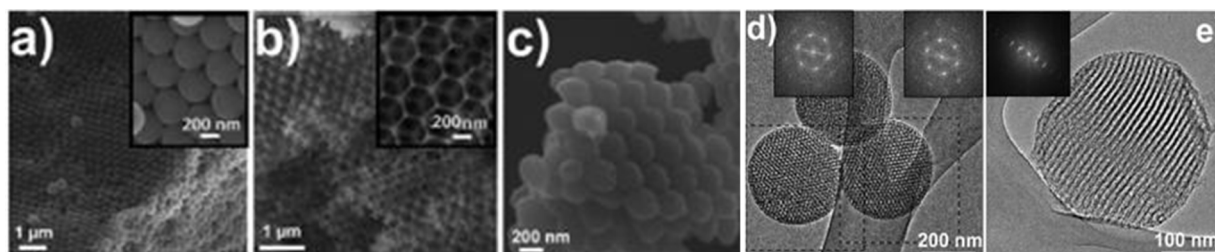


Fig. 3. Morphology of the materials during formation of porous carbon from PMMA as the carbon sources: (a) PMMA, (b) silica, (c) porous carbon products, (d, E) TEM of porous carbon products [50].

Carbon membranes have gained huge interests for desalination [68] and gas separation [69]. MCs based membrane has high pore volume and surface area, high resistance in rigorous circumstances, and is easy to regenerate. The pore size of a MC-based membrane is affected by the carbon precursors and the treatment method [62]. Carbon precursors such as thermosetting phenol resin (TPR), mesophase pitch (MP), and polyacrylonitrile (PAN) have been introduced for fabrication of MCs. MP is attractive to fabricate the porous material with excellent performances due to good graphitizability, high carbonization, and low organic content [62]. TPR offers higher surface area and pore volume of than MP and PAN. However, MP seems more stable during heat treatment [62]. The pores of MCs are formed by letting the small molecules of carbon precursors leach out during carbonization and by removal of the nanosized particles. The resulting pore properties are also affected by dispersion of the nanosized silica and the thermal stabilities.

2.3.2. Mobil crystalline material

Some researchers studied mesoporous silica structure as a template using MCM-48 [70], MCM-41 [71,72], MCM-50. The MCM-48 is very attractive as template for production of MCs because the precursor can form periodic pores arrangement with three-dimensional system. Homogeneous pores are contained in the MCM-48 molecular sieves [73]. MCM-41 is naturally hexagonal mesoporous silica with high surface, pore volume with the pores sizes ranging from 20 to 100 Å [74,75]. MCM-50 has pillared layer or lamellar pores. Among all, MCM-41 has gained the most interest because of its simple structure as shown in Fig. 8. In particular, the porous silica was created using sodium silicate or TEOS as the silicon source, and alkyl ammonium salts as the structure directing agent [74].

2.3.3. Santa Barbara Amorphous (SBA)

SBA-15 as a mesoporous material that has two-dimensional (2-D) hexagonal p6mm symmetry and a channel-type or 3-D mesopore structure. It contains the micropores inside the pore walls [77]. The pore wall structure of SBA-15 is thicker than the MCM-41 [78,79]. SBA-15 can be prepared from TEOS or sodium silicate [80,81] or sodium silicate derived from oil palm ash [82]. It has controllable pore sizes of 5–30 nm range [77,78] with good thermal and hydrothermal stability due to thick pore walls (2–6 nm). SBA-15 may show variety of morphologies such as rods, fibres, spheres, gyroids, doughnut-like and discoid-like shape depending on fabricate conditions [77,83,84].

Various methods of SBA-15 fabrication have been reported, to name a few: grafting and impregnation, direct synthesis, sol-gel and immobilization. Synthetic grafting and impregnation are used to produce covalent attachment of functional groups between organo-silane with silanol groups on surface material [85]. Direct synthesis is a method where the metal source is added directly to the synthesis gel. This method results in SBA-15 of high specific area and pore volumes, but owing to low pH, it requires a high amount of the extra aluminium network [86]. Pore structure, size and shape of SBA-15 can be properly arranged when employing sol-gel synthesis method that works under modest temperature and results in high purity [87].

2.3.4. Fudan University (FDU)

The 3D pore structures of FDU-12 s are face-centred cubic structure with close packing of spherical cages, each is connected to 12 nearest neighboring cages [88]. It can be fabricated from non-ionic triblock copolymer F127 as a template, TEOS as silica precursor with 1,3,5-trimethylbenzene (TMB) and potassium chloride (KCl) as additives.

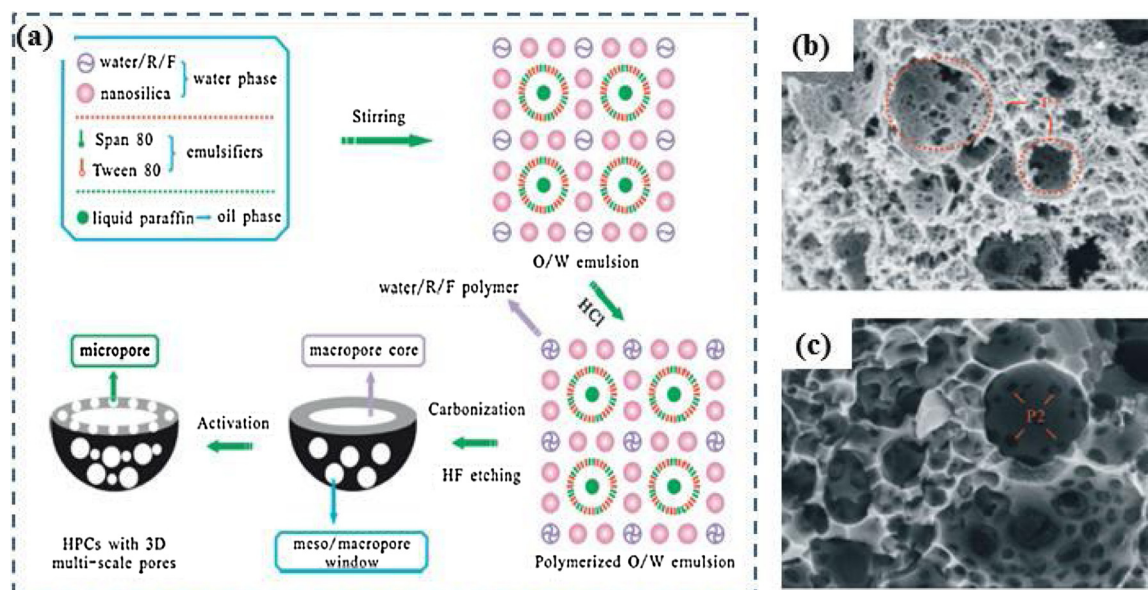


Fig. 4. (a) illustration of the porous carbon synthesis process, visualizing SEM from porous carbon with magnification: (b) Low and (c) high [52].

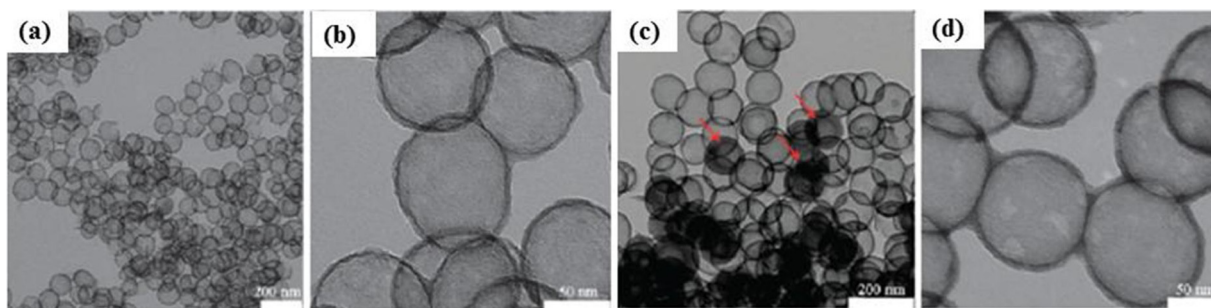


Fig. 5. TEM of carbon-based products: (A, B) Xylose and (c, D) glucose [52].

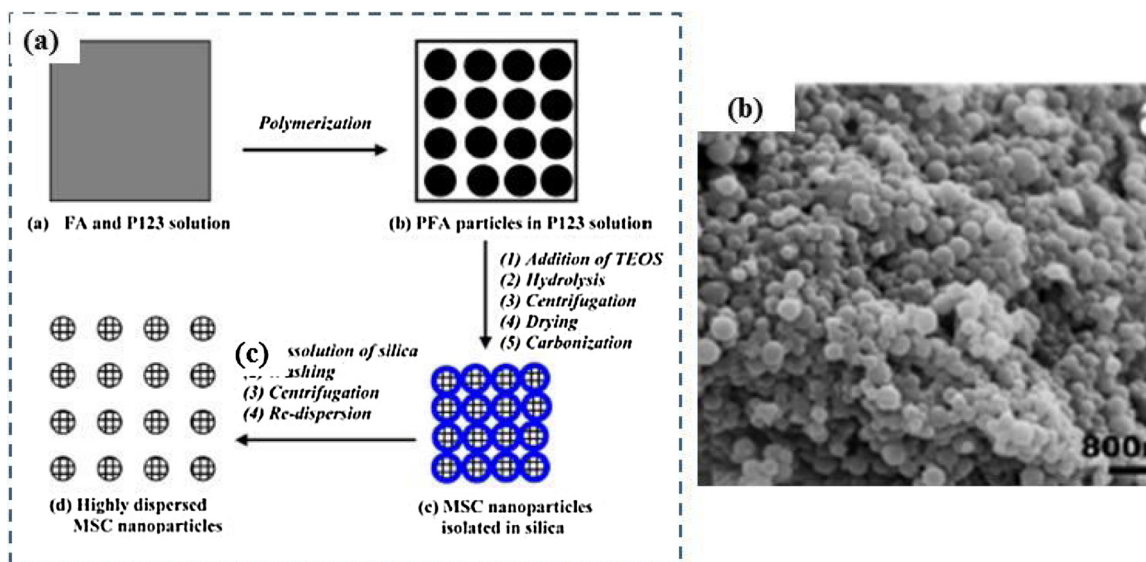


Fig. 6. (a) Illustration of porous carbon synthesis and (b) TEM of carbon [54].

TMB is used to enhance the volumetric ratio of the hydrophobic core and to turn it hydrophilic, which leads the structure changes from a body-centred cubic to a face-centred cubic [89]. Fabrication at low temperature (15 °C) results in highly ordered cubic of FDU-12 silica with pore diameters of 22–27 nm [89].

2.3.5. Messtructured MSU-H

The porous framework of MSU-H is similar to that of SBA-15 that consists of ordered large pores connected by micropores [90]. These large two-dimensional pore channels allow easy penetration of carbon with better pore sizes adjustment compared to the SBA-15 or the MCM-

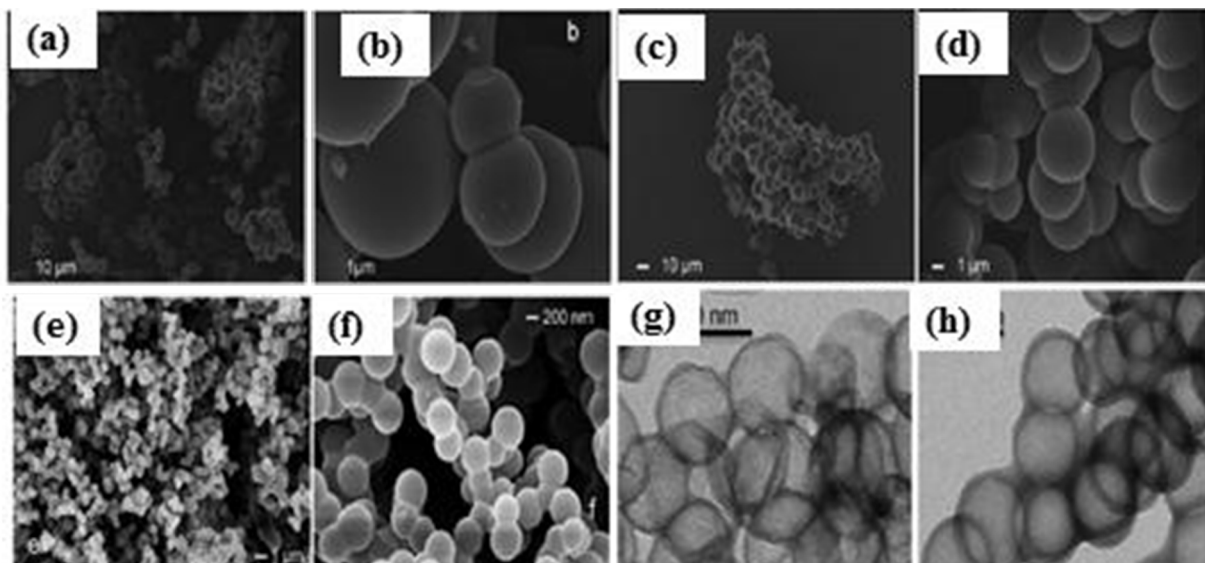


Fig. 7. Morphologies of porous carbon prepared from hydrothermal method: (A, b) hemicellulose hydrolysis, (c, D) Corn Cob, (e, F) glucose, and (g, h) TEM of carbon nanoparticle Products [55].

Table 1

List of pore size of mesoporous silica used as template for porous carbon membrane synthesis.

Material type	Pore size (nm)	References
MCM-48	2–5	[63,64]
MCM-41	1.5–8	[63,64]
MCM-50	2–5	[65]
SBA-15	6	[63]
FDU-12	5–36	[66]
MSU-H	3–10	[64]
HMS	2.9–4.1	[67]

41 [91]. MSU-H silica can be obtained from sodium silicate under neutral pH in the presence of triblock copolymer [92]. OMC membrane using sucrose as precursor and MSU-H as hard template was successfully fabricated Zeng, Zhao [91]. The resulting OMC has a large surface area of $1019 \text{ m}^2 \text{ g}^{-1}$, large volume ($1.46 \text{ cm}^3 \text{ g}^{-1}$) and uniform mesoporous structure (with pore size distribution with modus at 4.2 nm).

2.3.6. Hexagonal mesoporous silica

HMS is a mesoporous silica template with high surface area [93], prepared via soft templating from neutral long chain of *n*-dodecyl amine [94,95]. The long range hexagonal structure can be formed from a long chain template. There are few advantages of using HMS over MCM-458, namely inexpensive structure-directing agent (primary alkyl amines), high silica recovery yield (> 95 %, higher than the MCM-48 of ~50 %), fast synthesis (18 h for HMS and 4 days for MCM-48), does not involve hydrothermal reaction [96], thicker walls than SBA-15 [79], and the template is easy to remove. HMS has also been considered as a potential template for drug carriers thanks to its volume for drug molecule loadings [97].

2.4. Mesoporous silica through mesoporous carbon templated

Owing to excellent chemical, mechanical, thermal and molecular sieving properties [98–100], the mesoporous silica membranes have been favorably applied for gas and water desalination processes. The fabrications of such membranes involve several types of silica precursors such as TEOS as the most popular [101], tetramethoxysilane (TMOS), methyltrimethoxysilane (MTMS), and methyltriethoxysilane (MTES) [102].

In recent studies, ethyl orthosilicate-40 (ES-40) [103,104] was employed to fabricate this membrane. ES-40 contains about 40 wt% SiO_2 and an average of five Si atoms per molecule. It is produced by reacting ethanol, water and silicon tetrachloride or through partial hydrolysis and condensation processes of TEOS. However, unlike TEOS, ES40 has lower hydrolysis rate but higher condensation rate [105]. The produced silica is stable for up to 250 h of long term performance test [106]. However, the silica pores collapse easily because the hydrophilic silanol group (Si–OH) is reactive with water [107,108]. The hydrostability can be enhanced by templating the carbon source into the

silica resulting in improved properties of high mechanical strength, good electrochemical performance, and good thermal and adsorption properties [109] [110].

2.4.1. Pluronic surfactant

Pluronic has been used as a template during formation of CPM to create ordered porous structure. The pluronic concentration and the initial temperature are important aspects of forming a micelle. After the micelle formation in acid solution, poly(ethylene oxide) (PEO) blocks in micelle can interact with the framework precursor (TEOS or TMOS) [111]. Because of the high acidity of the solution, the framework condenses and forms a silica network around the micelle as shown in Fig. 9. During the synthesis of mesoporous organo-silica (PMO), PMO is formed when nonionic surfactant consisting of PEO is added. It results in formation of Si–C bonds through condensation of templated carbon surfactant, such as $(\text{RO})_3\text{-Si-R}^*\text{-Si-(OR)}_3$. Then, hydrolysis and cross-link occur between the terminal groups of the bridged bis(trialoxysilyl) organo-silanes [112,113].

SBA-16 can be prepared by employing Pluronic F127 to form high quality mesostructured [114]. Some studies report smaller pore sizes of SBA-16 from copolymer blends of P123 and F127 [115] or nonionic oligomeric surfactants [116]. F127 has critical micelle temperature of 31 °C at 0.1 % w/v. At higher concentration of 0.25 % w/v, the CMT is diminished at the 28 °C [111].

When Pluronic-123 (P123) as a carbon source is incorporated into silica structures, it produces more robust structures demonstrated by high performance of membrane filtration when using the silica-P123 than the pure-silica [103]. It was also found that at low P123 concentrations, the carbonized templates uniformly attached onto the silica matrix forming more microporous network. Higher concentrations of P123 lead to higher hydro-stability.

2.4.2. Natural carbon sources material

To address the challenge of providing renewable resources at low cost, it is very important to utilize non-food related materials as the carbon sources. Several studies report the use of pectin extracted from apple [118] and banana peel [119] as the carbon sources to fabricate carbon templated silica. The pectin in the silica matrix prevents the silica networks from collapsing toward water. The polysaccharides from pectin allow formation mesoporous structure. Sucrose has also been used as the carbon precursor through hard-template method for formation of MCM [120]. Sucrose is environmentally benign material that contains multiple adjacent hydroxyl groups that form hydrogen bonding with silica oligomers. However, there are only a few reports of sucrose incorporated into silica via the soft template.

3. Mesoporous silica materials

3.1. Recent techniques, fabrication and application

3.1.1. In-situ synthesis

In the modified in-situ synthesis, cetyltrimethylammonium (CTAB)

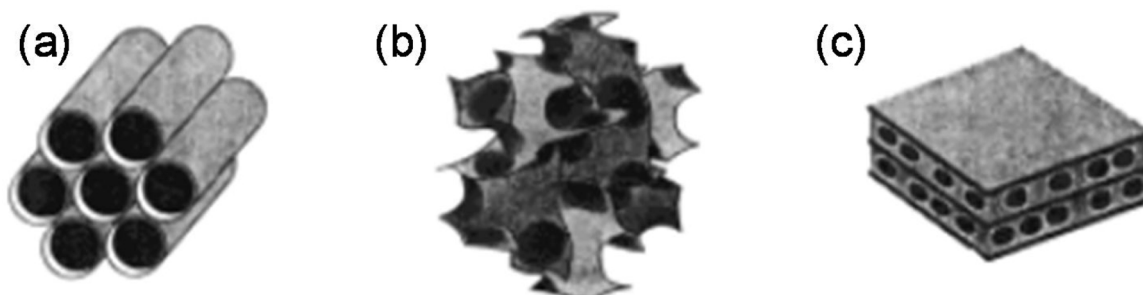


Fig. 8. Visualization of pore structures in MCM-41, MCM-48 and MCM-50 [76].

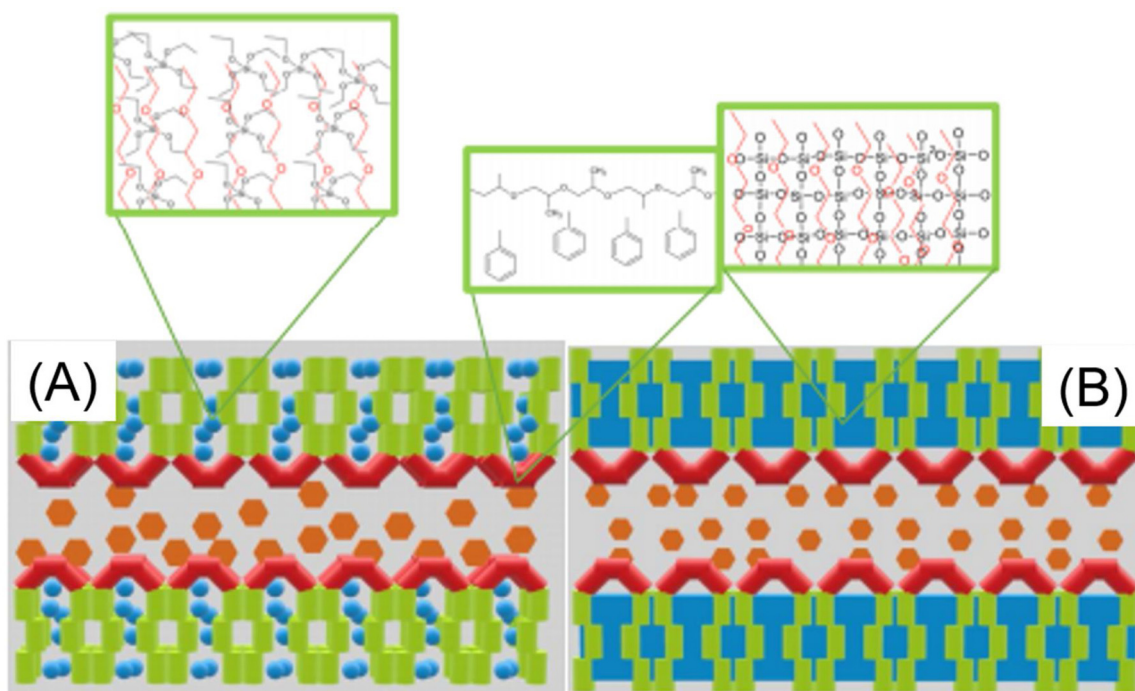


Fig. 9. Illustration of micelles formation with Pluronic-silica precursor and swelling agent before (A) after condensation (B) [117].

and urea were firstly dissolved in water. Next, cyclohexane, MI IPA, TEOS of 2.5 mL 3% mol (2-cyanoethyl)triethoxysilane (CETEOS) were added drop-wise [121]. After stirring for 30 min at room temperature, it was heated to 70 °C and was allowed to react for 16 h. The results obtained were silica fibrous particles or $\text{SiO}_2\text{-CN}_3$. By adopting the same method and by employing pure TEOS, it resulted in formation of Fi-SiO_2 [122].

Although in-situ synthesis produces mesoporous sizes of 10–20 nm on Fi-SiO_2 , $\text{SiO}_2\text{-CN}_3$ or $\text{SiO}_2\text{-CN400}$, addition of N_2 during the N_2 adsorption-desorption analysis increases the absorption and hysteresis H_3 at $\text{P/P}^\circ > 0.95$. It suggests that there are a number of macropore gaps related to the SiO_2 microspheres fibrous morphology [123,124], higher than the F-SiO_2 (of 55 nm). Both $\text{1-SiO}_2\text{-CN}_3$ and F-SiO_2 microspheres have relatively high specific surface area and total pore volume of microspheres [125,126]. The specific surface area ($\text{m}^2 \text{g}^{-1}$) sizes of 399.2 for F-SiO_2 , 252 for $\text{SiO}_2\text{-CN}_3$ and 298 for $\text{SiO}_2\text{-CN400}$ and the total pore volumes ($\text{cm}^3 \text{g}^{-1}$) for F-SiO_2 , $\text{SiO}_2\text{-CN}_3$, $\text{SiO}_2\text{-CN400}$ are 1.14, 0.99 and 0.89, respectively. Based on available data it shows that the in-situ method may produce mesoporous silica.

3.1.2. The spinning coating

Thin film synthesis using the spinning coating process has also been reported [127]. The fabrication starts from a mixture of NaOH, cetyltrimethylammonium chloride, CTAC, water and methanol mixture, tetramethylorthosilicate, mixture of MOS and aminopropyltrimethoxysilane and APT-MS to form a sol. The formed sol is stirred for 12 h at room temperature and is let idle for 8 h. To prepare a thin film via the spinning coating processes, a template of mesopore-free silica particles is dispersed in ethanol by ultrasonication at 2.5–10 % w/w. The dispersion is then coated on a substrate and spun at 500–2000 rpm for 40 s as detailed elsewhere [128].

The BET characterization shows that the resulting particles have diameter of 2.6 nm and surface area $499\text{--}942 \text{ m}^2 \text{g}^{-1}$, suggesting that they are mesoporous in structure. SEM images reveals that there are still some structural defects with variation in the thicknesses due to the presence of agglomerates either in the original dispersion or formed during spinning. In order to study the generality of the used spinning coating process, corresponding films were also prepared using amino-

functionalized mesoporous silica nanoparticles under otherwise identical conditions. The surface chemical properties of the nanoparticles are found to be important affecting the interactions of the nanoparticles and the biological environment [129].

3.1.3. The electrospinning coating

Mesoporous silica can also be prepared through the electrospinning coating process as reported elsewhere [130]. The base materials are TEOS mixture with H_3PO_4 that drop-wise added during stirring/mixing. Then a 10 % PVA solution is added into the silica sol as additive to ease the spinning. Next, an alumina sol with a molar composition of $\text{Al}(\text{NO}_3)_3 \cdot 9\text{H}_2\text{O}:\text{AlCl}_3 \cdot 6\text{H}_2\text{O}:\text{Al}(\text{O}-i\text{-Pr})_3:\text{Al}:\text{H}_2\text{O}$ of 1:1:2:4:178 is prepared through hydrolysis and condensation reactions under constant stirring at 80 °C. An appropriate amount of HNO_3 is then added to the mixture to adjust the reaction rate and control the pH of the final sol from 3.24 to 4.23. Then, 0.1 g of PEO and 6.0 g of P123 are added into 40 mL of as-prepared alumina to improve the spinnability of the sol and to direct the pore structure formation, respectively. The mixture is then stirred for 12 h to form a spinnable sol. To fabricate $\text{SiO}_2/\text{Al}_2\text{O}_3$ core-shell fibrous membrane, the sol silica and sol alumina are put into A separated syringes. The one for sol silica is connected to a core needle ($d = 0.4 \text{ mm}$), while the one for alumina sol is connected to a shell needle with an inner diameter of 1 mm. The flows in the needle are set alike at 2 mL/h. The distance between the spinneret and the aluminium collector is 17 cm and the voltage of 18 kV. The spinning is conducted under ambient condition. The electrospun xerogel core-shell fibrous membranes are collected on the aluminium foil and are further dried at 90 °C for 12 h, and then are calcined at 700, 800 or 900 °C for 2 h at a heating rate of $10 \text{ }^\circ\text{C min}^{-1}$ [131].

The BET analysis reveals that higher calcination temperature leads to lower specific surface areas [132], with the values of 134, 104 and 79 m^2/g at 700, 800 and 900 °C, respectively. The pH of the precursor also affects the pore volumes in which the pHs of 3.24, 3.53 and 4.23 correspond to the pore volumes are 0.387, 0.589 and 0.655 $\text{cm}^3 \text{g}^{-1}$, respectively. Considering that the high surface area corresponds to a large adsorption capacity, the reports [133] select the precursor pH of 4.23 as the most promising condition to fabricate the shell in the coaxial electrospinning process.

3.1.4. Extraction from pumice stone

Mesoporous silica can be fabricated from pumice via extraction. The resulting mesoporous silica has a high purity and shows the presence of siloxane and silanol groups. However, the extraction process takes so many steps and over a very long period. The fabrication process starts with dissolving a pumice in 3 M NaOH solutions in a three necks flask equipped with a condenser for 24 h at 100 °C and a stirring speed of 300 rpm to produce sodium silica. The obtained sodium silica is then washed and heated with distilled water. Silica settles at pH below 10, which is required to form silica gel under acidic condition. Furthermore, the solution is titrated with H₂SO₄ (5 M) until reaching pH 7, then is let idle for 24 h to allow formation of a white precipitate. The precipitate is then filtered, and the solid residue is dried at 80 OC for 24 h. The residue is then refluxed with 1 M HCl at 110 OC for 3 h to purify silica from other soluble minerals (Al, Ca, Fe and Mg). The refluxed solution is then filtered and dried at 110 OC. The last step is calcination at 800 OC to produce a white silica powder [134].

The resulting pumice powder composes of mostly silica (confirmed from FTIR and chemical analysis) main minerals content of clinopyroxene (diopside, augite or basanite types), forsterite and other (apatite and haematite) in minor quantities [135–138]. The pure silica structure is amorphous as demonstrated by strong peak at 2θ of 15–30°. FTIR peaks analysis show the narrow band centred at wavelength 1039 cm⁻¹ may be attributed to the presence of silica with the highest percentage [139], as also confirmed by chemical analysis. The predominant bands at wavelength 1101 cm⁻¹ and the shoulder at 1193 cm⁻¹ are associated with asymmetric stretching-vibrations of siloxane (Si-O-Si). The presence of bands at 470 cm⁻¹ and 810 cm⁻¹ is from symmetric siloxane groups (Si-O-Si). The existence of a band at 950 cm⁻¹ is associated with Si-OH groups from silanol groups with smaller particle sizes [140]. The shoulder appeared at 3750 cm⁻¹ indicates the presence of hydrogen bonds from interaction between the silanol groups (Si-OH) located at the surface of the nanosilica material [141]. BET results show that the pore size of the silica is in range of 2–6 nm indicating of the mesoporous structure, with a pore volume of 0.645 that exceeds the size of the nanoparticles of 0.195 cm g⁻¹ with the surface area of 422 m² g⁻¹.

3.2. Recent trends on the ordered and the disordered mesoporous silica materials

Summary of structure and pore size distribution of silica-carbon base materials is presented in Table 2. It summarizes the main properties of recently developed ordered and disordered mesoporous silica materials discussed in this sub-section.

3.2.1. TEOS : EtOH : C₆H₁₂O₆ : H₂O

Ordered mesoporous silica materials is a promising material in the field of technology membrane filtration. Synthesis of order mesoporous silica have recently been developed by directly assembly of organic or carbon template [149]. Elma et al. reported development of direct acid catalyst for preparation of mesoporous carbon template silica membranes with ordered structure on porous α -alumina support. The

ordered mesoporous silica membranes made from organocatalytic posed relatively high surface area and pore volume of 354 m² g⁻¹ and 0.215 cm³ g⁻¹ g⁻¹, respectively. The citric acid catalyst acts as a carbon source in the silica matrix and increases the hydro-stability of silica networks. Absorption of the N₂ curve shows xerogels refluxed at 0 and 50 °C are included in type IV H4 [142]. While Elma et al. work found surface area and pore size of 475 m² g⁻¹ and 1.94 cm³ g⁻¹ [143].

3.2.2. TEOS : EtOH : HNO₃ : H₂O : NH₃

Modified the sol-gel process is needed to reduce the amount of silanol group. Reflux temperature can be adjusted to get optimum condition for ordered mesoporous silica. The ordered mesoporous silica materials were also preserved during reflux temperature on sol-gel process. The sol-gel was refluxed at 0 and 50 °C to achieve the lowest and the highest siloxane concentrations with calcined xerogel at a pH of 6 or 9. Xerogel at pH 6 and 9 shows a tendency to form micro and mesoporous materials as adsorption saturation is achieved above 0.65 P/P° with capillary condensation leads to hysteresis near 0.5 P/P°. The average pore diameter each was measured around 2.6–2.7 nm and showed type IV isotherm curves with hysteresis loops indicating the mesopore structures. In other hand, silica-based materials of pH 7 and 8 had type I isotherms curves without hysteresis indicating of microporous material. The BET surface area (~ 420 m² g⁻¹) and total pore volume (~ 0.18 cm³ g⁻¹) were proportional to the pore size of about 1.8 nm. Therefore, micro-porosity was correlated well with high concentrations of silanol groups [143]. While silica sol mixed with various variations of cobalt oxide (5 %–35 % w/v) obtained at pH 6 and produced mesoporous membrane. The BET results show that the isotherms of the two samples were type IV, ascribing the characteristics of the mesoporous material. The greater addition of Si-Co concentration, the larger was the surface area, volume and pore size. This was because the cobalt oxide in xerogel increased the silanol and siloxane groups to enlarge the pores [150].

3.2.3. TEOS : TEVS : EtOH : HNO₃ : H₂O : NH₃ : P123

Triethoxyvinylsilane (TEVS) is frequently used to produce microporous silica membranes on interlayer porous substrates [146]. It contains vinyl groups as silica ligand pendants. The silica methyl ligand pendant group is known to produce high-quality microporous silica membranes. In order to form mesoporous structures, TEVS and other silica precursors are combined using TEOS with the addition of P123 non-ligand triblock copolymer as a template. Then the sol-gel synthesis is carried out with a base catalyst which allows its deposition directly to the porous substrate without using interlayers. The non-ligand surfactant is embedded into the silica matrix followed by carbonization. High-quality carbon can be prepared using ligand and non-ligand templates together with the co-polymerization reaction of two different silica precursors where TEOS does not have a template while TEVS has a ligand template based on the vinyl group. Then the xerogel and silica membrane are calcined under vacuum or N₂ atmosphere. Carbon silica hybrid membranes are represented as CS-N₂ (calcined under N₂) and CS-Vc (calcined under vacuum air) calcined at 450 °C. The isotherms of the order P123 template TEOS-TEVS is type IV of the mesoporous

Table 2

Summary of silica-carbon base material structure and pore size distribution.

Material type	Calcine technique/ temp. (°C)	BET surface area (m ² g ⁻¹)	Pore volume cm ³ g ⁻¹	Pore size (nm)	Ref
Organosilica	RTP (inert atm)/200	315	0.16	2.5	[142]
Pure silica	CTP (vacuum)/600	420	0.18	1.8	[143]
Silica P123	RTP (inert atm)/350	572	0.31	2.2	[144]
Silica P123	CTP (vacuum).450	965	0.50	2.3	[145]
TEVS	CTP (vacuum)/350	761	0.55	< 2	[146]
CTAB	CTP/550	925.1	0.20	3.1	[147]
Ni-Si	CTP	450	–	2.5	[148]

material. The interlayer-free carbon-silica hybrid membranes were successfully prepared by adding template of pluronic triblock copolymer (P123) and vinyl pendant ligands in TEVS in synthesis sol-gel also contain TEOS as the second silica precursor. Both the vacuum calcined and the N_2 samples exhibit mesoporous properties with high pore volume, but the calcined vacuum samples (CS-Vc) produces more carbon structure in the silica matrix resulting in better desalination performance. Surface area and pore volume of CS- N_2 membrane are $754 \text{ m}^2 \text{ g}^{-1}$ and $0.546 \text{ cm}^3 \text{ g}^{-1}$ while CS-Vc membrane are $761 \text{ m}^2 \text{ g}^{-1}$ and $0.615 \text{ cm}^3 \text{ g}^{-1}$. The CS-Vc membrane produces water flux much higher than previously reported for processing saltwater. The combine method of organo-silica hybrid with polymer template and vacuum calcination produces mesoporous silica membrane carbonization very well for the separation of water from hydrated salt ions, and exhibits high water flux especially for processing brine salt solutions [148].

3.2.4. TEOS : TEVS : EtOH : HNO₃ : H₂O : NH₃ : K₂S₂O₈

Hybrid silica membranes can be prepared by mixing TEOS and TEVS using K₂S₂O₈ (KPS) as an initiator Elma, Wang [146]. The KPS provides radical polymerization to create C–C bonds as a secondary network and then to produce more space in the silica network. The radical polymerization formed by KPS affects the growth of oriented particles. In order to avoid decomposition of C–C groups in the silica matrices, the calcination process is held up to 350 °C. Densification is then formed when the ratio of TEVS is greater than TEOS composition. The TEVS:TEOS molar ratio is 10:90 and produces micro-porosity. Pure TEVS is not suitable to produce amorphous silica material, because the functional groups formed were found blocked inside the pores. As such, the xerogel hybrids containing TEVS become microporous. The isotherms found the saturation process at very low relative pressures ($p/p^\circ < 0.05$). It is due to the mixing between TEVS and TEOS is greatly reduced and this trend continues as a function of TEVS [146].

3.2.5. TEOS : EtOH : NH₃ : H₂O : CTAB (cetyltrimethylammonium bromide)

Mesoporous silica carbon template materials have been explored and developed very fast to competes in desalination application. Carbon template is one of effective strategy to stabilized the silanol group of silica membrane. Recently, Ashrafi-Shahria, Ravaria [147] used CTAB surfactants as template to embedded into silica. Silica precursors were synthesized at 550 °C to remove cationic templates from CTAB required to form the mesoporous structures. Order mesoporous silica (MS) nanoparticles were synthesized and then functioned by Eriochrome Black T (ECBT) as a corrosion inhibitor. Composite coating systems (a combination between Ti-Zr conversion layers and organic/inorganic hybrid sol-gel) were applied instead of simple sol-gel films to provide better corrosion protection and adhesive strength. Nitrogen adsorption-desorption isotherms were plotted with BJH plots from MS nanoparticles before and after loading of the inhibitors. The N_2 physisorption data showed that the surface area and pore volume of MS were $925.1 \text{ m}^2 \text{ g}^{-1}$ and $0.2025 \text{ cm}^3 \text{ g}^{-1}$, while the surface area and pore volume of MS-ECBT were $103.1 \text{ m}^2 \text{ g}^{-1}$ and $0.0561 \text{ cm}^3 \text{ g}^{-1}$. It is clear that the specific surface area of MS nanoparticles is greatly decreased by the final functionalization process due to the addition of ECBT molecules in the mesoporous space. In addition, the pore volume of MS nanoparticles is greatly decreased by loading of inhibitors. However, the pore diameter of MS nanoparticles did not change significantly after the loading inhibitor because the structure of nanoparticles could not be affected by the functionalization process [147]. This is also similar to that study-explained by Vazquez, Gonzalez [151], in which surfactants play an important effect in changing the morphology of particles, but it cannot change pore size and pore diameter.

3.2.6. TEOS : EtOH : Ni(NO₃)₂ · 6H₂O : H₂O₂ : H₂O

The ordered of nickel oxide sol are synthesized by hydrolysis and condensation of TEOS in ethanol with and without 30 % H₂O₂ water

and nickel nitrate hexahydrate (Ni(NO₃)₂·6H₂O). The tendency of the silanol/siloxane ratio clearly showed that the role of H₂O₂ was favoured by the formation of silanol groups and slightly inhibited the condensation reaction. The presence of H₂O₂ acidified the the sol-gel process by the presence of nitric acid which promoted the formation of silanol groups and microporous materials.

Nitrogen adsorption isotherm of ordered xerogel doped with nickel by addition of H₂O₂ produced a type I isotherm curves ascribed by very strong initial adsorption at very low partial pressures ($P/P^\circ < 0.2$) followed by saturation ascribing the characteristic of type I micropores. Whereas nickel doped xerogels without H₂O₂ formed mesopores with higher adsorption saturation capacities above 0.4 P/P° and hysteresis with subtle inflection indicating the type IV isotherms. Surface area for ordered mesoporous nickel oxide with 10 % H₂O₂ was affected by the Ni/Si molar ratio. The average pore diameter with H₂O₂ remained constant at $2.1 \pm 0.05 \text{ nm}$. Addition of nickel oxide to silica gel matrix with H₂O₂ could maintain the micro-porosity of amorphous silica xerogel. Whereas samples without H₂O₂ produced meso-porosity that increased significantly as a function of Ni content as the average pore size increased while the BET surface area decreased for a Ni/Si ratio of 25–50%. This effect had also been observed for cobalt silica oxide, and increased meso-porosity is associated with cobalt oxide agglomeration. Perhaps, the same effect also occurs on increasing the shaft as a function of the Ni/Si molar ratio in this work [52].

4. The application of carbon templated mesoporous silica materials

Carbon templated mesoporous silica membranes are excellent material for pervaporation, a process to separate liquid mixtures by vaporization and selective permeation and through a membrane [152]. It uses molecular sieve type of membranes that permits only passage to water molecules under driving force of a water vapor pressure difference [10]. Highly permeable and selective membranes can be prepared via sol-gel method that offers great advantages in the control of pore sizes [10,143,152,153]. Recent advances in the preparation of carbon template mesoporous silica membranes have opened avenue to substantially improve pervaporation performance with respect to flux, selectivity and stability. Conscientious adjusting of carbon-silica template mesoporous structures makes it possible to design membranes as coveted of respective separation applications.

Carbon template silica membranes have also widely been applied for gas separation, particularly the ones with microporous structures [154–157]. Microporous molecular sieve carbon-silica base membranes can also offer the considerable advantages in comparison to the zeolite, the polymeric or the carbon-based membranes [157]. Whereas, membrane materials with mesoporous structure are more appropriate for water desalination [143,158,159]. The carbon templated molecular sieve mesoporous silica materials are gaining popularity for desalination, which is detailed in the following section.

4.1. Hydro-stability of silica-carbon templated and current strategies for water desalination

Desalination via pervaporation is promising to produce fresh water from non-potable saline sources. It offers advantages of a high salt rejection and the capability of treating a high salinity solution. Novel mesoporous silica base membranes for desalination have recently been developed. Because of the affinity of amorphous silica for water adsorption, pure silica-derived membranes suffer from structural degradation when in contact with water, leading to a loss of selectivity. Hydro-stability is therefore a severe problem which prompts the recent studies on altering the surface properties of the silica to lessen the interaction of water molecules with the membrane structure.

One strategy to address hydro-stability problems is by introducing a non-covalently bonded organic templates into the pure silica matrix



Fig. 10. Schematic of mechanism for stabilization of the carbon template silica pore structure.

[12,157,160]. The existence of carbon moieties embedded into the silica framework can inhibit the mobility of soluble silica groups under hydrolytic attack and consequently hinders micropore from collapsing [10,154]. The carbon templates and silanol groups (Si-OHs) interact weakly via the electrostatic interaction to form a peculiar structure derived from a hydrophobic core and hydrophilic exterior properties [161]. The carbon templates obstruct the micropore spaces to forbid the mobility and degradation of the silanol groups.

For the first time, Raman and Brinker [160] demonstrated a breakthrough organic templating approach to fabricate the molecular sieving organo-silica membranes. It results in high flux and selectivity membrane for gas separation. The hydrophobic carbon template improves the hydrothermal stability of the silica membranes. In similar research done by Duke, da Costa [154] report carbonized template molecular sieve silica (CTMSS) as new material for wet gas separation. The C6 surfactant hexyl trimethyl ammonium bromide is embedded into CTMSS as carbon template to achieve a great hydro-stability via hydrophobic surface functionalization. The mechanism of carbon templates in imposing hydro-stabilization toward exposure to water is illustrated in Fig. 10.

Both mesoporous silica and template carbon materials alter the surface chemistry to limit water in breaking the siloxane groups (hydrolysis) and allowing for dissociative chemisorption, as detailed elsewhere [162]. Normally, the rehydration on the silica surface is done by a physisorption of water to form a hydroxyl group, followed by a chemisorption with the nearby siloxane groups. As more silanol groups are formed, more sites become available for H₂O sorption and a chain reaction of siloxane breakage occurs across the surface. The mobility of silica groups then becomes localized in the higher-attraction-energy regions in the smaller pores, where thermal condition above 180 °C causes a subsequent cross-pore condensation leading to their closure.

Fig. 10 demonstrates how the carbon moieties templated into silica matrices prevent the mobility of silica groups under hydrolytic attack and inhibits micropore cave in. The entrapment of carbon moieties in the carbon template silica matrix is facilitated by carbonization of the templates under vacuum or an inert atmosphere, leading to a hybrid silica/carbon membrane. Carbon template membranes thus offers a great potential for achieving hydro-stability without compromising the selectivity [162]. The carbon-silica template membranes have also been tested for desalination of saline water (NaCl 3.5 wt%), demonstrating high salt rejection [163].

Carbon templated mesoporous silica materials have a pore size of 0.3–10 nm and thus are very suitable for desalination applications [145,158,163–165]. Wijaya, Duke [166] reported the investigation of carbon chain length of ionic surfactants effect toward CTMSS membranes for desalination by preparing sol-gels with C6, C12 and C16. The CTMSS membrane fabricated with the longest carbon chain C16 surfactant delivered the highest salt rejection, whilst also given the largest pore volume and surface area. Interestingly, the average pore sizes of

the membranes were identical for the three surfactants used.

Ladewig, Tan [165] investigated the potential of a polyethylene glycol-polypropylene glycol-polyethylene glycol (PEG-PPG-PEG) as the template non-ionic surfactant. The enhanced carbon content up to 10% increased the pore volume and the specific surface area. Consequently, the membrane demonstrated a slightly higher flux of 3.7 kg.m⁻².h⁻¹ and 985% of salt rejection at room temperature compared to the surfactant template membranes mentioned above, that is 2.2 and 3 kg.m⁻².h⁻¹, respectively. The embedded carbon has a beneficial role in silica matrices and the amount embedded has a direct impact to performance of the carbon-silica template.

4.1.1. Effect of operation condition on performance of carbon template silica membranes

Table 3 summarizes the reports on carbon template silica performance in terms of water flux and salt rejection. Performance of membrane in pervaporation is affected by the testing conditions such as feed temperature, feed salt concentration and permeate vapor pressure. To achieve optimum performance, it is necessary to study the effect of testing parameters on water flux and salt rejection. A change of feed concentration directly affects sorption at the liquid/membrane interface [161]. Since diffusion in the membrane is concentration dependent, the water flux generally decreases with increasing salt concentration in the feed [10,145]. Mass transfer in the liquid feed side may be limited by the extent of concentration polarization. In general, when the feed flow rate increases, water flux also increases due to a reduction of transport resistance in the liquid boundary layer and reduction of the concentration polarization.

The feed temperature exponentially increases the water flux. It is because when feed temperature increases, the vapor pressure on the feed side increases exponentially, while the vapor pressure on the permeate side remains constant. The raising of vapor pressure leads to an increase in the driving force of the water vapor transport, thus improving the water flux. The diffusion coefficient of water vapor increases by four times as the feed temperature is raised from 20 to 65 °C [153]. Moreover, high temperature increases the frequency and amplitude of thermal motions of the polymer chains, which can bring about the free channels of polymer promoting the water vapor transport. The carbon templated silica membranes have been widely reported and developed for water desalination application [17,19,99,109,144–146,159,163,164,166–170].

Pervaporation using inorganic membranes based on mesoporous silica offers high salt rejection, but rather low in water fluxes especially for saline solution (NaCl 3.5 wt%). These low performances diminish the chance of the pervaporation using inorganic membranes to compete against the reverse osmosis (RO) processes. It is, however, worth noting that the results are dependent upon many parameters related to testing condition, including the feed concentration, the feed temperature, the permeate vapor pressure and the fouling/scaling tendencies. In

Table 3

The summary of carbon template silica performance in terms of water flux and salt rejection in pervaporation for desalination.

Membrane types	Condition testing (calcination technique/ ΔP)	NaCl conc. (wt.%)	Water Flux (kg. m ⁻² h ⁻¹)	Salt Rejection (%)	Ref.
Silica-pectin CTMSS C6	RTP inert atmosphere/1 atm/25 °C	3.5	0.22–5.7	> 99	[107]
	CTP vacuum/7 bar/25 °C	0.3	3.2	86	[163]
		3.5	1.4	92	
CTMSS C12	CTP vacuum/7 bar/25 °C	0.3	2.8	86	[163]
		3.5	1.6	94	
		0.3	2.1	> 98	[163]
CTMSS C16	CTP vacuum/7 bar/25 °C	3.5	1.9		
		0.3	2.1	> 98	[163]
		3.5	1.9		
P123 Carbonized template silica	CTP vacuum/1 atm/22–60 °C	0.3	6–8.4	> 98	[145]
		3.5	2.4–7.8		
		7.5	1.8–6.6		
CTMSS C6	CTP vacuum/1 atm/22 °C	0.3	3.2	92	[166]
		3.5	2.2	97	
		7.5	0.4–2.3	> 92	[19]
Glucose carbonized template silica P123/TEVS/TEOS	RTP inert atmosphere/1 atm/25–60 °C	0.3	10–27	> 98	[148]
	CTP vacuum/1 atm/25–60 °C	3.5	9–17		
		7.5	8–16		
Interlayer-free silica-pectin	RTP inert atmosphere/1 atm/25–60 °C	3.5	5.9–8.9	> 99	[17]

addition, the listed membranes on Table 3 may have different geometries (flat, hollow fibre or tubular and sizes) and architecture (thickness of top layer, number interlayers or top layer, porosity and substrate) as such, all these factors play a role in the final performances.

Duke, O'Brien-Abraham [171] reported that a MTES membrane with pore diameter of 0.5 nm exhibits a higher water flux than carbonized template molecular sieve silica (CTMSS) membrane with pore diameters of 0.3 nm but with lower salt rejection. The comparison of three kinds of inorganic membranes: alumina, MTES and CTMSS for desalination by pervaporation have also been reported. Among them, CTMSS displayed the best performance with a flux of 2.2 kg.m⁻². h⁻¹, a rejection > 99.9 % and long-term testing at 25 °C was stable for 5 h. The findings suggest that the incorporation of carbon in a silica matrix plays a role in increasing salt rejection as well as matrix stabilization.

Wijaya, Duke [166] reported a CTS membrane derived from long carbon chain surfactant (C16) showed high salt rejection of up to 97 % with a flux of 3 kg.m⁻². h⁻¹. Carbon chain length of surfactants templates is a crucial factor that give direct impact in terms of desalination performance. The amount of embedded carbon has a beneficial role in silica matrices and is directly related to the number of residual carbons after the carbonization. However, if the surfactants concentration is too high, it forms micelles which block the possibility of using the sol-gel to coat the substrates.

Ladewig, Tan [165] to use the tri-block copolymer (polyethylene glycol)-(polypropylene glycol)-(polyethylene glycol) (PEG-PPG-PEG) as the template. The surfactant templates tend to form micelles at high concentrations and precipitate if in excess of 3 wt.% in the silica sol-gel. When the carbon content increased to 10 %, there was a rise in porosity despite still remained microporous. Consequently, the membrane demonstrated a slightly higher flux of 3.7 kg.m⁻². h⁻¹ and 985% of salt rejection for system operating at room temperature. Further increases of the tri-block copolymer to 20 wt.% altered the structure becomes mesopores. The performance is slightly higher than the surfactant template membranes (2.2 and 3 kg.m⁻². h⁻¹) mentioned earlier.

Mesopore CTAB silica membranes exhibited an excellent salt rejection > 99 % and water flux 2.6 kg.m⁻². h⁻¹ in seawater desalination at 25 °C. However, when it is exposed to high feed temperature (> 40 °C), the barrier layer of the mesostructured formed by a weak electrostatic interaction between CTAB and silica may suffer a disturbance, leading to a release of NaCl molecules to the permeate side and thus drastically decreases the salt rejection. This effect of temperature was reversible. The rejection came back to normal when reversed to lower feed temperature [172].

Recently, P123 carbon template silica prepared by the CTP technique by Elma, Wang [13] were successfully fabricated using the dual catalyst sol-gel method. Embedded P123 loading from 0–50 wt.% into

silica sol exhibited salt rejection of 99 %. The water fluxes varied depending on the loading of P123 in the silica sol, the feed temperature and the salt concentration in the feed. The water flux of the Silica-P123 membranes varied between 0.5–4.5 kg.m⁻². h⁻¹ (P123 5 wt. %), 0.9–5.5 kg.m⁻². h⁻¹ (P123 20 wt. %), 1.4–6.3 kg.m⁻². h⁻¹ (P123 35 wt. %), and 1.5–8.5 kg.m⁻². h⁻¹ (P123 50 wt.%). The major finding here was that the effect of salt concentration polarization was greatly reduced as the concentration of P123 in the silica matrix increased from 5 to 50 wt.%. Hence, high carbon content conferred salt concentration anti-polarization to the membrane surface as compared to the high silica content.

Glucose template silica membranes were investigated by Mujiyanti, Elma [19] for brine water desalination. The C–H stretching vibration showed from FTIR results indicating carbon from glucose successfully induced into the silica matrices. Silica-glucose membrane showed good performance with salt rejection of 93 %, but rather low water flux of 0.22–2.28 kg.m⁻². h⁻¹ under feed temperatures of 25, 40 and 60 °C). This work concluded that the addition of glucose as carbon template agents strengthen the silica network becomes stronger even though the water fluxes remains a bit lower.

Elma, Pratiwi [17] produced potable water from NaCl 3.5 wt.% solution. They found that the pectin template silica membranes gave similar water fluxes of 5.9–8.66 kg.m⁻². h⁻¹ (25–60 °C) with salt rejections of > 99.3 %, depending on the testing conditions and amount of pectin loading (2.5 wt.%, calcined at 300 °C). The membranes work well thanks to the presence of carbon chains from the pectin apple which strengthened silica membrane pore structure.

Syauqiyah, Elma [109] reported silica-P123 membrane for seawater desalination prepared under different calcined technique of (RTP). The RTP technique offered faster fabrication time with competitive performance against the CTP technique. This work reported comparing performance of silica-pectin and silica-P123 membranes by measuring water flux and salt rejection. Silica-pectin membrane displayed prominent water flux of 3 folds higher than the silica-P123. It is suggested that the number of carbon chains of P123 joined to silica matrices densified the membranes film.

Liang, Zhan [173] prepared GO (graphene oxide) films coated on polyacrylonitrile (PAN) by vacuum filtration method. As the new intriguing material, GO has ultra-thin two-dimensional structure with abundant functional groups such as epoxide, carbonyl on the surface. The resulting membrane displayed outstanding water permeability (of up to 65 kg.m⁻². h⁻¹) and salt rejection of > 99.8 % for desalination NaCl 3.5 wt.% via pervaporation at 90 °C. GO-based membranes have the potentials to become the preferred candidates to next-generation high performing membranes. However, fabrication method of GO membranes is rather complex, and the GO membranes tend to quickly

Table 4
Summary of carbon template based membranes for wetland saline water desalination.

Membrane	Feed temperature (°C)	NaCl conc. (wt%)	Water Flux (kg. m ⁻² h ⁻¹)	Salt Rejection (%)	Ref
Silica-P123	25	3.2	1.3–1.7	66–96	[169]
Silica-pectin	25	3.4	4.48	> 99	[174]
Pure silica	25–60	3.2	0.8–1.2	70–85	[168]
Organosilica	25	3	1.2	> 99	[99]

swell when immersed in water on a large Recent results show that pervaporation using inorganic membranes have undergone major improvement as water fluxes are now reaching values as high as 65 kg.m⁻². h⁻¹ (for feed of NaCl 3.5 wt.%). These results clearly show that pervaporation using inorganic membranes has closed the performance gap with the pervaporation using organic/polymer-based membrane, with performances now in the same range as commercial RO membranes.

4.1.2. Desalination of wetland saline water by carbon template silica membranes

Desalination of wetland saline water is an interesting application for pervaporation by carbon template silica membranes. Reports on desalination of wetland saline water by pervaporation using carbon-silica template membrane are listed on Table 4. Wetland saline water is abundant in Indonesia, especially in South Kalimantan. Generally, wetland saline water has unique characteristics such as low pH, brownish colour and consists of high natural organic matter (NOM) [99], that typically increases membrane vulnerability from fouling. Even more, sea water infiltrates into wetland aquifers during the rainy season and increase the salinity of the wetland water. In many wetland areas, wetland water is often seen as the only water resource, but its utilization is highly limited by the salt concentration and NOM contents.

Elma, Fitriani [169] reported the application of mesopore carbonized template silica membrane by employing P123 triblock copolymers calcinated at different temperatures (350–600 °C) for desalination of wetland saline water. The silica-P123 membranes showed good water flux and salt rejection. The water flux of silica-P123 increased from 1.3 to 1.7 kg.m⁻². h⁻¹ by raising the calcination temperatures from 300 to 600 °C. In the contrary, the salt rejection decreased sharply from 96 % to 66 %. Such behaviours are attributed to the carbon moieties tight at low temperature in arranging the silica pore structure leading to the reduction of water fluxes. Therefore, silica-P123 membranes calcined at high temperature having loose indeed the membrane structure become unstable and force the selectivity decreases.

In another study Elma, Hairullah [168], pure silica membrane was proved effective to reduce the salt concentration of wetland saline water feed via pervaporation process. The highest water flux obtained at feed temperature of 60 °C was 1.2 kg.m⁻². h⁻¹. Unfortunately, the salt rejection was still poor, only 69 % at the highest feed temperature. A phenomena equivocal with the one discussed earlier. Interestingly, another study Lestari, Elma [99] also reported organosilica membrane with similar water flux of 1.2 kg.m⁻². h⁻¹ at lower feed temperature (25 °C) coupled with high salt rejection over 99 % (Fig. 11). The organosilica membranes was prepared by employing citric acid with dual roles as the carbon sources and catalyst. Such membrane poses advantages such as inexpensive, easy to fabricate and fast in production. The pure mesoporous silica has slightly lower performance than other carbon mesopore template silica membranes. Overall it can be deduced that carbon template effective and yet affordable material for preparation of silica-based membranes for wetland saline water desalination.

Silica-pectin membrane showed excellent water fluxes of 2–3 folds higher than various silica-based membranes applied for wetland saline

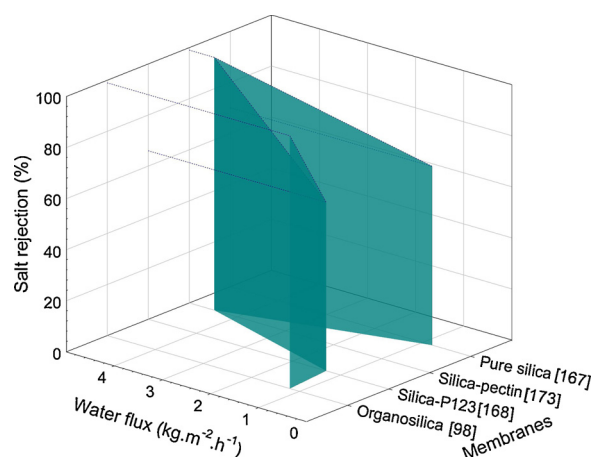


Fig. 11. Pervaporation performance at room temperature (25 °C) for desalination of wetland saline water.

water desalination (Fig. 11). Rahma, Elma [174] investigated pectin templated silica membrane and claimed that it achieved almost complete salt rejection of > 99 %. The NOM content was effectively reduced by incorporating a coagulation process as the pre-treatment. The highest NOM (UV₂₅₄) rejection was over 90 % [174]. Mechanism of pervaporation process for wetland saline water using carbon-silica template membrane is shown in Fig. 12.

Selectively of pure silica membranes are greatly reduced as the mobility of the silica enlarge the pore in the silica film facilitating salt diffusion. Water molecules react with the hydrophilic silanol groups because the silica matrix becomes mobile. The carbon template provides a barrier in the silica matrix that blocks the mobility of silica (Fig. 12). In this application, carbon can be attributed as a strong agent that switches the weakly silanol groups to avoid shrinkage of the silica matrices. At higher temperature, carbon-silica template materials are needed.

4.1.3. Long term stability of carbon template silica membranes

The stability of pervaporation process is judged by the ability to maintain the performance over time. Flux decline can happen due to hydration of the ions in solution and on the pore mouths which blocks the entry of water molecules. Therefore, during long-time testing the membrane fouling becomes critical due to the tendency of salt deposition that block the membrane pores. Deposition of salt shrinks the pore structure that block the transport of water which lowers the flux [143,153]. Fig. 13 summarizes the stability performance of various membranes types for desalination application.

Regarding the long-term testing of pure silica membrane (inorganic based material), an excellent result was reported by Elma, Yacou [143] for desalination of feed solution of 3.5 wt.% of NaCl. It was observed that pure silica membranes have stable long-term performances for 250 h at feed temperature of 22 °C. The first part of the operation of 150 h showed water fluxes ~8.5 kg.m⁻². h⁻¹, and the 250 h test yielded the water fluxes of 6.7 kg.m⁻². h⁻¹. The salt rejections were maintained high (of > 98 %). However, Elma, Yacou [143] also reported that water flux slightly reduced attributed to micropore blocking by hydrated salt ions due to the pure silica matrices cave during the submergence in water.

Despite the importance of performance stability, only a few reports are available (Table 5). In the longest performance evaluation reported so far, Lin, Ding [175] demonstrated cobalt oxide silica membranes (CoOxSi) est with multiples salt solutions i.e. 1 % (288 h), 3,5 wt.% (144 h), 7,5 wt.% (72 h) and 15 wt.% (72 h), totalling of 570 h. Water flux of the CoOxSi membrane tended to stabilize after 5 days ascribed to initial structural changes in the CoOxSi matrices. The long-term testing successfully demonstrated the improved hydro-stability of CoOxSi

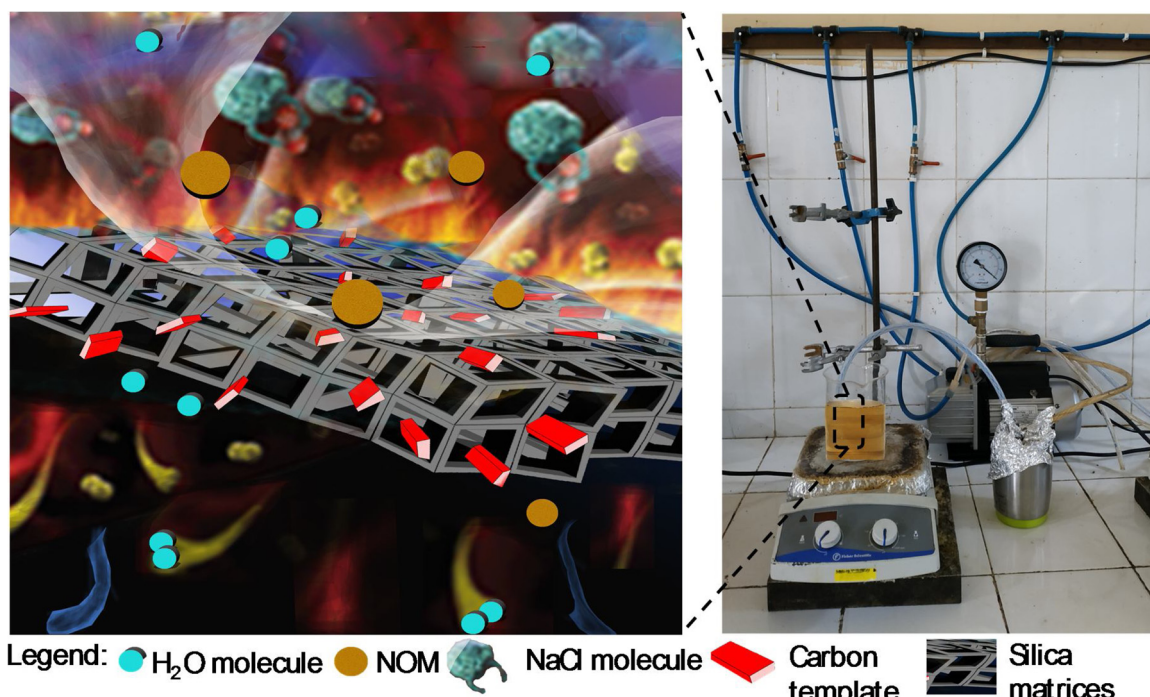


Fig. 12. Illustration of pervaporation mechanism of wetland saline water desalination via carbon template silica matrices.

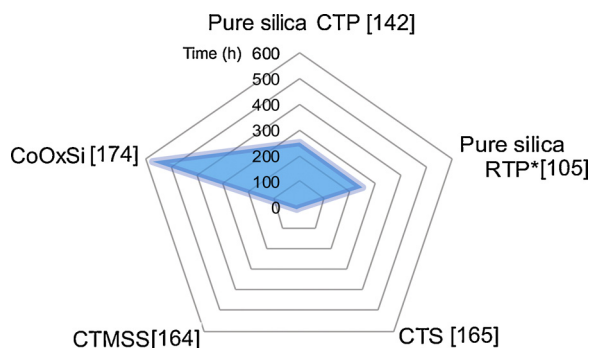


Fig. 13. Stability of various membranes type toward operation time (hour) for desalination of seawater and *wetland saline water.

membranes at various feed concentrations. In the several other studies, CTMSS (C6) membranes showed stable performance over 5 h, Wijaya, Duke [166] and over 12 h [165] due to the benefit of the carbonized templating method to improve the hydro-stability of the silica membranes. The report of long term stability study of carbon templated mesoporous silica membranes is still limited.

Zwijnenberg, Koops [176] demonstrated the longest stability performance of non-porous polyether amide membranes using solar driven pervaporation. The test was carried out using three different feed: de-ionized formation water, untreated seawater and artificial seawater (3.5 wt.% NaCl). The water flux remained stable over 250 day. In the

beginning of the experiment, a slightly lower flux was observed due to the hold-up volume on the permeate side of the system. However, water flux reached a steady state after 10 days tests. The occurrence of membrane fouling was not obvious over the experiment duration. The decrease in water flux due to fouling also reduced the heat loss via evaporation. This automatically resulted in an increase in the feed temperature. Consequently, the increased feed temperature enhanced the evaporation rate to about the same level that occurred as that without fouling.

4.2. Future challenges

Carbon template silica-based membranes for desalination application are still at the premature stages of research and development. Therefore, this type of material requires significant enhancements to be able to compete against both established membranes and/or established technologies. Indeed, the RO process using polymeric based membranes is now the golden standard as a result of major research, development, and deployment in the last 30 years.

Silica based membranes have shown potential in providing excellent molecular sieving properties for gas separation applications, but less so in water desalination. It is primarily due to the shortage of hydro-stability of silica structures when contact with water. The final challenge for the membrane researchers is to establish the carbon materials which are favourable, most technically and economically viable applied for water desalination using silica-based membranes. GO and polyetherimide materials have been reported to be effective carbon

Table 5
The stability performance of silica based membranes for water desalination.

Membrane type	Testing condition (Pressure, Temp.)	Feed salt conc. (wt%) Lower/Higher	Water Flux (Kg. m ⁻² . h ⁻¹)	Salt Rejection (%)	Long Term Stability test	Ref
Pure silica CTP	ΔP < 1 bar, 22 °C	3.5	8.5 – 6.89	> 98	250 h	[143]
Pure silica RTP	ΔP < 1 bar, 25 °C	3.2 (wetland saline water)	1.7 – 1.25	98 – 92	250 h	[106]
CTS	P = 7 bar, 20 °C	0.3/3.5	2.1/1.9	99.9/98	5 h	[166]
CTMSS	ΔP < 1 bar, 20 °C	0.3/3.5	6.3/4.9	87/97	12 h	[165]
CoOxSi	ΔP < 1 bar, 20 °C	0.3/15	0.4/0.3	99.7/99.9	570 h	[175]

template into silica matrices. In wetland saline water desalination, improvement is required to have membrane material that can handle the presence of NOM in the feed.

Application of mesoporous carbon template silica membranes by pervaporation is also restricted by the high energy input in comparison to the RO. Analysis of the thermodynamics also indicates that parity will never be reached when utilizing primary energy sources. However, if the pervaporation process is successfully integrated with solar heat sources, waste heat or other sustainable energy source then the technology may be attractive for niche applications such as brine processing or salt recovery.

Currently, there is limited study on membrane fouling for the silica-carbon based membranes mainly due to the immature stages of the testing. Most studies still utilize laboratory scale using artificial salt-water as the feed. Similarly, for fouling study of wetland saline water desalination. Given the scale of the problem for RO membranes, this is a problem that will require substantial research in the future to ensure that mesoporous carbon template silica membranes can be deployed in an industrial context.

5. Conclusions

Many approaches have been developed to prepare carbon templated mesoporous silica. Hard templating methods have often been applied, in which the incorporated carbon sources are deposited through mesoporous silica. However, this method is costly, involves toxic substances and complicated, which limit its application. Soft templating is favourable strategies to tailor well defined mesoporous structure. Sustainable carbon sources material as templating agents are very attractive technically and economically. Sucrose has been explored as carbon templates because it is an environmentally friendly product and contains multiple adjacent hydroxyl groups which will make the formation of hydrogen bonding with silica oligomers possible. In addition, GO and polyetherimide material can also be considered as effective carbon templating into silica matrices due to their excellent properties. Application of carbon templated mesoporous silica membranes is promising for water desalination. Future challenges for desalination of wetland saline water are on improve membrane performances (high flux and salt rejection), as well as handle NOM content. To tackle the energy input issue, application of mesoporous carbon template silica membranes by pervaporation systems can be coupled with renewable energy such as solar heat sources, waste heat or others as such it can be competitive against RO for niche applications such as brine processing or salt recovery.

Declaration of Competing Interest

The authors report no declarations of interest.

Acknowledgements

Muthia thanks to Applied Research Universities Grant 2019-2020, Thesis Magister Grant 2019-2020, World Class Research Grant 2020-2022 Deputy of Research and Development National Research and Innovation Agency, The Ministry of Research and Technology Republic of Indonesia and Lambung Mangkurat University Research Grant 2020.

References

- [1] K. Ariga, et al., Nanoarchitectonics for mesoporous materials, *Bull. Chem. Soc. Jpn.* 85 (1) (2012) 1–32, <https://doi.org/10.1246/bcsj.20110162>.
- [2] X. Zhu, et al., Facile surface modification of mesoporous silica with heterocyclic silanes for efficiently removing arsenic, *Chinese Chem. Lett.* 30 (6) (2019) 1133–1136, <https://doi.org/10.1016/j.ccl.2019.02.022>.
- [3] U. Ciesla, F. Schüth, Ordered mesoporous materials, *Microporous Mesoporous Mater.* 27 (2) (1999) 131–149, [https://doi.org/10.1016/S1387-1811\(98\)00249-2](https://doi.org/10.1016/S1387-1811(98)00249-2).
- [4] V. Meynen, P. Cool, E.F. Vansant, Verified syntheses of mesoporous materials,

- Microporous Mesoporous Mater.* 125 (3) (2009) 170–223, <https://doi.org/10.1016/j.micromeso.2009.03.046>.
- [5] W. Cheng, et al., A multifunctional nanoplatform against multidrug resistant Cancer: merging the best of targeted Chemo/Gene/Photothermal therapy, *Adv. Funct. Mater.* 27 (45) (2017) 1704135, <https://doi.org/10.1002/adfm.201704135>.
- [6] W. Zeng, et al., Dual-response oxygen-generating MnO₂ nanoparticles with poly-dopamine modification for combined photothermal-photodynamic therapy, *Chem. Eng. J.* 389 (2020) 124494, <https://doi.org/10.1016/j.cej.2020.124494>.
- [7] W. Ji, et al., Mesoporous silica nanospheres with the ability of photo-driven releasing sandela 803 for the application to wallpaper, *Chinese Chem. Lett.* 30 (03, 2019-03-22) (2019) 747–749, <https://doi.org/10.1016/j.ccl.2018.09.015>.
- [8] F. Schüth, W. Schmidt, Microporous and mesoporous materials, *Adv. Eng. Mater.* 4 (5) (2002) 269–279, [https://doi.org/10.1002/1527-2648\(20020503\)4:5<269::Aid-adem269>3.0.Co;2-7](https://doi.org/10.1002/1527-2648(20020503)4:5<269::Aid-adem269>3.0.Co;2-7).
- [9] A. Taguchi, F. Schüth, Ordered mesoporous materials in catalysis, *Microporous Mesoporous Mater.* 77 (1) (2005) 1–45, <https://doi.org/10.1016/j.micromeso.2004.06.030>.
- [10] M. Elma, et al., Microporous silica based membranes for desalination, *Water.* 4 (2012) 629–649, <https://doi.org/10.3390/w4030629>.
- [11] Heiner Strathmann, Enrico Drioli L.G, *An Introduction to Membrane Science and Technology*, Consiglio Nazionale Delle Ricerche, Italy, 2006.
- [12] S.J.C. Giessler, Dinizda Costa, G. Lu, Hydrophobicity of templated silica xerogels for molecular sieving applications, *J. Nanosci. Nanotechnol.* 1 (3) (2001) 331–336.
- [13] M. Elma, et al., Interlayer-free P123 carbonised template silica membranes for desalination with reduced salt concentration polarisation, *J. Memb. Sci.* 475 (2015) 376–383, <https://doi.org/10.1016/j.memsci.2014.10.026>.
- [14] C. Liang, S. Dai, Synthesis of mesoporous carbon materials via enhanced hydrogen-bonding interaction, *J. Am. Chem. Soc.* 128 (16) (2006) 5316–5317, <https://doi.org/10.1021/ja060242k>.
- [15] S. Tanaka, N. Nishiyama, Morphology control of ordered mesoporous carbon using organic-templating approach, *Progress in Molecular and Environmental Bioengineering-From Analysis and Modeling to Technology Applications*, IntechOpen, 2011.
- [16] R. Ayu Lestari, et al., Functionalization of Si-C Using TEOS (Tetra Ethyl Ortho Silica) As Precursor and Organic Catalyst, 148, (2020) 07008.
- [17] M. Elma, et al., The performance of membranes interlayer-free silica-pectin templated for seawater desalination via pervaporation operated at high temperature of feed solution, *Mater. Sci. Forum* 981 (2020) 349–355.
- [18] M. Elma, et al., Effect of banana pectin concentration on silica membran performance for brackish water, *Jurnal Teknik Lingkungan* 5 (2) (2019) 60–66, <https://doi.org/10.20527/jukung.v5i2.7318>.
- [19] D.R. Mujiyanti, M. Elma, M. Amalia, Interlayer-free glucose carbonised template silica membranes for brine water desalination, *MATEC Web Conf.* 280 (2019) 03010.
- [20] R. Babicheva, et al., New carbon membrane for water desalination via reverse osmosis, *IOP Conference Series: Materials Science and Engineering*, IOP Publishing, 2018.
- [21] V. Malgras, et al., Templated synthesis for nanoarchitected porous materials, *Bull. Chem. Soc. Jpn.* 88 (9) (2015) 1171–1200.
- [22] V. Malgras, et al., Nanoarchitectures for mesoporous metals, *Adv. Mater.* 28 (6) (2016) 993–1010.
- [23] N.L. Rosi, et al., Hydrogen storage in microporous metal-organic frameworks, *Science.* 300 (5622) (2003) 1127–1129.
- [24] Y.S. Bae, R.Q. Snurr, Development and evaluation of porous materials for carbon dioxide separation and capture, *Angew. Chemie Int. Ed.* 50 (49) (2011) 11586–11596.
- [25] Y.H. Deng, et al., A drying-free, water-based process for fabricating mixed-matrix membranes with outstanding pervaporation performance, *Angew. Chemie Int. Ed.* 55 (41) (2016) 12793–12796.
- [26] H.-L. Jiang, et al., Synergistic catalysis of Au@ Ag core– shell nanoparticles stabilized on metal– organic framework, *J. Am. Chem. Soc.* 133 (5) (2011) 1304–1306.
- [27] Y.D. Chiang, et al., Functionalized Fe₃O₄@ silica core–shell nanoparticles as microalgae harvester and catalyst for biodiesel production, *ChemSusChem.* 8 (5) (2015) 789–794.
- [28] Y.-H. Yang, et al., Hollow mesoporous hydroxyapatite nanoparticles (hmHANPs) with enhanced drug loading and pH-responsive release properties for intracellular drug delivery, *J. Mater. Chem. B* 1 (19) (2013) 2447–2450.
- [29] N.L. Torad, et al., MOF-derived nanoporous carbon as intracellular drug delivery carriers, *Chem. Lett.* 43 (5) (2014) 717–719.
- [30] R.E. Morris, P.S. Wheatley, Gas storage in nanoporous materials, *Angew. Chemie Int. Ed.* 47 (27) (2008) 4966–4981.
- [31] J. Ruparelia, et al., Potential of carbon nanomaterials for removal of heavy metals from water, *Desalination* 232 (1–3) (2008) 145–156.
- [32] F.-K. Shieh, et al., Size-adjustable annular ring-functionalized mesoporous silica as effective and selective adsorbents for heavy metal ions, *RSC Adv.* 3 (48) (2013) 25686–25689.
- [33] S. Dutta, A. Bhaumik, K.C.-W. Wu, Hierarchically porous carbon derived from polymers and biomass: effect of interconnected pores on energy applications, *Polym. Environ. Sci.* 7 (11) (2014) 3574–3592.
- [34] C. Van Nguyen, et al., A metal-free, high nitrogen-doped nanoporous graphitic carbon catalyst for an effective aerobic HMF-to-FDCA conversion, *Green Chem.* 18 (22) (2016) 5957–5961.
- [35] N.-L. Liu, et al., ZIF-8 derived, nitrogen-doped porous electrodes of carbon

- polyhedron particles for high-performance electrosorption of salt ions, *Sci. Rep.* 6 (1) (2016) 1–7.
- [36] Y. Gao, et al., Preparation of polyaniline nanotubes via “thin glass tubes template” approach and its gas response, *Macromol. Rapid Commun.* 28 (3) (2007) 286–291.
- [37] Y. Xie, et al., The effect of novel synthetic methods and parameters control on morphology of nano-alumina particles, *Nanoscale Res. Lett.* 11 (1) (2016) 1–11.
- [38] Y. Xie, et al., Review of research on template methods in preparation of nano-materials, . 2016 (2016).
- [39] M. Zhou, Z. Wei, H. Qiao, et al., Particle size and pore structure characterization of silver nanoparticles prepared by confined arc plasma, *Contributions to Atmospheric Physics* 2009 (8) (2009) 219–229.
- [40] E.M. Johansson, J.M. C´ordoba, M. Od´en, Effect of heptane addition on pore size and particle morphology of mesoporous silica SBA-15, *Microporous Mesoporous Mater.* 133 (1–3) (2010) 66–74.
- [41] H. Tamon, et al., Preparation of mesoporous carbon by freeze drying, *Carbon.* 37 (12) (1999) 2049–2055.
- [42] K. Nielsch, et al., Self-ordering regimes of porous alumina: the 10 porosity rule, *Nano Lett.* 2 (7) (2002) 677–680.
- [43] L. Zhang, et al., Templated growth of crystalline mesoporous materials: from Soft/Hard templates to colloidal templates, *Front. Chem.* 7 (2019) 22.
- [44] Y. Meng, et al., Ordered mesoporous polymers and homologous carbon frameworks: amphiphilic surfactant templating and direct transformation, *Angew. Chemie Int. Ed.* 44 (43) (2005) 7053–7059.
- [45] W. Li, et al., A perspective on mesoporous TiO₂ materials, *Chem. Mater.* 26 (1) (2014) 287–298.
- [46] H.N. Lokupitiya, et al., Ordered mesoporous to macroporous oxides with tunable isomorphic architectures: solution criteria for persistent micelle templates, *Chem. Mater.* 28 (6) (2016) 1653–1667.
- [47] M.D. Goodman, et al., Enabling new classes of templated materials through mesoporous carbon colloidal crystals, *Adv. Opt. Mater.* 1 (4) (2013) 300–304.
- [48] J. Pang, et al., Silica-templated continuous mesoporous carbon films by a spin-coating technique, *Adv. Mater.* 16 (11) (2004) 884–886.
- [49] B. Hu, et al., Functional carbonaceous materials from hydrothermal carbonization of biomass: an effective chemical process, *J. Chem. Soc. Dalton Trans.* (40) (2008) 5414–5423.
- [50] J. Schuster, et al., Spherical ordered mesoporous carbon nanoparticles with high porosity for lithium–sulfur batteries, *Angew. Chemie Int. Ed.* 51 (15) (2012) 3591–3595.
- [51] M.-X. Liu, et al., Synthesis and electrochemical performance of hierarchical porous carbons with 3D open-cell structure based on nanosilica-embedded emulsion-templated polymerization, *Chinese Chem. Lett.* 25 (6) (2014) 897–901.
- [52] A. Darmawan, et al., Structural evolution of nickel oxide silica sol-gel for the preparation of interlayer-free membranes, *J. Non. Solids* 447 (2016) 9–15.
- [53] N. Brun, et al., Hydrothermal carbon-based nanostructured hollow spheres as electrode materials for high-power lithium–sulfur batteries, *J. Chem. Soc. Faraday Trans.* 15 (16) (2013) 6080–6087.
- [54] J. Liu, et al., Highly dispersible microporous carbon particles from furfuryl alcohol, *NSTI Nanotech.* (2005).
- [55] C. Falco, et al., Hydrothermal carbons from hemicellulose-derived aqueous hydrolysis products as electrode materials for supercapacitors, *ChemSusChem.* 6 (2) (2013) 374–382.
- [56] J.H. Knox, K.K. Unger, H. Mueller, Prospects for carbon as packing material in high-performance liquid chromatography, *J. Liq. Chromatogr.* 6 (sup001) (1983) 1–36, <https://doi.org/10.1080/01483918308067647>.
- [57] T. Morishita, et al., A review of the control of pore structure in MgO-templated nanoporous carbons, *Carbon.* 48 (10) (2010) 2690–2707, <https://doi.org/10.1016/j.carbon.2010.03.064>.
- [58] Y. Yan, et al., Controlled synthesis of mesoporous carbon nanosheets and their enhanced supercapacitive performance, *J. Solid State Electrochem.* 17 (6) (2013) 1677–1684, <https://doi.org/10.1007/s10008-013-2025-3>.
- [59] X. He, et al., Synthesis of mesoporous carbons for supercapacitors from coal tar pitch by coupling microwave-assisted KOH activation with a MgO template, *Carbon* 50 (13) (2012) 4911–4921, <https://doi.org/10.1016/j.carbon.2012.06.020>.
- [60] A. Eftekhari, Z. Fan, Ordered mesoporous carbon and its applications for electrochemical energy storage and conversion, *Mater. Chem. Front.* 1 (6) (2017) 1001–1027, <https://doi.org/10.1039/C6QM00298F>.
- [61] S.B. Yoon, et al., New mesoporous silica/carbon composites by in situ transformation of silica template in carbon/silica nanocomposite, *J. Exp. Nanosci.* 9 (3) (2014) 221–229, <https://doi.org/10.1080/17458080.2011.654275>.
- [62] Z.-h. Tang, et al., Properties of mesoporous carbons prepared from different carbon precursors using nanosize silica as a template, *New Carbon Mater.* 25 (6) (2010) 465–469, [https://doi.org/10.1016/S1872-5805\(09\)60045-7](https://doi.org/10.1016/S1872-5805(09)60045-7).
- [63] S.J.M. Wang, Ordered mesoporous materials for drug delivery, *Microporous Mesoporous Mater.* 117 (1–2) (2009) 1–9.
- [64] H.I. Lee, et al., Rational synthesis pathway for ordered mesoporous carbon with controllable 30- to 100-Angstrom pores, *Adv. Mater.* 20 (4) (2008) 757–762, <https://doi.org/10.1002/adma.200702209>.
- [65] S. Wang, H.J.M. Li, Structure directed reversible adsorption of organic dye on mesoporous silica in aqueous solution, *Microporous Mesoporous Mater.* 97 (1–3) (2006) 21–26.
- [66] L. Huang, M. Kruk, Synthesis of ultra-large-pore FDU-12 silica using ethylbenzene as micelle expander, *J. Colloid Interface Sci.* 365 (1) (2012) 137–142, <https://doi.org/10.1016/j.jcis.2011.09.044>.
- [67] T.R. Pauly, T.J. Pinnavaia, Pore size modification of mesoporous HMS molecular sieve silicas with wormhole framework structures, *Chem. Mater.* 13 (3) (2001) 987–993, <https://doi.org/10.1021/cm000762t>.
- [68] R.I. Babicheva, et al., New carbon membrane for water desalination via reverse osmosis, *IOP Conference Series: Materials Science and Engineering* 447 (2018) 012053, <https://doi.org/10.1088/1757-899x/447/1/012053>.
- [69] B. Zhang, et al., Towards the preparation of ordered mesoporous Carbon/Carbon composite membranes for gas separation, *Sep. Sci. Technol.* 49 (2014), <https://doi.org/10.1080/01496395.2013.838684>.
- [70] R. Ryoo, S.H. Joo, S. Jun, Synthesis of highly ordered carbon molecular sieves via template-mediated structural transformation, *J. Phys. Chem. B* 103 (37) (1999) 7743–7746, <https://doi.org/10.1021/jp991673a>.
- [71] C. Lin, et al., Synthesis of ordered mesoporous carbon using MCM-41 mesoporous silica as template, *Adv. Mat. Res.* 11–12 (2006) 543–546, <https://doi.org/10.4028/www.scientific.net/AMR.11-12.543>.
- [72] M. Brankovic, et al., Mesoporous silica (MCM-41): Synthesis/modification, characterization and removal of selected organic micro-pollutants from water, *Adv. Technol.* 6 (2017) 50–57, <https://doi.org/10.5937/savteh1701050B>.
- [73] K. Erdmann, et al., Al-MCM-48 As a Template for Synthesis of Porous Carbons – Adsorption Study, (2005).
- [74] C. Kresge, et al., Ordered mesoporous molecular sieves synthesized by a liquid-crystal template mechanism, *nature* 359 (6397) (1992) 710–712.
- [75] J.S. Beck, et al., A new family of mesoporous molecular sieves prepared with liquid crystal templates, *J. Am. Chem. Soc.* 114 (27) (1992) 10834–10843.
- [76] J.C. Vartuli, et al., Chapter 1 - designed synthesis of mesoporous molecular sieve systems using surfactant-directing agents, in: W.R. Moser (Ed.), *Advanced Catalysts and Nanostructured Materials*, Academic Press, San Diego, 1996, pp. 1–19.
- [77] A. Sayari, B.-H. Han, Y. Yang, Simple synthesis route to monodispersed SBA-15 silica rods, *J. Am. Chem. Soc.* 126 (44) (2004) 14348–14349, <https://doi.org/10.1021/ja0478734>.
- [78] D. Zhao, et al., Triblock copolymer syntheses of mesoporous silica with periodic 50 to 300 angstrom pores, *Science.* 279 (5350) (1998) 548–552, <https://doi.org/10.1126/science.279.5350.548>.
- [79] D. Zhao, et al., Nonionic triblock and star diblock copolymer and oligomeric surfactant syntheses of highly ordered, hydrothermally stable, mesoporous silica structures, *J. Am. Chem. Soc.* 120 (24) (1998) 6024–6036, <https://doi.org/10.1021/ja974025i>.
- [80] P. Fulvio, S. Pikus, M. Jaroniec, Short-time synthesis of SBA-15 using various silica sources, *J. Colloid Interface Sci.* 287 (2005) 717–720, <https://doi.org/10.1016/j.jcis.2005.02.045>.
- [81] J. Wang, et al., Hydrothermal synthesis of SBA-15 using sodium silicate derived from coal gangue, *J. Nanomaterials.* 2013 (2013), <https://doi.org/10.1155/2013/352157> Article 6.
- [82] H. Razak, et al., Refluxed synthesis of SBA-15 using sodium silicate extracted from Oil Palm Ash for dry reforming of methane, *Mater. Today Proc.* 19 (2019) 1363–1372, <https://doi.org/10.1016/j.matpr.2019.11.150>.
- [83] A. Sayari, Y. Yang, SBA-15 templated mesoporous carbon: new insights into the SBA-15 pore structure, *Chem. Mater.* 17 (24) (2005) 6108–6113, <https://doi.org/10.1021/cm050960q>.
- [84] M. Koh, et al., Surface morphology and physicochemical properties of ordered mesoporous silica SBA-15 synthesized at low temperature, *IOP Conference Series: Materials Science and Engineering* 206 (2017) 012056, <https://doi.org/10.1088/1757-899X/206/1/012056>.
- [85] N. Rahmat, A.Z. Abdullah, A. Mohamed, A review: mesoporous santa barbara Amorphous-15, types, synthesis and its applications towards biorefinery production, *Am. J. Appl. Sci.* 7 (2010), <https://doi.org/10.3844/ajassp.2010.1579.1586>.
- [86] M.S.Md. Oliveira, et al., Incorporating aluminum into the structure of SBA-15 by adjusting the pH and adding NaF, *Mater. Res.* 22 (2019).
- [87] E. Rivera-Muñoz, R. Huirache-Acuña, Sol gel-derived SBA-16 mesoporous material, *Int. J. Mol. Sci.* 11 (2010) 3069–3086, <https://doi.org/10.3390/ijms11093069>.
- [88] T. Yu, et al., Pore structures of ordered large cage-type mesoporous silica FDU-12s, *J. Phys. Chem. B* 110 (43) (2006) 21467–21472, <https://doi.org/10.1021/jp064534j>.
- [89] J. Fan, et al., Cubic mesoporous silica with large controllable entrance sizes and advanced adsorption properties, *Angew. Chem. Int. Ed. Engl.* 42 (27) (2003) 3146–3150, <https://doi.org/10.1002/anie.200351027>.
- [90] S.S. Kim, et al., Synthesis and characterization of ordered, very large pore MSU-H silicas assembled from water-soluble silicates, *J. Phys. Chem. B* 105 (32) (2001) 7663–7670, <https://doi.org/10.1021/jp010773p>.
- [91] J. Zeng, et al., Ordered mesoporous carbon/Nafion as a versatile and selective solid-phase microextraction coating, *J. Chromatogr. A* 1365 (2014) 29–34, <https://doi.org/10.1016/j.chroma.2014.08.094>.
- [92] S.-S. Kim, T.J. Pinnavaia, A low cost route to hexagonal mesostructured carbon molecular sieves, *Chem. Commun.* 23 (2001) 2418–2419, <https://doi.org/10.1039/B107896H>.
- [93] Á.A. Beltrán-Osuna, J.E. Perilla, Colloidal and spherical mesoporous silica particles: synthesis and new technologies for delivery applications, *J. Solgel Sci. Technol.* 77 (2) (2016) 480–496.
- [94] D. Macquarrie, et al., Organomodified hexagonal mesoporous silicates, *New J. Chem.* 23 (5) (1999) 539–544.
- [95] F. Farjadian, et al., Phosphinite-functionalized silica and hexagonal mesoporous silica containing palladium nanoparticles in Heck coupling reaction: synthesis, characterization, and catalytic activity, *RSC Adv.* 5 (97) (2015) 79976–79987.
- [96] P.T. Tanev, T.J. Pinnavaia, A neutral templating route to mesoporous molecular sieves, *Science.* 267 (5199) (1995) 865–867, <https://doi.org/10.1126/science.267.5199.865>.

- [97] M.A. Al Roaya, F. Manteghi, M. Haghighverdi, Synthesis and characterization of hollow mesoporous silica spheres and studying the load and release of dexamethasone, *Silicon*. 11 (3) (2019) 1401–1411, <https://doi.org/10.1007/s12633-018-9943-8>.
- [98] M. Elma, et al., Microporous silica based membranes for desalination, *Water*. 4 (3) (2012) 629, <https://doi.org/10.3390/w4030629>.
- [99] R.A. Lestari, et al., Organo silica membranes for wetland saline water desalination: effect of membranes calcination temperatures, *E3S Web Conf.* 148 (2020) 07006.
- [100] S. Benfer, et al., Development and characterization of ceramic nanofiltration membranes, *Sep. Purif. Technol.* 22-23 (2001) 231–237, [https://doi.org/10.1016/S1383-5866\(00\)00133-7](https://doi.org/10.1016/S1383-5866(00)00133-7).
- [101] R. Ayu Lestari, et al., Functionalization of Si-C using TEOS (Tetra ethyl ortho silica) as precursor and organic catalyst, *E3S Web Conf.* 148 (2020) 07008.
- [102] D. Nadargi, A. Rao, Methyltriethoxysilane: New precursor for synthesizing silica aerogels, *Journal of Alloys and Compounds - J ALLOYS COMPOUNDS*. 467 (2009) 397–404, <https://doi.org/10.1016/j.jallcom.2007.12.019>.
- [103] Maimunawaro, et al., Deconvolution of carbon silica templated thin film using ES40 and P123 via rapid thermal processing method, *Mater. Today Proc.* (2020), <https://doi.org/10.1016/j.matpr.2020.01.195>.
- [104] S.K. Rahman, et al., Functionalization of hybrid organosilica based membranes for water desalination – preparation using Ethyl Silicate 40 and P123, *Mater. Today Proc.* (2020), <https://doi.org/10.1016/j.matpr.2020.01.187>.
- [105] J. Cihlář, Hydrolysis and polycondensation of ethyl silicates. 2. Hydrolysis and polycondensation of ETS40 (ethyl silicate 40), *Colloids Surf. A Physicochem. Eng. Asp.* 70 (3) (1993) 253–268, [https://doi.org/10.1016/0927-7757\(93\)80299-T](https://doi.org/10.1016/0927-7757(93)80299-T).
- [106] M. Elma, N. Riskawati, Marhamah, Silica membranes for wetland saline water desalination: performance and long term stability, *IOP Conference Series: Earth and Environmental Science* 175 (1) (2018) 012006, <https://doi.org/10.1088/1755-1315/175/1/012006>.
- [107] E.L.A. Rampun, et al., Interlayer-free silica-pectin membrane for sea-water desalination, *Membr. Technol.* 2019 (12) (2019) 5–9, [https://doi.org/10.1016/S0958-2118\(19\)30222-8](https://doi.org/10.1016/S0958-2118(19)30222-8).
- [108] E.L.A. Rampun, et al., Interlayer-free Silica Pectin Membrane for Wetland Saline Water via Pervaporation, *J. Kim. Sains Dan Apl.* 22 (3) (2019) 6 10.14710/jksa.22.3.99-104.
- [109] I. Syaunqiyah, et al., Interlayer-free silica-carbon template membranes from pectin and P123 for water desalination, *MATEC Web Conf.* 280 (2019) 03017.
- [110] A. Lamy-Mendes, R.F. Silva, L. Durães, Advances in carbon nanostructure-silica aerogel composites: a review, *J. Mater. Chem. A* 6 (4) (2018) 1340–1369, <https://doi.org/10.1039/C7TA08959G>.
- [111] P. Alexandridis, J.F. Holzwarth, T.A. Hatton, Micellization of poly(ethylene oxide)-Poly(propylene oxide)-Poly(ethylene oxide) triblock copolymers in aqueous solutions: thermodynamics of copolymer association, *Macromolecules*. 27 (9) (1994) 2414–2425, <https://doi.org/10.1021/ma00087a009>.
- [112] B. Hatton, et al., Past, present, and future of periodic mesoporous organosilicas-the PMOs, *Acc. Chem. Res.* 38 (4) (2005) 305–312, <https://doi.org/10.1021/ar040164a>.
- [113] F. Hoffmann, et al., Periodic mesoporous organosilicas (PMOs): past, present, and future, *J. Nanosci. Nanotechnol.* 6 (2) (2006) 265–288, <https://doi.org/10.1166/jnn.2006.902>.
- [114] D. Zhao, et al., Triblock copolymer syntheses of mesoporous silica with periodic 50 to 300 angstrom pores, *science* 279 (5350) (1998) 548–552.
- [115] T.-W. Kim, et al., Tailoring the pore structure of SBA-16 silica molecular sieve through the use of copolymer blends and control of synthesis temperature and time, *J. Phys. Chem. B* 108 (31) (2004) 11480–11489.
- [116] L. Wang, et al., Synthesis and characterization of small pore thick-walled SBA-16 templated by oligomeric surfactant with ultra-long hydrophilic chains, *Microporous Mesoporous Mater.* 67 (2–3) (2004) 135–141.
- [117] G. Farid, Flexible and Versatile Soft Templates for Mesoporous Silicas and Organosilicas Based on Pluronic Block Copolymer Surfactants and Their Mixtures, (2018).
- [118] A.E. Pratiwi, et al., Innovation of carbon from pectin templated in fabrication of interlayer-free silica-pectin membrane, *J. Kim. Sains Dan Apl.* 22 (3) (2019) 6, <https://doi.org/10.14710/jksa.22.3.93-98>.
- [119] M. Elma, et al., The effect of banana pectin concentration on silica membrane performance for brackish water, *Jukung Jurnal Teknik Lingkungan*. 5 (2) (2019) 45–51.
- [120] R. Zhong, et al., An eco-friendly Soft template synthesis of mesostructured silica-carbon nanocomposites for acid catalysis, *ChemCatChem*. 7 (2015), <https://doi.org/10.1002/cctc.201500728> n/a-n/a.
- [121] C.M. Yang, B. Zibrowius, F. Schuth, Formation of cyanide-functionalized SBA-15 and its transformation to carboxylate-functionalized SBA-15, *Chemistry* (2004) 2461–2467.
- [122] Yunyun Xie, Mozhen Wang J.W, Xuewu Ge, Fabrication of fibrous amidoxime-functionalized mesoporous silicamicrosphere and its selectively adsorption property for Pb²⁺ in aqueous solution, *J. Hazard. Mater.* 297 (2015) 66–73.
- [123] S. Brunauer, W.E. Deming, E. Teller, On a theory of the van derWaals adsorption of gases, *J. Am. Chem. Soc.* 62 (1940) 1723–1732.
- [124] K.S.W. Sing, R.A.W. Haul, L. Moscou, R.A. Pierotti, J. Rouquérol, T. Siemieniowska, Reporting physisorption data for gas/solid systems with special reference to the determination of surface area and porosity (recommendations 1984), *Pure Appl. Chem.* 57 (1985) 603–619.
- [125] D.S. Moon, J.K. Lee, Tunable synthesis of hierarchical mesoporous silicananoparticles with radial wrinkle structure, *Langmuir*. 28 (2012) 12341–12347.
- [126] F. Juillerat, P.B., H. Hofmann, 22 (2006) 5287–5291.
- [127] J.M. Rosenholm, E. Peuhu, R. Niemi, J.E. Eriksson, C. Sahlgrén, *MI INDEN, ACS Nano* 3 (2009) 197–268.
- [128] Oliver Wiltshchka, D. Böcking, Larissa Miller, Rolf E. Brenner, Cecilia Sahlgrén, Mika Lindén, Preparation, characterization, and preliminary biocompatibility evaluation of particulate spin-coated mesoporous silica films, *Microporous Mesoporous Mater.* 188 (2013) 203–209.
- [129] J.H. Prosser, S.Lee T.B, A.J. Nolte, D. Lee, *Nano Lett.* 11 (1999) 2132–2140.
- [130] X. Mao, Y. Chen, L. Yang, F. Zhao, B. Ding, J. Yu, *RSC Adv.* (2012) 12216–12223.
- [131] Yang Wang, Xiuling Jiao W.D, Dairong Chen, Electrospun flexible self-standing silica/mesoporous alumina core-shell fibrous membranes as adsorbents toward Congo red, *RSC Adv.* 30790 (2014).
- [132] S. Zhan, X. Jiao, C. Tao, *J. Phys. Chem. B* 110 (11199-11204) (2006).
- [133] J.H. Yu, S.V. Fridrikh, G.C. Rutledge, *Adv Mater* 16 (1562-1566) (2004).
- [134] Asmaa Mourhly, Adnane E. Hamidi, Mohammed Kacimi, Mohammed Halim, Said Arsalane, The synthesis and characterization of low-cost mesoporous silica SiO₂ from local pumice rock, *Nanomater. Nanotechnol.* (2015).
- [135] S. Nasserli, M. Heidari, Evaluation and comparison of aluminum coated-pumice and zeolite in arsenic removal from water resources, *Iranian J. Environ. Health Sci. Eng.* 9 (2012) 256–268.
- [136] A.H. Mahvi, A. Mesdaghinia, A.R. Yari, Fluoride adsorption by pumice from aqueous solutions, *E-journal Chem.* 9 (2012) 1843–1853.
- [137] M. Tapan, Use of pumice and scoria aggregates, *Problems of Minerals Processing* 50 (2014) 467–475.
- [138] B. Cekova, B. Pavlovski, D. Spasev, A. Reka, Structural examinations of natural raw materials pumice and trepel from republic of Macedonia, *Balkan Mineral Processing Congress, Bulgaria*, 2013, pp. 73–75.
- [139] M.N. Sepehr, Kazemian Z.M, H. Amrane, A. Yaghmaian, K. Ghaffar, Removal of hardness agents, calcium and magnesium, by natural and alkaline modified pumice stones in single and binary systems, *Appl. Surf. Sci.* 274 (2013) 295–305.
- [140] I.A. Rahman, P. Vejayakumar, C.S. Sipaut, J. Ismail, C.K. Chee, Size-dependent physicochemical and optical properties of silica nanoparticles, *Mater. Chem. Phys.* 114 (2009) 328–332.
- [141] J. Yang, E. Wang, Reaction of water on silica surfaces, *Curr. Opin. Solid State Mater. Sci.* 10 (2006) 33–39.
- [142] M. Elma, et al., Fabrication of interlayer-free silica-based membranes – effect of low calcination temperature using an organo-catalyst, *Membr. Technol.* 2019 (2) (2019) 6–10, [https://doi.org/10.1016/S0958-2118\(19\)30037-0](https://doi.org/10.1016/S0958-2118(19)30037-0).
- [143] M. Elma, et al., Performance and Long Term Stability of Mesoporous Silica Membranes for Desalination, *Membranes* 3 (2013) 136–150, <https://doi.org/10.3390/membranes3030136>.
- [144] M. Elma, et al., Fabrication of interlayer-free P123 coronised template silica membranes for Water desalination: conventional versus Rapid thermal processing (CTP vs RTP) techniques, *IOP Conference Series: Materials Science and Engineering*, IOP Publishing, 2019.
- [145] M. Elma, et al., Interlayer-free P123 carbonised template silica membranes for desalination with reduced salt concentration polarisation, *J. Memb. Sci.* 475 (2015) 376–383, <https://doi.org/10.1016/j.memsci.2014.10.026>.
- [146] M. Elma, et al., Interlayer-Free hybrid organo-silica membranes based teos and tevs for Water desalination, *International Conference on Oleo and Petrochemical Engineering* (2015) 49–57 https://www.researchgate.net/publication/294715939_INTERLAYER-FREE_HYBRID_ORGANO-SILICA_MEMBRANES_BASED_TEOS_AND_TEVS_FOR_WATER_DESALINATION.
- [147] S.M. Ashrafi-Shahria, F. Ravaria, D. Seifzadeh, Smart Organic/Inorganic sol-gel nanocomposite containing functionalized mesoporous silica for corrosion protection, *Progress in Organic Coatings*. 133 (2019) 44–54.
- [148] H. Yang, et al., Interlayer-free hybrid carbon-silica membranes for processing brackish to brine salt solutions by pervaporation, *J. Memb. Sci.* (2017).
- [149] S. Tanaka, et al., Preparation of ordered mesoporous carbon membranes by a soft-templating method, *Carbon*. 49 (10) (2011) 3184–3189, <https://doi.org/10.1016/j.carbon.2011.03.042>.
- [150] M. Elma, G.S. Saputro, Performance of cobalt-silica membranes through pervaporation process with different feed solution concentrations, *Mater. Sci. Forum* 981 (2020) 342–348.
- [151] N.I. Vazquez, et al., Synthesis of mesoporous silica nanoparticles by sol-Gel as nanocontainer for future drug delivery applications, *Boletín De La Sociedad Espanola De Ceramica y Vidrio*. 56 (2017) 139–145.
- [152] H. Nagasawa, T. Tsuru, Chapter 9 - silica membrane application for pervaporation process, in: A. Basile, K. Ghasemzadeh (Eds.), *Current Trends and Future Developments on (Bio-) Membranes*, Elsevier, 2017, pp. 217–241.
- [153] Q. Wang, et al., Desalination by pervaporation: a review, *Desalination* 387 (2016) 46–60, <https://doi.org/10.1016/j.desal.2016.02.036>.
- [154] M.C. Duke, et al., Hydrothermally robust molecular sieve silica for wet gas separation, *Adv. Funct. Mater.* 16 (9) (2006) 1215–1220, <https://doi.org/10.1002/adfm.200500456>.
- [155] P.-S. Lee, et al., Carbon molecular sieve membranes on porous composite tubular supports for high performance gas separations, *Microporous Mesoporous Mater.* 224 (2016) 332–338, <https://doi.org/10.1016/j.micromeso.2015.12.054>.
- [156] S.M. Saufi, A.F. Ismail, Fabrication of carbon membranes for gas separation—a review, *Carbon* 42 (2) (2004) 241–259, <https://doi.org/10.1016/j.carbon.2003.10.022>.
- [157] G. Xomeritakis, et al., Organic-templated silica membranes: I. Gas and vapor transport properties, *J. Memb. Sci.* 215 (1) (2003) 225–233, [https://doi.org/10.1016/S0376-7388\(02\)00616-6](https://doi.org/10.1016/S0376-7388(02)00616-6).
- [158] M. Elma, et al., High performance interlayer-free mesoporous cobalt oxide silica membranes for desalination applications, *Desalination* 365 (2015) 308–315, <https://doi.org/10.1016/j.desal.2015.02.034>.
- [159] Y. Chua, et al., Mesoporous organosilica membranes: effects of pore geometry and

- calcination conditions on the membrane distillation performance for desalination, *Desalination*. 370 (2015) 53–62, <https://doi.org/10.1016/j.desal.2015.05.015>.
- [160] N.K. Raman, C.J. Brinker, Organic “template” approach to molecular sieving silica membranes, *J. Memb. Sci.* 105 (3) (1995) 273–279, [https://doi.org/10.1016/0376-7388\(95\)00067-M](https://doi.org/10.1016/0376-7388(95)00067-M).
- [161] Z. Xie, et al., 6 - desalination by pervaporation, in: V.G. Gude (Ed.), *Emerging Technologies for Sustainable Desalination Handbook*, Butterworth-Heinemann, 2018, pp. 205–226.
- [162] M.C. Duke, et al., Hydrothermally robust molecular sieve silica for wet gas separation, *Adv. Funct. Mater.* 16 (9) (2006) 1215–1220, <https://doi.org/10.1002/adfm.200500456>.
- [163] M.C. Duke, S. Mee, J.C.D. da Costa, Performance of porous inorganic membranes in non-osmotic desalination, *Water Res.* 41 (17) (2007) 3998–4004, <https://doi.org/10.1016/j.watres.2007.05.028>.
- [164] H. Yang, et al., Hybrid vinyl silane and P123 template sol–gel derived carbon silica membrane for desalination, *J. Solgel Sci. Technol.* (2017), <https://doi.org/10.1007/s10971-017-4562-1>.
- [165] B.P. Ladewig, et al., Preparation, characterization and performance of templated silica membranes in non-osmotic desalination, *Materials*. 4 (5) (2011) 845.
- [166] S. Wijaya, M.C. Duke, J.C. Diniz da Costa, Carbonised template silica membranes for desalination, *Desalination*. 236 (1) (2009) 291–298, <https://doi.org/10.1016/j.desal.2007.10.079>.
- [167] E.L.A. Rampun, et al., Interlayer-free silica pectin membrane for wetland saline water via pervaporation, *J. Kim. Sains Dan Apl.* 22 (3) (2019) 99–104.
- [168] M. Elma, Hairullah, Z.L. Assyaifi, Desalination process via pervaporation of wetland saline Water, *IOP Conference Series: Earth and Environmental Science*, IOP Publishing, 2018.
- [169] M. Elma, et al., Silica P123 membranes for desalination of wetland saline Water in South Kalimantan, *IOP Conference Series: Earth and Environmental Science*, IOP Publishing, 2018.
- [170] Y.T. Chua, et al., Nanoporous organosilica membrane for water desalination: theoretical study on the water transport, *J. Memb. Sci.* 482 (2015) 56–66, <https://doi.org/10.1016/j.memsci.2015.01.060>.
- [171] M.C. Duke, et al., Seawater desalination performance of MFI type membranes made by secondary growth, *Sep. Purif. Technol.* 68 (3) (2009) 343–350, <https://doi.org/10.1016/j.seppur.2009.06.003>.
- [172] P.S. Singh, et al., Cetyltrimethylammonium bromide–silica membrane for seawater desalination through pervaporation, *Bull. Mater. Sci.* 38 (2) (2015) 565–572.
- [173] B. Liang, et al., High performance graphene oxide/polyacrylonitrile composite pervaporation membranes for desalination applications, *J. Mater. Chem. A* 3 (9) (2015) 5140–5147, <https://doi.org/10.1039/C4TA06573E>.
- [174] A. Rahma, et al., Removal of natural organic matter for wetland saline water desalination by coagulation-pervaporation, *J. Kim. Sains Dan Apl.* 22 (3) (2019) 85–92, <https://doi.org/10.14710/jksa.22.3.85-92>.
- [175] C.X.C. Lin, et al., Cobalt oxide silica membranes for desalination, *J. Colloid Interface Sci.* 368 (1) (2012) 70–76.
- [176] H.J. Zwijnenberg, G.H. Koops, M. Wessling, Solar driven membrane pervaporation for desalination processes, *J. Memb. Sci.* 250 (1) (2005) 235–246, <https://doi.org/10.1016/j.memsci.2004.10.029>.